

EVALUATION OF HEAT REJECTION STRATEGIES FOR LIQUID DESICCANT AIR-CONDITIONING SYSTEMS

by

Danial Salimizad

A thesis submitted to the Department of Mechanical and Materials Engineering
in conformity with the requirements for the degree of Master of Applied Science

Queen's University
Kingston, Ontario, Canada
(September, 2015)

Copyright © Danial Salimizad, 2015

Abstract

The increased demand for space cooling and the resulting summer peak in electrical demands are motivating research into thermally-driven air-conditioning systems that can use renewable or waste heat. One promising technology is the use of a Liquid Desiccant Air-Conditioning (LDAC).

An evaporative cooling tower (ECT) was used as a cooling device to reject the heat from a LDAC at Queen's University. Investigation of the ECT showed significant power consumption and ineffective operation in humid conditions which contributed to the low electrical and thermal coefficients of performance (COP_E and COP_T). Therefore, the present study was undertaken to identify and evaluate alternative heat rejection strategies that can provide a better thermal and electrical system performance.

The relationship between the relative humidity and the ambient air temperature at a variety of cooling water temperatures was modelled using TRNSYS, a transient simulation program, as the first stage of the study. To find the most promising heat rejection technologies, available cooling methods were reviewed and two were selected (based on the results of the first phase of the study), namely, (i) a cooling water storage (CWS) system and (ii) a ground-source heat exchanger (GSHX) system. These were simulated and evaluated in detail. Finally, an experimental investigation of a stratified cooling water storage tank (SCWS) and night cooling water storage (NCWS) was undertaken to confirm the results of an additional simulation on the use of a stratified cooling tank.

From the simulation results and the overall comparison of the selected heat rejection strategies of the LDAC, it was concluded that GSHX system with 25 boreholes showed better COP_E than the CWS system whereas the COP_T improvement of both systems was almost same. The improved performance of the GSHX however, is expensive as the capital cost for boreholes is higher than the other systems. When comparing the CWS system (with mixed tank) and the SCWS (with stratified tank) it was observed that the stratified tank had the better potential of improving the COP_T , depending upon the water flow rate and initial tank temperature.

Acknowledgements

There have been a few people whose inspiration and support on me shaped my life. I would like to express my sincere gratitude to my advisor Prof. Stephen Harrison for the continuous support of my study. This research would not have been possible without his valuable guidance, enthusiasm, and immense knowledge.

I thank my fellow labmates at the Solar Calorimetry Laboratory who have made my time here more enjoyable and memorable.

I would also like to thank Natural Resources Canada (NRCan), Natural Sciences and Engineering Research Council (NSERC), and the Canadian Smart Net Zero Energy Buildings Strategic Research Network (SNEBRN) for their financial contribution towards this project and my studies.

Last but not the least, I would like to thank my family for their support, love and patience.

Table of Contents

Chapter 1 Introduction	1
1.1 Background	1
1.2 Traditional Air-Conditioning Systems	4
1.3 Alternative Approaches to Traditional Vapour-compression Air-Conditioning systems	6
1.3.1 Open Cooling Cycles.....	9
1.3.2 Desiccant cooling system	10
1.4 Thermodynamics of Air-Conditioning.....	14
1.5 International Energy Agency Task 38.....	16
1.6 Problem Definition of the LDAC System	17
1.6.1 Cold Water Supply	17
1.6.2 Electrical Consumption	18
1.7 Available Cooling Water Technologies	19
1.8 Objective, Approach, and Scope	21
1.9 Format and Thesis Organization	24
Chapter 2 Literature Review	26
2.1 Heat rejection for Desiccant Absorber Designs	27
2.1.1 Dry coolers	27
2.1.2 Evaporative Cooling towers	30
2.1.3 Cold Storage	33
2.1.4 Ground Source Heat Storage and Control strategies	37
2.1.5 Selected Heat Rejection Strategies	39
2.2 Previous Work at the Queen’s Solar Calorimetry Laboratory	40
2.2.1 Queen’s System Description	40
Chapter 3 Numerical and Experimental Modeling	45
3.1 Basic Simulation Model of LDAC System	46
3.1.1 Introduction	46
3.1.2 Basic TRNSYS Simulation	47
3.2 Case A: Cooling Water Temperature Model.....	52
3.2.1 Introduction	52

3.2.2 TRNSYS Simulation Model.....	53
3.3 Case B: Cooling Water Storage System (Load-shifting Model).....	54
3.3.1 Introduction	54
3.3.2 TRNSYS Simulation Model.....	56
3.4 Case C: Ground-source Heat Exchanger Model	59
3.4.1 Introduction	59
3.4.2 TRNSYS Simulation Model.....	59
3.5 Experimental Investigation of Stratified Cooling Water Storage Tank (SCWS) (Case D).....	63
3.5.1 Introduction	63
3.5.2 Experimental Set-up and Design	64
Chapter 4 Results and Analysis	69
4.1 Case A: Cooling Water Temperature Results	69
4.1.1 Daily System Performance	69
4.1.2 Thermal comfort and cooling water	77
4.1.3 Annual System Performance	79
4.2 Case B: Cold Water Storage System (Load shifting Model)	82
4.3 Case C: Ground Source Heat Exchanger Results for LDAC System	86
4.4 Experimental Investigation of a Stratified Cooling Water Storage Tank (SCWS) (Case D).....	91
4.4.1 SCWS Simulation.....	95
Chapter 5 Discussion of Results	97
5.1 Case A: Cooling Water Temperature Model.....	97
5.2 Case B: Cold Water Storage System (Load shifting Model)	100
5.3 Case C: Ground-source Heat Exchanger Results for LDAC System.....	102
5.4 Experimental Investigation of Stratified Cooling Water Storage Tank (SCWS) (Case D).....	104
5.5 Comparison of Different Cases	106
Chapter 6 Conclusions and Recommendations.....	111
6.1 Conclusions	111
6.2 Recommendations for Future Research	114

References.....	115
Appendix A- Modeling of a Conditioner/Regenerator	123
Appendix B- Stratified tank simulation	130

List of Figures

Fig. 1-1: Residential secondary energy use [1].....	1
Fig. 1-2: Thermal comfort zone according [4].....	2
Fig. 1-3: Latent and sensible Ventilation Load Index (VLI) for several cities with a set-point of 24°C and 50% relative humidity [8].	4
Fig. 1-4: Psychrometric charts showing sensible cooling, latent cooling, and cooling and dehumidification process.	6
Fig. 1-5: Types of Thermal Driven A/C systems.....	7
Fig. 1-6: LHS- basic components of a vapour-compression refrigeration unit; and, RHS- schematic of an absorption chiller [9]	8
Fig. 1-7: Solid desiccant dehumidifier schematic [15]	11
Fig. 1-8: Psychrometric chart of thermodynamic processes of: vapour-compression system (green line), solid desiccant (brown line), and liquid desiccant (blue line) [8].....	12
Fig. 1-9: Typical desiccant cycle [14].....	13
Fig. 1-10: Electrical power consumption of LDAC system components [22].	19
Fig. 1-11: Different techniques for rejecting heat from air conditioning systems	20
Fig. 1-12: Flow chart of research method.....	23
Fig. 2-1: Thermal COP and ambient relative humidity [8].....	33
Fig. 2-2: Classification of energy storage materials [51].....	36
Fig. 2-3: Annual range of ground temperature in Ottawa, Canada [58]	38
Fig. 2-4: Schematic of air handling unit	41
Fig. 2-5: Cooling water system at a commercial LDAC system at Queen’s University ..	42
Fig. 2-6: Simplified schematic operation of solar driven liquid desiccant air conditioner	44
Fig. 3-1: Schematic of basic TRNSYS model (dark blue, light blue, and green lines represent desiccant, cooling water, and weather data connections respectively; purple, and red lines represent heating water loop [8].....	48
Fig. 3-2: Minimum water vapour pressure of Lithium Chloride [70].....	51
Fig. 3-3: Cooling pattern of ECT and operating conditions over a single test day.....	55

Fig. 3-4: Schematic of cooling water storage system integrated with the liquid desiccant air-conditioning system	57
Fig. 3-5: Schematic of U-tube geo-exchanger integrated with the liquid desiccant air-conditioning system [78]	61
Fig. 3-6: 6000 liter CWS tank at Queen’s University.....	64
Fig. 3-7: Plan View and Details of the perforated single-pipe diffuser (PSD).....	65
Fig. 3-8: Queen’s University CWS tank instrumentation diagram.....	67
Fig. 3-9: Night cooling water storage (NCWS) system diagram.....	68
Fig. 4-1: Simulated average COP_R at different fixed relative humidity values determined using July 11 th weather data.....	71
Fig. 4-2: Results for July 11 th - Top: simulated values of average COP_T as a function of cooling water temperature and relative humidity; Bottom: Actual hourly and daily average values of COP_T measured over the day.....	72
Fig. 4-3: Results for July 17 th - Top: simulated values of average COP_T as a function of cooling water temperature and relative humidity; Bottom: Actual hourly and daily average values of COP_T measured over the day.....	73
Fig. 4-4: Results for July 23 rd - Top: simulated values of average COP_T as a function of cooling water temperature and relative humidity; Bottom: Actual hourly and daily average values of COP_T measured over the day.....	74
Fig. 4-5: Results for Aug 13 th - Top: simulated values of average COP_T as a function of cooling water temperature and relative humidity; Bottom: Actual hourly and daily average values of COP_T measured over the day.....	75
Fig. 4-6: Results for Aug 15 th - Top: simulated values of average COP_T as a function of cooling water temperature and relative humidity; Bottom: Actual hourly and daily average values of COP_T measured over the day.....	76
Fig. 4-7: Example of simulated process air inlet and outlet conditions (i.e., Condition 1: 70% RH; Condition 2: 60% RH) at different cooling water temperatures for August 15 th 2012.....	78
Fig. 4-8: Simulated average COP_T for each month and ΔT values at a fixed relative humidity of 65% in Toronto. The heat rejection technologies capable of producing each temperature are also shown.	80

Fig. 4-9: Simulated average COP_T for each month and ΔT values at a fixed relative humidity of 75% in Toronto. The heat rejection technologies capable of producing each temperature are also shown.	81
Fig. 4-10: Measured weather data for July 11 th , 2013 [8].....	82
Fig. 4-11: Simulated performance for 25 boreholes on July 11 th	90
Fig. 4-12: Tank stratification for ten hours of operation for on September 9 th	92
Fig. 4-13: Tank stratification for ten hours of operation on September 16 th	92
Fig. 4-14: Tank stratification for ten hours of operation on September 17 th	93
Fig. 4-15: Evaporative cooling tower operating condition and average efficiency for 8 th and 9 th of September	94
Fig. 4-16: Evaporative cooling tower operating condition and average efficiency for 15 th and 16 th of September	95
Fig. 4-17: Simulated average air cooling power and thermal COP for various cooling water flow rates on July 17 th	96
Fig. 5-1: Case A, thermal COP improvement for every three degree change in cooling water temperature for different operating days in Kingston.....	99
Fig. 5-2: Stored cooling energy at various storage volume.	101
Fig. 5-3: Improvement in system COP_T as a function of the number of boreholes as compared to the base case (ECT only system) for three reference days	103
Fig. 5-4: Improvement in system COP_E as a function of the number of boreholes as compared to the base case (ECT only system) for three reference days	103
Fig. 5-5: Cost of borehole storage based on 2006 estimates [83].....	104
Fig. 5-6: Electrical COP improvement comparison for case B and C for July 11 th	108
Fig. 5-7: Electrical COP improvement comparison for case B and C for July 17 th	108
Fig. 5-8: Electrical COP improvement comparison for case B and C for August 13 th	109
Fig. A-1: Schematic of heat and mass transfer in liquid desiccant conditioner.....	123
Fig. A-2: Schematic of inputs, outputs, and parameters for the TYPE251	127
Fig. A-3: Schematic of heat and mass transfer in internally heated regenerator	128
Fig. B-1: Schematic of components used for TRNSYS simulation validation.....	131
Fig. B-2: Schematic of liquid tank stratification nodes and heat and mass flow into and out of a node [67].....	133

Fig. B-3: Comparison of experimental and simulation stratification for September 16th.
..... 135

Fig. B-4: Comparison of experimental (EXP) and predicted (SIM) average water
temperature for three operating days in September. 136

Fig. B-5: Simulated average air cooling power and thermal COP for various tanks cooling
water flow rate on July 17th. 140

List of Tables

Table 3-1: TRNSYS components used in the base case simulation including the standard TRNSYS library TYPES and custom TYPES.....	49
Table 3-2: Effectiveness values used in TRNSYS simulation [8].....	52
Table 3-3: Input parameters used in Type 577.	62
Table 3-4: CWS Tank and PSD Characteristics	65
Table 4-1: Average value from day long operating condition.....	70
Table 4-2: Ambient air temperature variations from May to August [67]	79
Table 4-3: Summary of the CWS simulation applied to experimental data recorded for the LDAC system on July 11, 2012.....	83
Table 4-4: Summary of the CWS simulation applied to experimental data recorded for the LDAC system on July 17 th 2012.....	84
Table 4-5: Summary of the CWS simulation applied to experimental data recorded for the LDAC system on Aug 13 th 2012.	85
Table 4-6: Summary of geo-exchange (boreholes) simulation and experimental value from previous LDAC testing for 11 th of July	87
Table 4-7: Summary of geo-exchange (boreholes) simulation and experimental value from previous LDAC testing for 17 th of July	88
Table 4-8: Summary of geo-exchange (boreholes) simulation and experimental value from previous LDAC testing for 13 th of August.....	89
Table B-1: Summary of LD-SCWS simulation and experimental values from LDAC testing in summer.....	139

Nomenclature

Abbreviations

A/C	Air-conditioning
COP_E	Electrical coefficient of performance
COP_T	Thermal coefficient of performance
CWS	Cooling water storage
ECT	Evaporative cooling tower
EXP	Experimental results
GSHX	Ground source heat exchanger
LDAC	Liquid-desiccant air-conditioning
LD-WSECT	Water storage assisted evaporative cooling tower integrated with liquid desiccant air-conditioning system
LD-SCWS	Stratified cooling water storage integrated with liquid desiccant air-conditioning system
OAC	Open absorption cycle
SIM	Numerical simulation results
SCWS	Stratified cooling water storage
NCWS	Night cooling water storage

Variables

c_p	Heat capacity (kJ/kg·K)
h	Enthalpy (kJ/kg)
m	Mass (kg)
\dot{m}	Mass flow rate (kg/s)
T	Temperature (°C)
t	Time (s)
UA	Overall heat transfer coefficient (kW/K)

Subscripts

air	Process-air stream
amb	Ambient outdoor air
cond	Conditioner
cw	Cooling water
in	Inlet
ld	Liquid desiccant solution
out	Outlet

Greek symbols

$\epsilon_{\text{dehumid}}$	Dehumidification effectiveness
ϵ_h	Enthalpy effectiveness
$\epsilon_{\text{ld,cw}}$	Desiccant-cooling water effectiveness
ω	Humidity ratio ($\text{kg}_{\text{water}}/\text{kg}_{\text{air}}$)
ϕ	Relative humidity

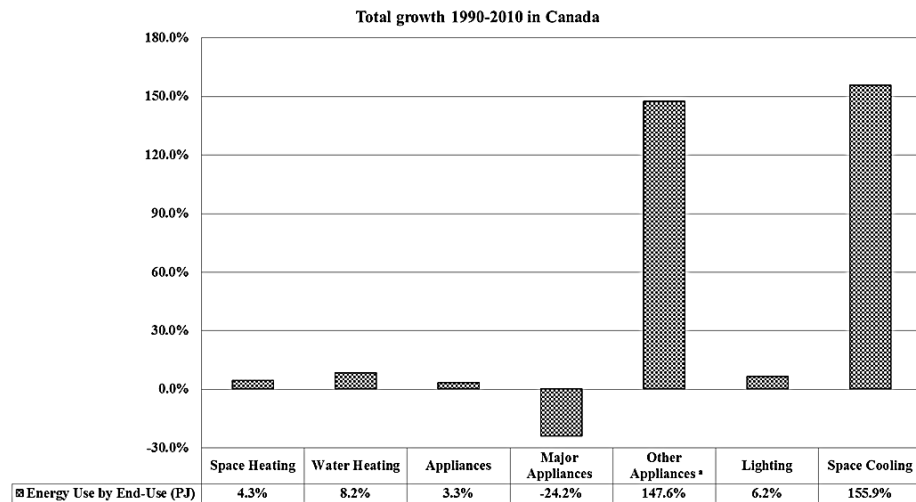
Chapter 1

Introduction

This thesis addresses alternative methods for rejecting heat from thermally driven liquid desiccant air-conditioning systems. Both analytical and experimental investigations were performed and are described in the following sections.

1.1 Background

Between 1990 and 2010, the total air-conditioned residential space area in Canada almost tripled from 267 to 788 million square meters [1]. This has increased the demand for space cooling systems and tripled the overall energy consumption of air-conditioning (A/C) units (Fig. 1-1). This demand also places a significant peak load on the electricity grid during hot summer afternoons and early evenings.



a) *Other Appliances* includes small appliances such as televisions, video cassette recorders, digital video disc players, radios, computers and toasters.

Fig. 1-1: Residential secondary energy use [1].

Heating Ventilation and Air-Conditioning (HVAC) systems are primarily used to control the temperature and humidity of a particular space and to provide adequate ventilation to ensure acceptable indoor air quality (IAQ) for the occupants or intended use. Maintaining a desired condition in a space will depend on the internal loads, ventilation requirements and local climatic conditions, and may require significant conditioning of the air to adjust temperature and relative humidity level.

In the case of building spaces that are intended for human occupancy, in addition to fresh-air ventilation requirements, it is recognized that both the temperature and relative humidity of the air in the space should be controlled to produce a comfortable environment. The American Society of Heating, Refrigerating and Air-Conditioning Engineers (ASHRAE) proposed acceptable ranges of humidity and temperature) in Standard 62.1 for non-residential spaces [2], and ASHRAE 62.2 for residences [3]. Acceptable values were defined for either summer or winter conditions, (Fig. 1-2).

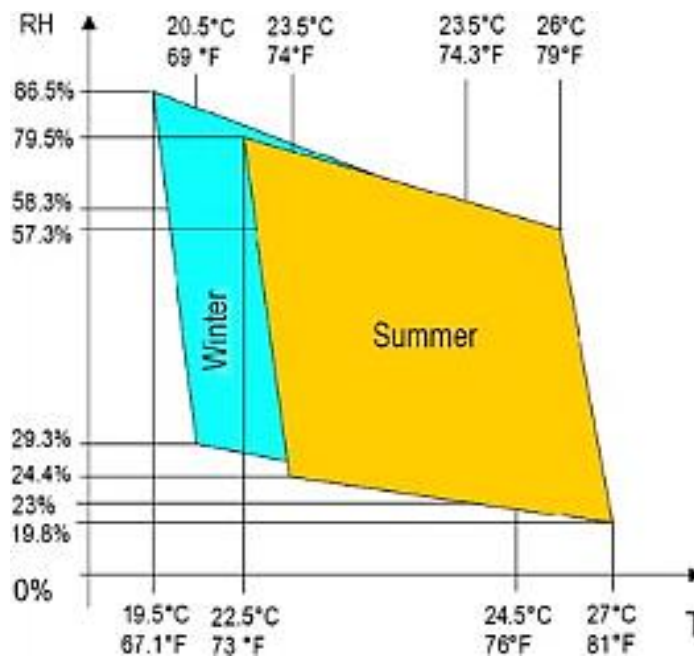


Fig. 1-2: Thermal comfort zone according [4].

Air-conditioning loads are a result of internal heat and moisture sources, and sinks, heat and moisture transmission through walls, and the infiltration of unconditioned air into the space. The energy demand associated with maintaining the desired air temperature, humidity and ventilation requirements within a conditioned space depends on the air-conditioning approach used. It can be estimated by determining the sensible loads (associated with maintaining a desired air temperature) and the latent loads (associated with maintaining a desired humidity level) in the conditioned space, accounting for the sensible or latent loads associated with outdoor air that has entered the space due to air leakage or ventilation requirements [5].

To quantify the energy load associated with a particular ventilation rate, the Ventilation Load Index (VLI) may be calculated. It can be used to indicate the proportions of sensible and latent cooling associated with a particular ventilation load. The Latent VLI and Sensible VLI, expressed in energy per unit flow rate of air (kWh/m³/hr) may be calculated according to Eq. 1.2.1 and 1.2.2 [6] i.e.,

$$\text{Latent VLI} = \int_0^{8760\text{hrs}} \frac{h_{fg} \rho_{air} (\omega_{air} - \omega_{set})}{3600} dt \quad (1.2.1)$$

$$\text{Sensible VLI} = \int_0^{8760\text{hrs}} \frac{Cp_{air} \rho_{air} (T_{air} - T_{set})}{3600} dt \quad (1.2.2)$$

where, ρ_{air} , ω_{air} , T_{air} , and Cp_{air} are ambient air density per volumetric flow rate (kg/m³/s), specific humidity (kg_w/kg_a), temperature (°C), and specific heat of air respectively. h_{fg} , ω_{set} , and T_{set} are the latent heat of condensation (kJ/kg), set-point humidity and temperature respectively, and 3600 is the conversion unit from kJ to kWh. The

ventilation load index is shown for a variety of locations, Fig. 1-3. An examination of typical weather conditions in humid climates shows that latent loads usually exceed sensible loads in ventilation air. VLC is useful for evaluating configurations, components and controls [7].

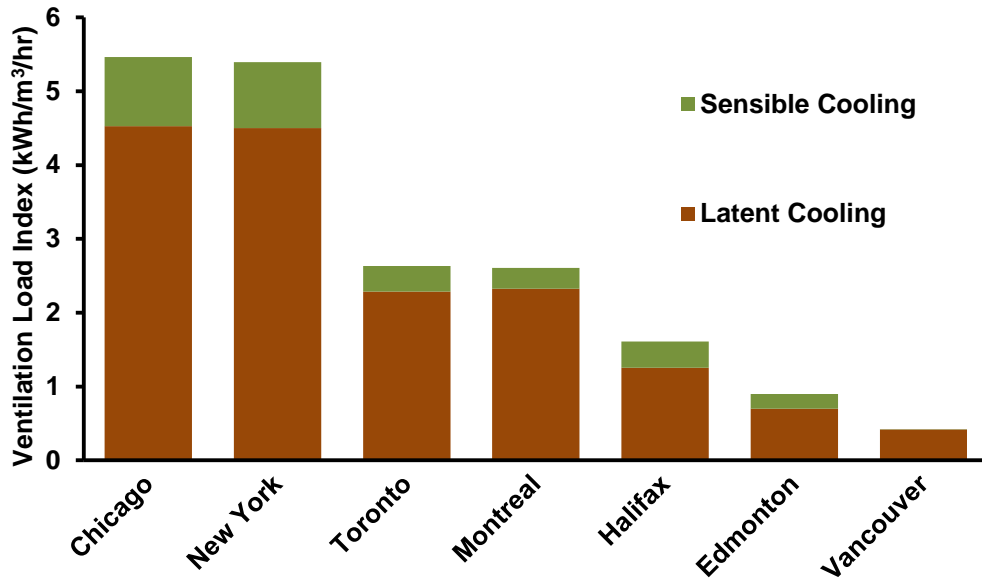


Fig. 1-3: Latent and sensible Ventilation Load Index (VLI) for several cities with a set-point of 24°C and 50% relative humidity [8].

1.2 Traditional Air-Conditioning Systems

The basic function of an air-conditioning unit is to control the temperature and humidity of the air within a conditioned space or to precondition ventilation air prior to its entry into the space. In traditional air-conditioning systems, a vapour-compression refrigeration unit [9] is used to cool room or ventilation air by passing it over a cooling coil. Depending on the types of A/C unit selected, the coils may be cooled by a refrigerant (e.g., direct-expansion vapour compression), or by chilled water produced by a central cooling plant or cold source.

Both sensible and latent cooling of moist air can be accomplished by heat removal. Sensible cooling generally involves the removal of heat from an air stream that only results in a reduction in temperature. This is most obvious for cooling of moist air above its dew-point temperature where the absolute or specific humidity level, ω , remains constant. Sensible cooling will result in the reduction of the dry bulb (DB) and wet bulb (WB) temperature of the air. Relative humidity, ϕ , will increase as heat is removed until the dew-point temperature of the air is reached (i.e., 100% relative humidity) without affecting the moisture content of the air. Further heat removal will result in the condensation of moisture from the air-stream and the removal of the “latent heat of vapourization”. This latter process is generally referred to as latent cooling or dehumidification and involves the removal of moisture from the air-stream. Both sensible and latent cooling by this technique involves the removal of heat from the air-stream with an associated reduction in enthalpy in the processed air (Fig. 1-4).

Air-conditioning by this process would result in the delivery of air at or near to 100% relative humidity. To achieve the required thermal comfort level in an occupied space, it is normal to mix this saturated air with dryer room air, or to reheat the air-stream to bring the relative humidity level back to recommended levels. A disadvantage of this reheating process is that it involves the supply of additional thermal energy to raise the temperature of the air-stream which is considered inefficient.

Decoupling of sensible cooling (i.e., temperature reduction) and moisture removal (i.e., dehumidification) has been used as an alternative method of maintaining a particular comfort level within a conditioned space. It has the potential to be more energy efficient and provide a more precise environmental control as it can avoid the reheat process often

required in conventional air-conditioning. To achieve this “decoupling” a variety of alternative air-conditioning approaches have been proposed. These are discussed in the next section.

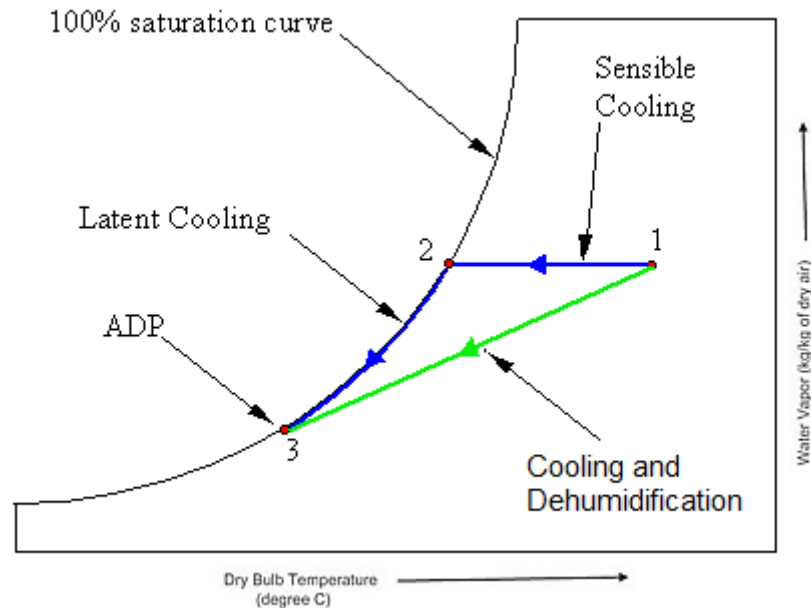


Fig. 1-4: Psychrometric charts showing sensible cooling, latent cooling, and cooling and dehumidification process.

1.3 Alternative Approaches to Traditional Vapour-compression Air-Conditioning systems

Numerous alternative approaches to traditional vapour-compression refrigeration exist and have been developed over time for air-conditioning applications. The most common approaches consist of thermally driven cycles that use a heat input to drive the refrigeration cycle rather than an electrical or mechanical gas compressor. The use of thermal energy to drive a cycle allows alternative fuels to be used including renewable energy such as solar heat or bio-mass or waste heat from industrial processes.

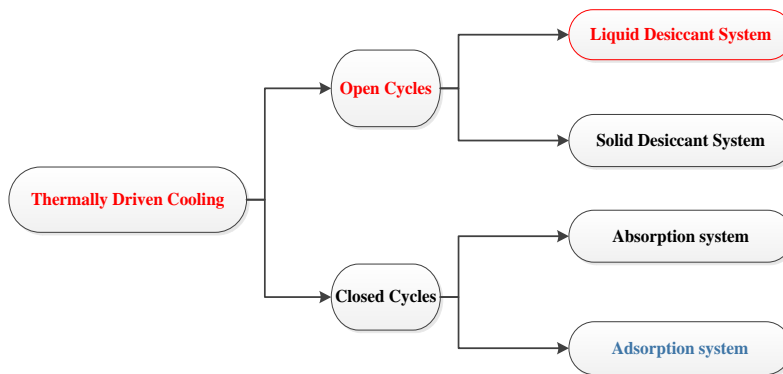


Fig. 1-5: Types of Thermal Driven A/C systems

As shown in Fig. 1-5, thermally driven cycles can be generally classified as open or closed cycles, however, closed cycle absorption systems are more common [10]. The primary difference between vapour-compression and absorption cycles is the nature of the compression process. Instead of compressing a vapour between the evaporator and the condenser by a mechanical compressor, the refrigerant of an absorption system (e.g., ammonia) is absorbed in an intermediate fluid (e.g., water). The solution is then pumped to a high pressure by a solution pump where heat is applied in a generator to liberate the refrigerant from the absorber fluid. The fluid is then drained back to the absorber sump and the refrigerant is circulated through a condenser (liberating heat) and an expansion valve, back to the evaporator, where heat is absorbed, Fig.1-6 [11].

For chilled water above 0°C, as it is used in air-conditioning, a liquid H₂O/LiBr or H₂O/LiCl solution may be used with water as a refrigerant. In these systems, the water evaporates at very low pressure in the evaporator and is absorbed in the absorber, thereby diluting the H₂O/LiBr or H₂O/LiCl solution. To improve the efficiency of the process, the absorber is usually cooled, and heat is applied in the generator. In effect the

mechanical compression process has been replaced by a chemical absorption process driven by thermal energy. The power consumed by the pump in the system is considerably lower than would be required by a mechanical gas-compressor. The detailed operation of an absorption chiller can be found in Moran et al. [9] and Herold et al. [12].

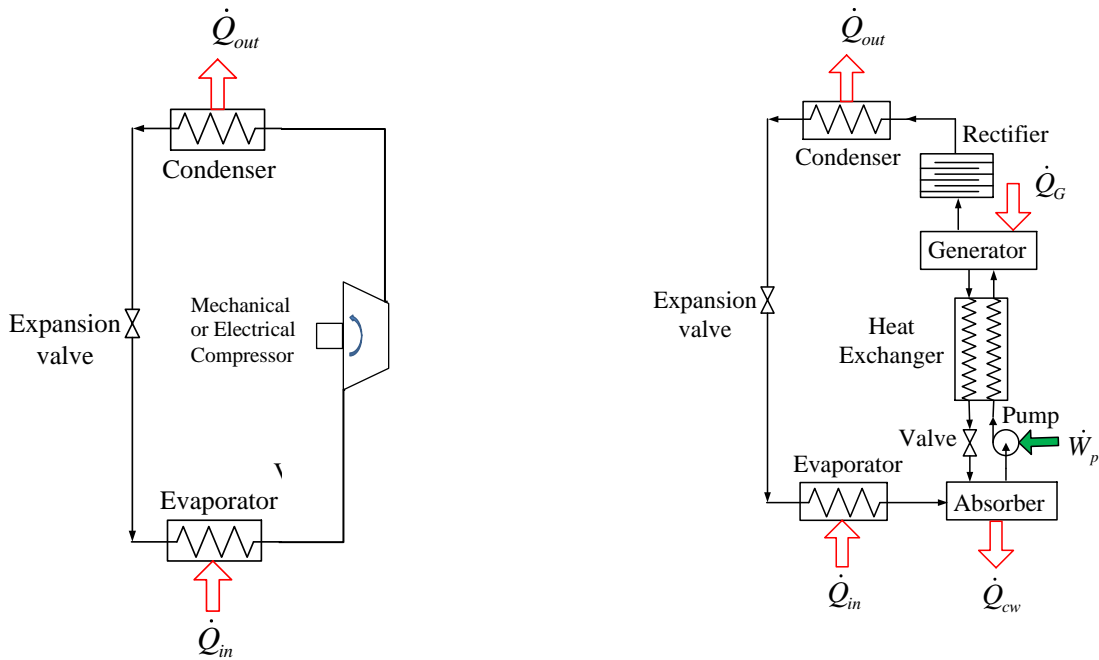


Fig. 1-6: LHS- basic components of a vapour-compression refrigeration unit; and, RHS- schematic of an absorption chiller [9]

The performance of absorption systems is governed by thermodynamics and is limited by the temperatures and pressures available in the cycle. The operation of absorption air-conditioning systems is similar to vapour-compression systems in that dehumidification is achieved by cooling the processed air to the dew point, followed by a reheat process. In addition, significant thermal energy is usually required to drive these cycles and higher heat rejection rates are required usually increasing capital cost and unit size.

Many commercial absorption chillers are available but their typical capacities are above 100kW. Most are supplied with district heat, waste heat or heat from co-generation and require a heat source temperature above 80 °C for single-effect machines or 140 °C for double-effect machines. The coefficient of performance (COP) for these machines ranges from 0.6 to 0.8. for single effect and up to 1.2 for double effect [10].

1.3.1 Open Cooling Cycles

There are a variety of open cooling cycles. For example, the reverse Brayton (i.e., Bell-Coleman) Cycle is used on jet aircraft to cool cabin air by expanding compressed air bled from the engine compressors. In the context of this thesis, however, we are concerned with open cycles in which outdoor ambient air, or air from a conditioned space, is brought into direct contact with a solid or liquid desiccant, (i.e., a hygroscopic material or solution) [13]. In this context, the term ‘open’ is used to indicate that the refrigerant (water) is discarded from the system after providing the cooling effect and new refrigerant (water) is supplied in its place in an open-ended loop. The cooling cycle is thermally driven and consists of a combination of evaporative cooling and air dehumidification by the desiccant [14]. A common technology uses rotating desiccant wheels, equipped either with silica gel or lithium-chloride as a sorption material (i.e., solid desiccant systems).

Closed cycles are classified based on whether liquid (absorption cycle) or solid (adsorption cycle) sorption is used in the cycle. The absorption/adsorption cycles involve two separate process loops coupled with heat exchangers and work under the same principle as the vapour-compression cycle. One loop is for the refrigeration process, and the other is for the rejection of heat from the cooling load.

The main difference between vapour-compression cycles and absorption cycles is the nature of the compression process. Instead of compressing a vapour between the evaporator and the condenser by a mechanical compressor, the refrigerant of an absorption system is absorbed by a thermal compressor which includes the absorber, and the solution pump. The solution circuit circulates from low pressure in the absorber to the high pressure in the desorber [11].

1.3.2 Desiccant cooling system

Desiccant cooling systems refer to solid or liquid desiccant systems that are used to transfer moisture from one airstream to another by using two components of the sorption process (dehumidification process) and desorption process (regeneration process). For this reason they are primarily used for dehumidification processes in air-conditioning applications. The main difference between solid and liquid desiccant systems is the regenerator system and the type of desiccant used. In the solid desiccant systems, the regenerator is constructed by using a thin layer of desiccant material, such as silica gel or molecular sieves deposited on a solid substrate mounted on the rotary disk. Regions of the disk are alternatively exposed to process and regeneration air streams (Fig. 1-7) [15].

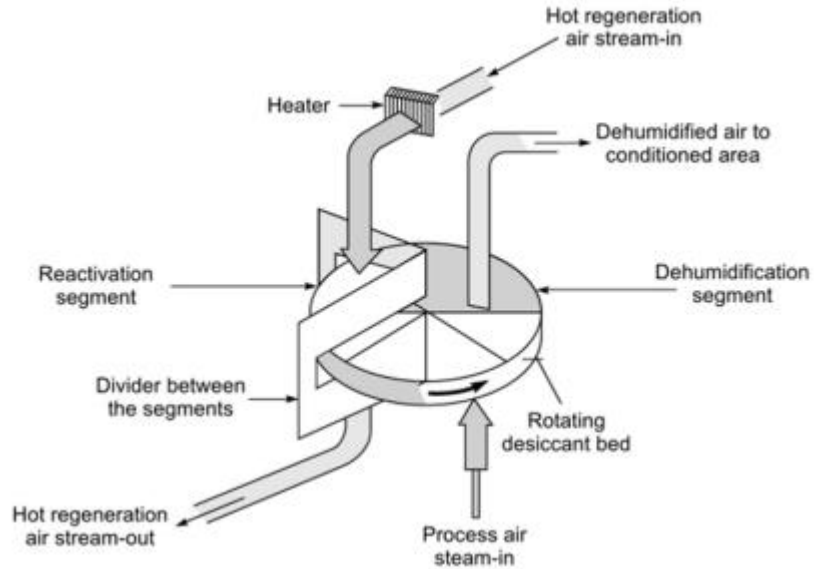


Fig. 1-7: Solid desiccant dehumidifier schematic [15]

A typical solid desiccant dehumidification process is shown on a psychrometric chart in (brown line). A concentrated solid sorbent (e.g., silicate gel) adsorbs the water vapour in the supply air during process (1-2') and increases in temperature due to the heat of condensation. The air is then cooled sensibly during the (2'-3') process (brown line). If further sensible cooling is required then an evaporative cooling process (3'-4) can be used to produce the desired temperature. Solid desiccant systems can be compact, less subject to corrosion and carryover of the desiccant into the airstream, however, solid desiccant systems do not provide practical options for storing of cooling capacity, a potential feature of liquid desiccant systems.

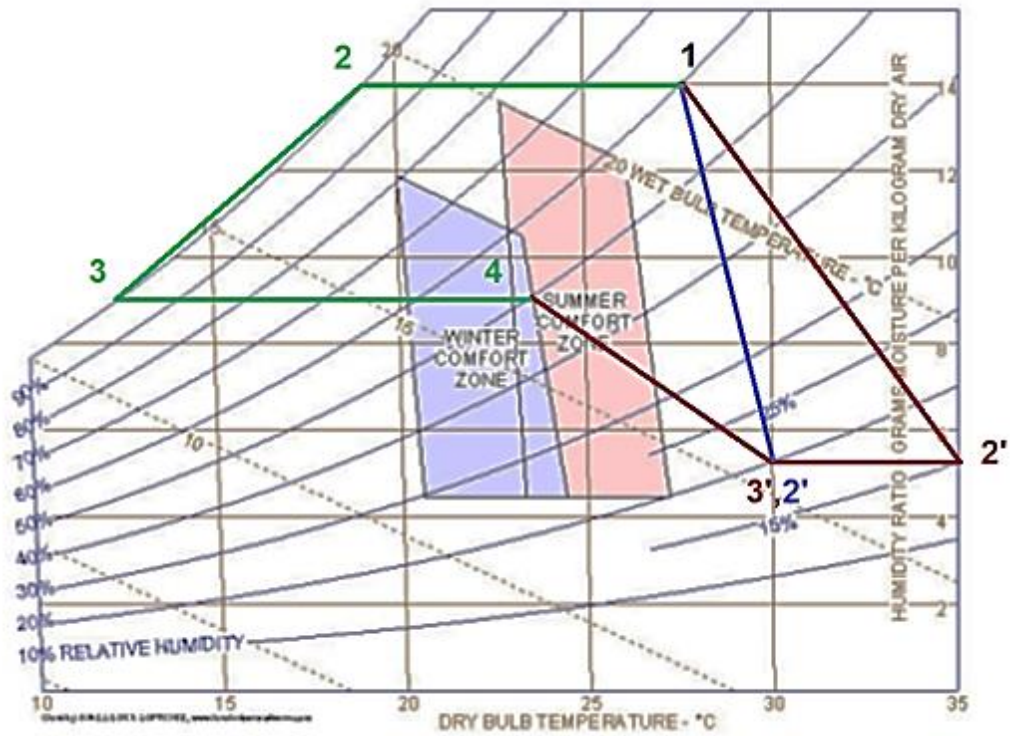


Fig. 1-8: Psychrometric chart of thermodynamic processes of: vapour-compression system (green line), solid desiccant (brown line), and liquid desiccant (blue line) [8].

Liquid desiccant systems operate on an open absorption cycle (OAC). The typical components of the OAC are the absorber and regenerator which are heat and mass exchangers. Desiccant solutions typically used are based on lithium chloride (LiCl), calcium chloride (CaCl), lithium bromide (LiBr) or triethelene-glycol [13]. The chemical dehumidification process is based on the water vapour removal from the process air at the surface of the desiccant due to the difference in the partial pressure of the water in solution and the partial pressure of the water vapour the air stream (P_v). The water vapour pressure is a function of both the temperature and concentration of the desiccant solution [14].

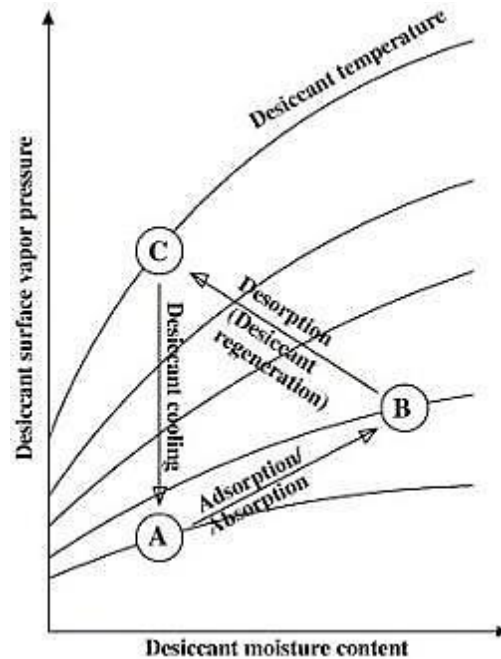


Fig. 1-9: Typical desiccant cycle [14]

The typical cycle of the desiccant in a dehumidification system is made up by three steps as shown in Fig. 1-9.

- A-B: an *absorption process* where cool, concentrated desiccant solution is brought into contact with humid air. Water vapour is absorbed into the desiccant solution diluting it and increasing its surface vapour pressure
- B-C: a *desorption process* where the dilute desiccant solution is heated, increasing its vapour pressure above a scavenging air stream. Water vapour is removed from the solution increasing its concentration and rejected in the air stream
- C-A: a cooling process in which the concentrated desiccant solution is cooled returning it to its original states so that the cycle can be repeated.

The process steps B-C and C-A constitute the desiccant *regeneration* process. To facilitate this cycle, a source of thermal input is required, as well as, a mechanism for rejecting heat. If the temperature of the desiccant in the absorber is not kept low enough, then the machine's latent cooling (i.e., dehumidification) capability will be reduced. Similarly, an adequate heat input is required to raise the temperature of the desiccant such the absorbed water vapour can be regenerated. In most commercial Liquid desiccant machines adequate performance can be obtained by heating the desiccant solution to relatively low temperatures, (i.e., 60 - 80°C). The initial temperature of the desiccant significantly affects its ability to absorb water vapor. Consequently, the apparent temperature and effectiveness of the heat rejection process is an important aspect of liquid-desiccant system performance. This heat rejection, desiccant cooling process usually relies on active cooling with a water stream, itself, cooled by rejecting heat to the surrounding ambient. This may present a significant disadvantage for this type of system as cooling is often required during period of high ambient temperature and humidity.

1.4 Thermodynamics of Air-Conditioning

Air-conditioning cooling systems are normally rated based on the coefficient of performance (COP) [9]. The coefficient of performance (COP) of VC refrigeration system is the ratio between the amount of heat absorbed and net power input (Eq.1.4.1).

$$COP_{vc} = \frac{Q_{in}}{W_c} = \frac{Q_{in}}{Q_{out} - Q_{in}} \quad (1.4.1)$$

This is also true for liquid desiccant cooling system; however, three common COPs are used to describe system performance: Thermal, which is based on the thermal cooling power output per unit of available thermal energy, Electrical, which represents the ratio of cooling power to electrical power consumption, and Regenerator, which is the rate of desorption per heat input, e.g., [16]:

$$COP_T = \frac{\dot{Q}_{total,cooling}}{\dot{Q}_{heat,in}}; \quad (1.4.2)$$

$$COP_E = \frac{\dot{Q}_{total,cooling}}{P_{el}}; \quad (1.4.3)$$

$$COP_{regenerator} = \frac{Q_{Desorption}}{Q_{heat,in}} \quad (1.4.4)$$

For thermally driven air-conditioning systems such as liquid desiccant systems, COP_T are typically low [17] (i.e., 0.25 – 0.7) means that during operation significant heat must be supplied per unit of cooling (dehumidification), This is normally tolerated as their low operating temperature requirement means that waste process heat or alternative energy may be used as a source. The low COP_T also means that a significant amount of heat must be rejected during operation putting additional strain on the heat rejection equipment. In conventional vapour-compression systems COP_E is the primary measure of performance and these systems are able to typically operate at COP_E ranging from 1.5 to 4 depending on conditions [18].

These values underline an important fact. For thermally driven air-conditioning to be competitive with vapour-compression systems, it is imperative that their COP_E be significantly lower than a similar capacity vapour-compression system.

Recent research on a prototype LDAC unit at Queen's University [8] has recently shown that power consumed in the pumps and fans associated with the heat rejection equipment (i.e., cooling tower) is significant and overall COP_E are lower than expected. Similar results have been reported by other researchers as described in Chapter 2.

1.5 International Energy Agency Task 38

Recognizing the potential benefits of improved heat rejection strategies, the International Energy Agency (IEA) established Task 38 to promote international collaboration to address this problem.

According to IEA road map report, the current thermal cooling systems require optimized, thermally-driven cooling cycles (sorption chillers and desiccant systems), with higher coefficients of performance (COP_T and COP_E), lower cost and easier hybridization with other waste heat, backup heating and backup cooling technologies. The IEA technology roadmap recommends $COP_E > 10$ for the whole system and standardization of solar thermally driven cooling technology by 2020 [19]. Therefore, one of the major goals of this project is to develop techniques that result in improving COPs.

According to the solar heating and cooling Task 38, the main aspects of technical problems associated with heat rejection are [20]:

- Evaporative cooling towers often consume too much electric power. Investigations of realized systems show that up to 50-60 % of the total

electrical consumption is used in the heat rejection system, depending on the type and design of the system. Small capacity ECTs are relatively expensive and require high-maintenance.

- Dry coolers consume more electricity than ECT due to larger fan and air pressure drop.
- Hybrid systems (dry/wet) seem to be a promising solution, but very few systems are available on the market and they are expensive.

1.6 Problem Definition of the LDAC System

1.6.1 Cold Water Supply

As mentioned previously, thermal COP of the system depends on the ratio of the total cooling power to the heat input. The total cooling capacity and COP_T of a LDAC also depend on: the type of desiccant used, its concentration and temperature, the unit's thermal design and the temperature of the heat supply and rejection sinks.

The high relative humidity of the ambient air results in a reduced cooling rate of water. The higher inlet humidity reduces the amount of water that can be evaporated from the cooling water (due to increased vapour pressure of air) thus reducing the heat rejection rate and the cooling performance of the evaporative cooler. The air that leaves the direct evaporative cooler typically has 80-90% relative humidity [21].

Higher temperature cooling water will be less effective at reducing the desiccant vapour pressure which leads to a reduction in absorption rate. Therefore, replacing the

direct evaporative cooler with other available techniques depends mainly on heat sink temperature, cooling capacity, and cost.

1.6.2 Electrical Consumption

A liquid desiccant air-conditioner has the potential of achieving a high electrical coefficient of performance (COP_E) resulting in lower electrical energy consumption. Unfortunately, the twenty days of operation of a commercial LDAC at Queen's has revealed that the electrical COP_E was up to 2.42, which is lower than expected [8]. This is a result of high energy consumption of pumps and fans associated with the operation of the unit. In particular, power consumption associated with the rejection of heat from the unit is significant and severely reduces the advantages of the unit. Cooling towers often consume significant amounts of electricity and are often not modulated under partial loads. An investigation of the existing LD air-conditioning system [8] at Queen's University shows that up to 40-50 % of the total electrical consumption in these systems is used for heat rejection. This is shown as the separated sections in Fig. 1-10.

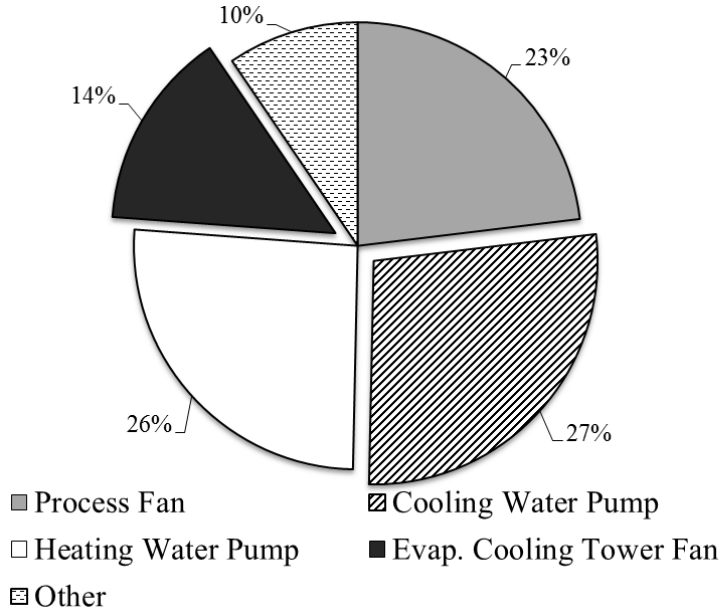


Fig. 1-10: Electrical power consumption of LDAC system components [22].

An alternative approach to reducing demands on the “grid-supplied” electricity is to power fans with photovoltaic modules. Recent cost reductions in PV solar cells have made this a promising alternative if access to sunlight can be achieved. The focus of this research is to identify and compare the most promising cooling methods to replace the ECT in the existing Queen’s system.

1.7 Available Cooling Water Technologies

Thermally driven cooling systems have a strong dependence on the heat rejection capacity and the heat sink temperature. In the case of utilizing wet cooling towers and dry coolers for heat rejection; their effectiveness depends on ambient air temperature and humidity levels respectively. The ultimate feasibility of replacing a direct evaporative (i.e., wet) cooler with other available options, such as dry coolers, geothermal sinks,

natural ventilation circulation, or spray ponds will depend on their capacity, heat sink temperature and cost.

If the heat sink is ambient air, given the ambient conditions, the lowest cooling water temperatures are based on either the wet bulb temperature, in the case of evaporative cooling (latent cooling) or the dry bulb temperature (sensible cooling), in the case of dry cooling.

If the heat sink is the earth, the cooling water temperatures supplied to LDAC unit would be close to the average annual ground temperature [23]. The different options available to replace an open wet cooling tower are shown Fig. 1-11.

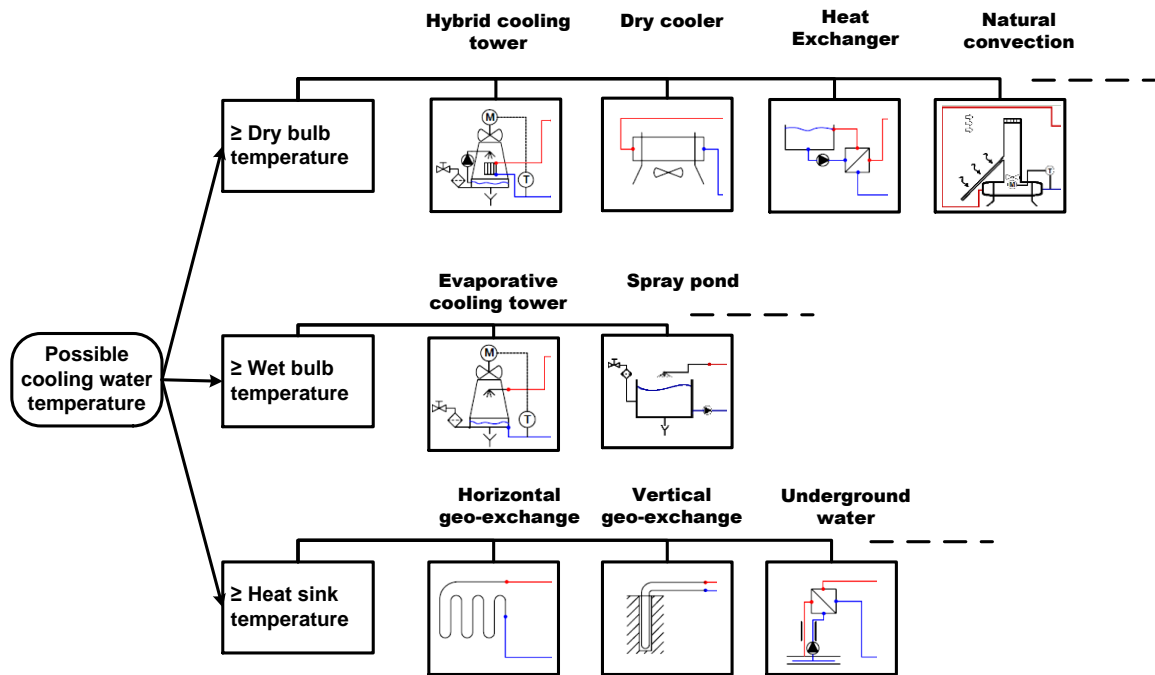


Fig. 1-11: Different techniques for rejecting heat from air conditioning systems

There are many cooling water techniques that can be considered as the most promising methods of cooling. The cold water that enters the air handling unit has a high mass flow rate ranging from 7200- 10800 (kg/hr), and it continuously operates for at least ten hours per day. The previous experimental data (taken in 2012) taken for the hot water leaving the conditioner indicates a temperature range of 25-35°C. This range in temperature eliminates the possibility of using hot water for heating applications. Other barriers for selecting cooling technologies are operational cost, technical feasibility and space limitations. Therefore, this study investigates the effect of heat sink temperature range on cooling performance and offers the most promising cooling devices.

1.8 Objective, Approach, and Scope

This project builds on previous studies conducted by Jones [24] and Crofoot [8] on the solar LDAC system at Queen's University. These studies indicated that the LDAC system's performance could be improved and that the heat rejection sub-system was a key weak point of the system.

This study analyzed the effect of the heat rejection sub-system on the overall system's performance and then, based on these results, identified and analyzed new heat rejection sub-systems to improve the overall performance.

The primary objective of this study was to improve the LDAC system's COP_E by investigating alternative heat rejection strategies that could reduce the power consumption of the system. There was a strong focus on the COP_E because, in theory, this is suggested as one of the LDAC system's main advantages over a traditional vapour compression HVAC system.

Although the COP_E was the chief concern, there were other performance metrics that also showed room for improvement. This led to the secondary objective: i.e., to investigate the effect of the heat rejection system on the thermal performance of the LDAC system (i.e., COP_T).

A structured approach was used to achieve these objectives. Firstly, an extensive literature review was conducted to determine what alternative heat rejection strategies could be used in this application and what their expected performance could be. The weather data gathered from the system's operation in 2012 was then used in a system scale TRNSYS model of the LDAC system to determine the effect of the cooling water temperature on the LDAC systems performance. The temperature ranges of the different heat rejection systems were then studied to identify the most promising concepts. These approaches were then integrated into the TRNSYS model and simulations run to determine the effect of several critical parameters on the overall system's performance. Where possible, experimental data was used to verify the simulation results. This approach is shown in the flow chart, Fig. 1-12.

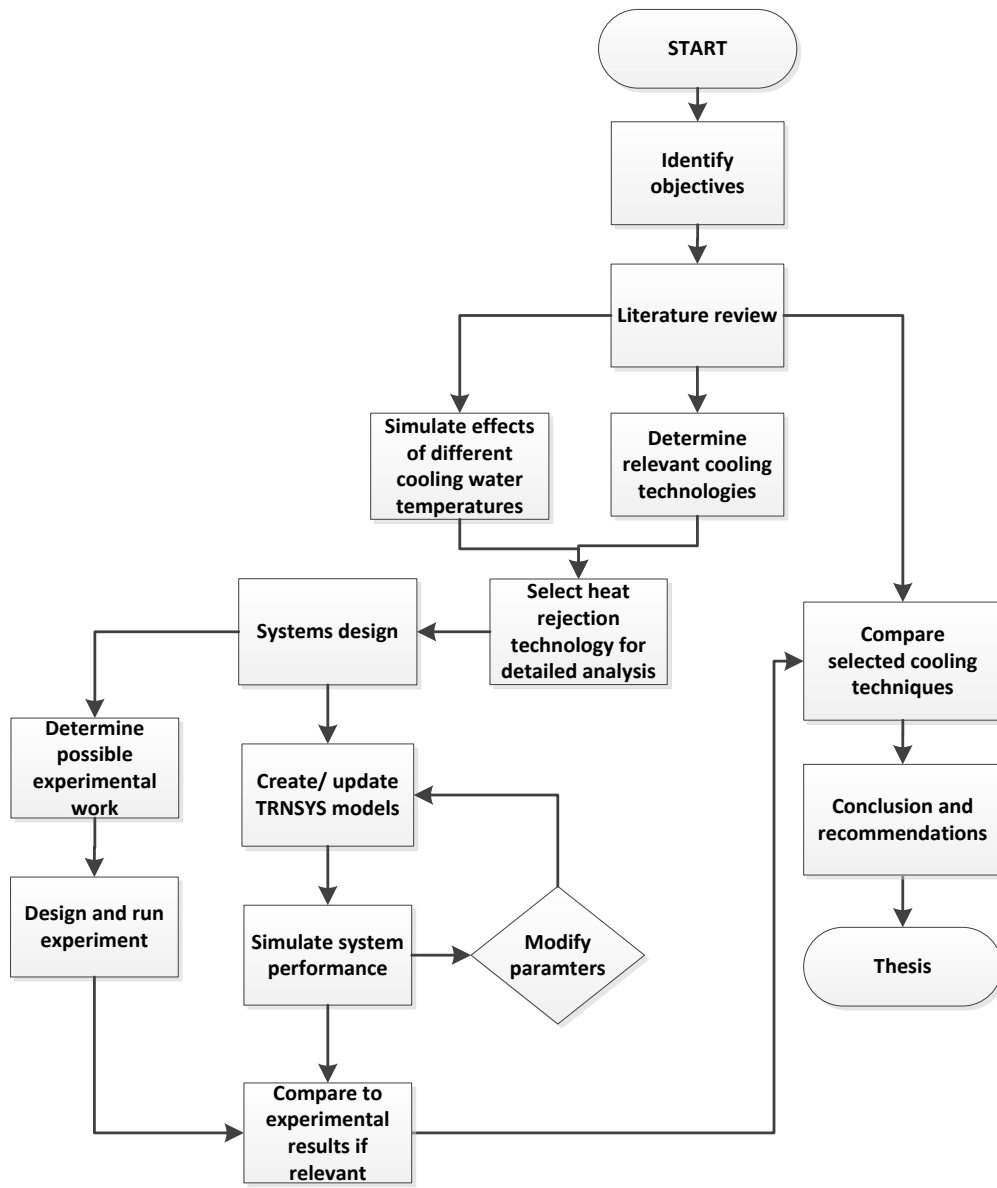


Fig. 1-12: Flow chart of research method

The scope of this research included only the heat rejection technologies that would be applicable to the LDAC system at Queen's University. There are many of methods of heat rejection possible in other applications (e.g., using cool lake or ocean water in coastal installations, or using radiative cooling in space stations), that will not be studied as part of this research. this research will also be limited to that the local climate of Kingston Although this analysis was conducted for the Queen's LDAC system, the results have applications to other thermal cooling and A/C systems that currently rely on traditional evaporative cooling systems.

1.9 Format and Thesis Organization

The format used in this thesis follows the guidelines laid out in the Queen's University, School of Graduate Studies, Traditional Manuscript Format. The chapters of this thesis were arranged and organized as follows:

- Chapter 1 provides a background on air-conditioning and heat rejection technology as well as the purpose, the objectives and the outline of the present work.
- Chapter 2 is a review of relevant previous research on related technologies with the overall goal of providing context for the reader to aids their understanding of the present work.
- Chapter 3 describes the modeling software, the various simulations, and the experiments conducted for this study.
- Chapter 4 presents the results of the simulations and experiments described in Chapter 3

- Chapter 5 provides a discussion of the results and compares the heat rejection systems' performance
- Chapter 6 contains the overall conclusions and gives recommendations for future studies.

Chapter 2

Literature Review

As described in the previous chapter, the performance (i.e., COP) of an air-conditioning unit can be improved by reducing the electrical consumption associated with heat rejection and by lowering the temperature required for heat rejection. This is particularly evident for thermally driven air-conditioning systems that typically have lower thermal COP's, meaning that greater quantities of heat input and rejection are required for a particular cooling capacity. As well, this implies that greater heat transfer rates are required to limit temperature differences across heat rejection equipment and to the surroundings. In typical applications this is usually accomplished by using forced convection and extended surface areas (e.g., finned surfaces). Unfortunately, fan power required for these solutions is typically large, leading to lower electrical COP's.

As described in Chapter 1, efforts are underway to identify alternative approaches to allow for heat rejection with reduced power consumption. With these new heat rejection strategies, it should be possible to reduce the electrical consumption associated with heat rejection for the Queen's Liquid Desiccant Air-Conditioning unit (LDAC).

As a first step in the evaluation of alternative approaches to heat rejection in thermally driven AC, review of relevant literature was conducted to investigate the most common heat rejection methods (with a focus on studies related to desiccant absorbers) and to identify cooling technologies for further study. In addition, previous work on the effects of heat rejection temperature on system performance was reviewed in an effort to identify its impact on LDAC performance.

2.1 Heat rejection for Desiccant Absorber Designs

Basic thermodynamics indicates that it is necessary to reject heat to sustain a continuous cooling cycle. As well, it has been shown that systems that have to reject heat to a higher temperature “sink” will operate at a lower performance level. This is particularly important for thermally driven absorption systems as they tend to operate at lower COP_T meaning that they must reject more heat per unit of cooling than comparable vapour-compression systems that operate at higher COP’s.

This is true for liquid and solid desiccant dehumidification systems that rely on “cooling” a desiccant in a dehumidifier (i.e., absorber) to increase its ability to absorb moisture. In most commercial LDAC systems, the desiccant is indirectly cooled by a water circulation loop chilled by an evaporative cooling tower. The desiccant is “regenerated” by heat addition to a “conditioner” where absorbed water vapour is rejecting to an exhaust air stream.

For continuous operation of an LDAC unit, a source of cooling is required. To maintain moisture absorption rates, low cooling water temperatures and effective heat rejection are needed. This is usually accomplished by increasing external heat transfer area and rates, and by lowering the heat sink temperature. Various strategies for heat rejection have been used and these are reviewed in the following sections.

2.1.1 Dry coolers

One of the simplest forms of heat rejection is the dry-cooler. In a dry-cooler the refrigerant (of a vapour-compression system) or an intermediate heat transfer fluid (in the case of thermally driven AC equipment) is used to reject heat from the AC unit. Heat is rejected from the heat transfer fluid by heat conduction through the walls of an array of

tubes exposed to the ambient air. To enhance heat transfer on the air-side of a dry-cooler, finned surfaces are added to increase the surface area, thereby compensating for the relatively low heat transfer rates associated with the air-side. Although, dry coolers can rely on natural convection on the air-side, they typically use “forced” (i.e., fan driven) convection. This increases heat transfer rates on the air-side and lowers the temperature difference between the fluid and the ambient air. Dry coolers come in many configurations and use various fin-tube arrangements to: maximize overall heat rejection; reduce overall size and cost; and, reduce pressure drops on the fluid- and air-sides to lower pump and fan power consumption [25].

Advantages of dry coolers are:

- they are relatively inexpensive, robust and do not require extensive maintenance;
- the working fluid can be a refrigerant or freeze-protected fluid (e.g., water/glycol solutions) allowing winter operation;

Dry coolers to have significant disadvantages, however, including:

- fan power consumption may be high, particularly if it is desired to keep the temperature as low as practically possible;
- heat rejection is only possible to the ambient-air dry-bulb temperature which may be high during times of high cooling demand;
- in the case of thermally driven AC units such as liquid desiccant systems, the use of an intermediate heat transfer fluid that requires the use of a heat

exchanger that lowers overall heat rejection capacity and effective “sink” temperature.

These limitations may be severe in the case of thermally driven AC (e.g., absorption or liquid desiccant systems, etc.) as the overall COP_T of these unit depends on the cycle heat rejection temperature and the COP_E depends on the units electrical consumption including pump and fan power.

Dry cooler technology is well established and design criteria is extensively described in various handbooks and guides [26]. Literature on their use in LDAC systems is limited however the work of Khan [27] numerically investigated an internally-cooled LDAC that used a tube-fin heat exchanger in a cross-flow configuration to reject heat. He simulated the load removal performance using the different absorber dimensions with different cooling water temperature (5 to 30°C), and found that total load removal (kJ/kg) reduced by 63% - 56%.

Bansal et al. [28] investigated the performance of a structured packed-bed dehumidifier with and without internal cooling using water. Their results indicated that the maximum COP_E achieved was between 0.55-0.70 for internal cooling, and 0.38-0.55 without cooling for the same range of operating parameters.

MD et al. [29] compared an air-cooled absorption chiller system with a water-cooled system and found air-cooled absorption chiller systems have higher outlet, absorber, and condenser temperatures than the water cooled systems. This results in higher desiccant concentrations, lower absorption rates and the potential of harmful crystallization of the desiccant.

Similarly, Yoon and Kwon [30] simulated a double effect absorption system using air as the cooling medium for the heat rejection system. In their study, they varied the cooling air inlet temperature from 28 to 40 °C and concluded that COP_T reduces by 16% as the cooling air inlet temperature increases.

Izquierdo et al. [31] tested a commercial air-cooled absorption chiller. In this system, the heat was rejected to the environment by a water-air finned tube heat exchanger and a fan. They found the performance and the average COP_T were 4.5 kW and 0.49 respectively. Similarly, González-Gil et al. [32] tested air-cooled Li/Br absorption system and obtained a COP_T of 0.6 and cooling capacity of 2-3.8 kW.

Dry coolers continue to be used in small AC units as condensers and as an alternative to wet-cooling towers but their impact on thermal system performance can be significant particularly during times of high ambient temperature.

2.1.2 Evaporative Cooling towers

Evaporative cooling towers (ECT) are widely used to reject heat from commercial air-conditioning equipment. Typically, an indirect water circulation loop sends heated water to the cooling tower where it is sprayed into a natural or forced circulation of ambient air. In contrast to dry coolers (that do not allow evaporation of the circulation water), evaporative cooling towers are designed to facilitate the evaporation of a portion of the cooling water. In this process, the latent heat of evaporation, is removed from the remaining fluid stream, cooling it. The cooled fluid is captured in a “sump” and pumped back to the AC unit. The water volume lost due to evaporation is added to the sump as “make-up water”. This latent heat exchange produces high heat transfer rates and allows the fluid to be cooled below the ambient dry-bulb temperature. The “direct contact”

between the cooling water and the ambient air stream, allow the heat transfer area and fan power to be reduced relative to a similar capacity dry-cooler. In addition, dry coolers are limited to heat transfer to the dry-bulb temperature that is always higher than the wet-bulb temperature except at the dew-point [25].

Although compact and effective, ECTs do have some major drawbacks:

- high ambient humidity will decrease the capability of the evaporative cooler (due to the higher dew point temperature) exactly when the latent air-conditioning load is high;
- cooling towers must be drained to protect them from freezing during the winter months;
- the fact that the circulation water is in direct contact with the ambient air, means that the water may become contaminated by atmospheric constituents or be subject to biological fouling.
- as water is consumed by the evaporation process (e.g., approx. 1% for each 7°C), make-up water will be required and may have to be chemically treated to avoid fouling [33];
- ECTs have been identified as a source for the growth and spread of Legionnaires' disease due to their normal operational temperature that is optimum for growth of the bacteria. For this reason, strict operational protocols must be followed and frequent bacterial testing conducted; increasing operational and maintenance costs [34] [35].

Even with these considerable drawbacks, ETCs continue to be widely used and studied due to the lack of alternative technologies. For example, Qi and Lu [36] studied the performance of an internally cooled/heated LDAC system equipped with an ECT in Hong Kong. Their system was designed to handle the entire building latent load by dehumidifying the fresh air used in the ventilation system. Monitored results recorded for a May to October period revealed that the cooling tower's capacity was limited by the high humidity of the ambient air during that period. Moreover, they reported that adding an auxiliary cooler for the desiccant solution entering the dehumidifier could effectively reduce energy consumption of chiller by 20–30%.

Gommed and Grossman [37] experimentally tested a LDAC system with an ECT in a Mediterranean climate. They monitored the performance of the nominal 16 kW dehumidification system for five summer months (May–November) under various operating conditions. The data analysis indicated that an average COP_T of 0.8 was achieved using a cooling tower that supplied water for heat rejection at 22–27 °C.

Kessling et al. [38] simulated an internally cooled LiCl dehumidification system combined with an evaporative cooler for heat rejection. The focus of their research was on the absorption of moisture into the LDAC at different desiccant mass flow rates. Hartmann et al. [39] combined an evaporative cooler with an adsorption chiller to provide cooling for a solar thermal system and PV system. The performance of these two systems was then compared to a reference system which consisted of a compression chiller.

Jones [40] tested the low-flow LDAC system at Queen's that is equipped with an ECT and found total cooling power varied between 4.3 kW– 22.8 kW and COP_E of the system varied between 0.58– 4.48.

Similarly, Crofoot et al. in 2012 [8] found that high relative humidity decreased the rate of mass and heat transfer inside the ECT, resulting in high cooling water temperatures (19-28°C) being supplied to the conditioner. The high cooling water temperature decreases the rate of absorption, which is reflected by a lower COP_T of the system. Fig. 2-1 indicates this effect for various degrees of relative humidity.

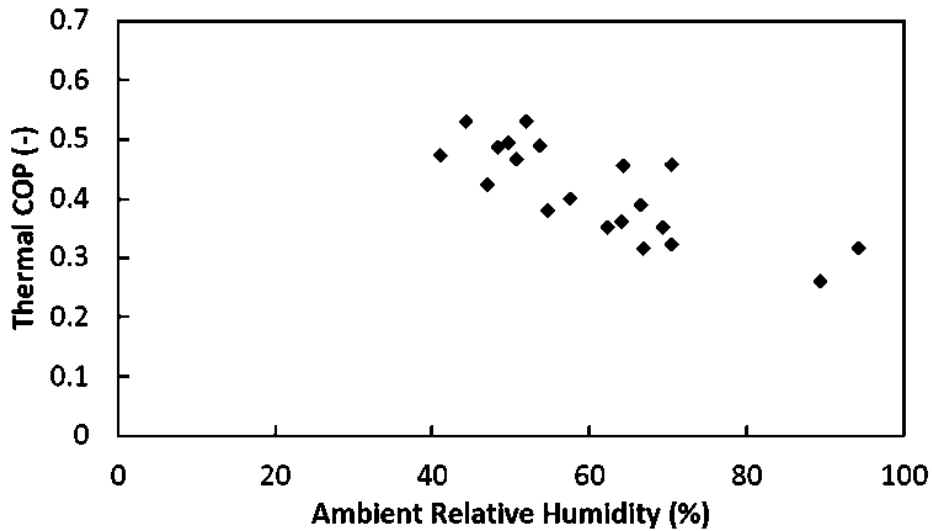


Fig. 2-1: Thermal COP and ambient relative humidity [8].

2.1.3 Cold Storage

As an alternative to the on-demand use of a wet or dry-cooler, cooling potential can be stored in the heat rejection cooling loop for use during peak load periods. There are two options for cold storage operation: full storage and partial storage. For full storage operation, the complete chilled water demand is met by the cooling water storage during peak hours. In contrast, partial storage utilizes both the cooling storage and another cooling device [41]. A thermal storage system can reduce the electric demand of a LDAC system and partially, or fully, shift the electric energy consumption from peak hours to off-peak hours (i.e., load shifting) and therefore reduce operating costs.

There are three main methods of cold storage: phase change materials, ice, and chilled water. These will be discussed in the following sections.

2.1.3.1 Cold Water Storage (CWS)

Cold water storage tanks can store sensible cooling capacity during off-peak hours and provide cooling capacity for the absorption process during periods of high cooling demand and peak hours. This was confirmed by Fields and Knebel [42] who tested applications of over one hundred cold storage systems and found a reduction in energy consumption and operational cost. Additionally, it was found that these systems can improve indoor air quality due to constant lower relative temperature during night hours; they also provide lower initial and maintenance costs in comparison with non-storage mechanical chilling systems. Similar results were found by Sebzali and Rubini who investigated the impact of using water storage on an air-conditioning system and concluded that this system can reduce the peak electrical load up to 100% [43].

The cold water storage also can be integrated with other components or cooling devices to extract additional heat during off-peak periods. Ayadi et al. [44] tested a LiBr/water absorption chiller with 17.6 kW cooling power and COP of 0.7 at nominal operation temperature. In their study, they used a cooling tower for the absorber and a 1000 liter, cold water storage coupled with a heat pump for the evaporator. They found an average COP_T of 0.55 and COP_E of 4 for summer operation. Agyenim et al. [45] tested a 4.5 kW LiBr/H₂O absorption chiller with a 1000 liter cold storage tank and a 6 kW fan coil. They found an average COP_T and COP_E of 0.58 and 3.6 respectively.

Cold water storage can reduce the cooling water temperature during operation of LDAC systems. Yin et al. [46] experimentally tested an internally cooled/heated

conditioner/regenerator liquid desiccant system. They utilized a water tank and chilling unit to provide cold water for the conditioner. The results indicated that the dehumidification efficiency decreased from 0.75 to 0.3 as the cooling water temperature increased from 20.5 to 24.5°C. Desiccants at low temperatures should have higher mass transfer coefficients (due to lower vapour partial pressure). Zhang et al. [47], Gao [48], and Liu et al. [49] also tested an internally-cooled LD system and reported the same effect of cooling water temperature on dehumidification performance.

2.1.3.2 Phase Change Materials (PCMs)

Thermal energy can be stored in phase-change materials. A phase change material will absorb the “heat of fusion” as it changes phase from a solid to a liquid providing sensible cooling capacity or to store thermal energy. Unlike sensible storage, PCM’s may provide a higher storage density over a small temperature range. PCMs can be encapsulated in plastic containers and arranged to provide a reduced storage volume when compared to chilled water [50].

In 1983 Abhat [51] gave a useful classification of phase change materials used for Thermal Energy Storage (TES). Depending on the application, the PCMs should first be selected based on their melting temperature. Materials that melt below 15 °C are typically used for cold storage in air-conditioning applications [52].

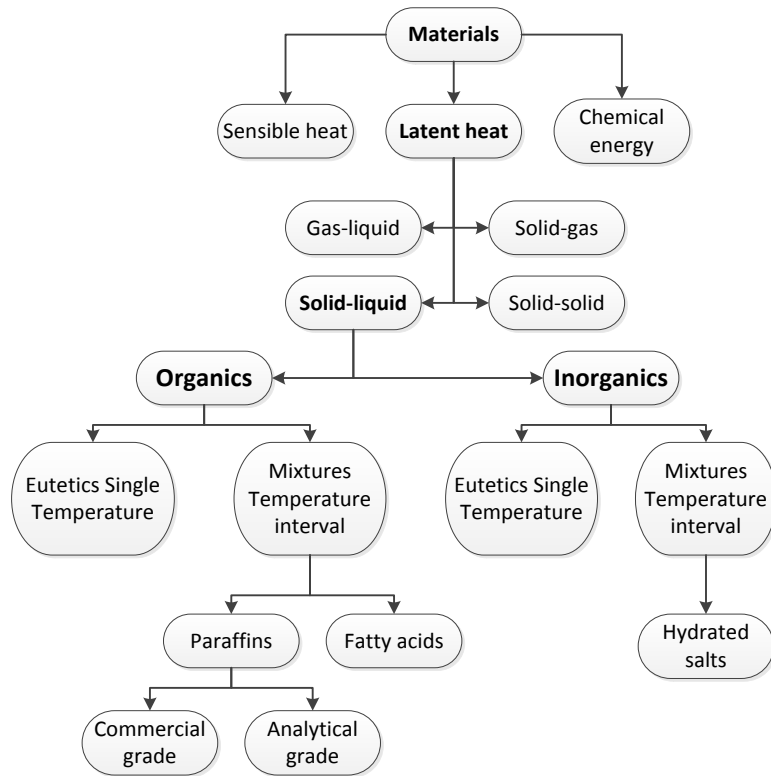


Fig. 2-2: Classification of energy storage materials [51]

A wide range of thermo-physical properties (e.g., melting point, heat of fusion, thermal conductivity, and density) of PCMs have been studied by different researchers and their potential use for thermal storage has been summarized by Manish and Rathod [53]. The most common mixture used for PCM cool thermal storage is a combination of inorganic salts (e.g., Eutectic salts), water, and nucleating and stabilizing agents which melt and freeze at 8.3°C (47°F) [54].

PCMs are primarily used for latent heat storage and therefore are effective for load shifting applications. Helm et al. (2009) [55] used latent heat storage in conjunction with a dry cooling system to reject heat from a LiBr solution-based absorption cooling system. In their system, heat rejection from the chiller is shifted to periods with lower ambient temperatures. It was found that the volume of the storage was decreased tenfold

when compared to conventional cold water storage systems. In later research, Helm et al. (2014) [56] simulated and compared a dry cooler with and without latent heat storage for an absorber chiller operating under different climatic conditions. The results indicated that a dry cooler using a phase change material (PCM) can increase system efficiency up to 64% in comparison with a system using solely dry cooling.

An ice based storage system is considered a form of phase change storage and may be considerably more compact than single-phase (i.e., liquid) water storage. For example, ice-based storage has a typical cooling storage density of 0.019 to 0.027(m³/kWh), which is 80-90% smaller than a comparable cold water tank and 50-70% smaller than a PCM storage tank [35].

The selection of the sensible heat storage tanks for thermal applications was studied by Dincer et al. [57]. In this study, they reported that cold water storage requires almost ten times more volume than ice storage and the selection of storage tank depends on the diurnal or seasonal operating time.

Unfortunately, ice-based storage systems require refrigeration equipment to provide the cooling capacity to produce ice. Electrical reciprocating, screw scroll or multi-stage centrifugal chillers, and gas reciprocating chillers are normally used to produce ice for cold storage [50]. Therefore, replacing ECT with ice storage would require an additional operational system. This would result in higher electrical power consumption and cost, and therefore will not be discussed in this study.

2.1.4 Ground Source Heat Storage and Control strategies

Weather and climate conditions, particularly the amount of solar radiation, result in temperature fluctuation during the summer and winter months in the upper few meters

of the ground. However, temperatures for depths below 5-6 m are relatively constant throughout the year. Fig. 2-3 illustrates two simplified schematics of ground temperature fluctuations at various depths of the ground surface in Ottawa, Canada [58].

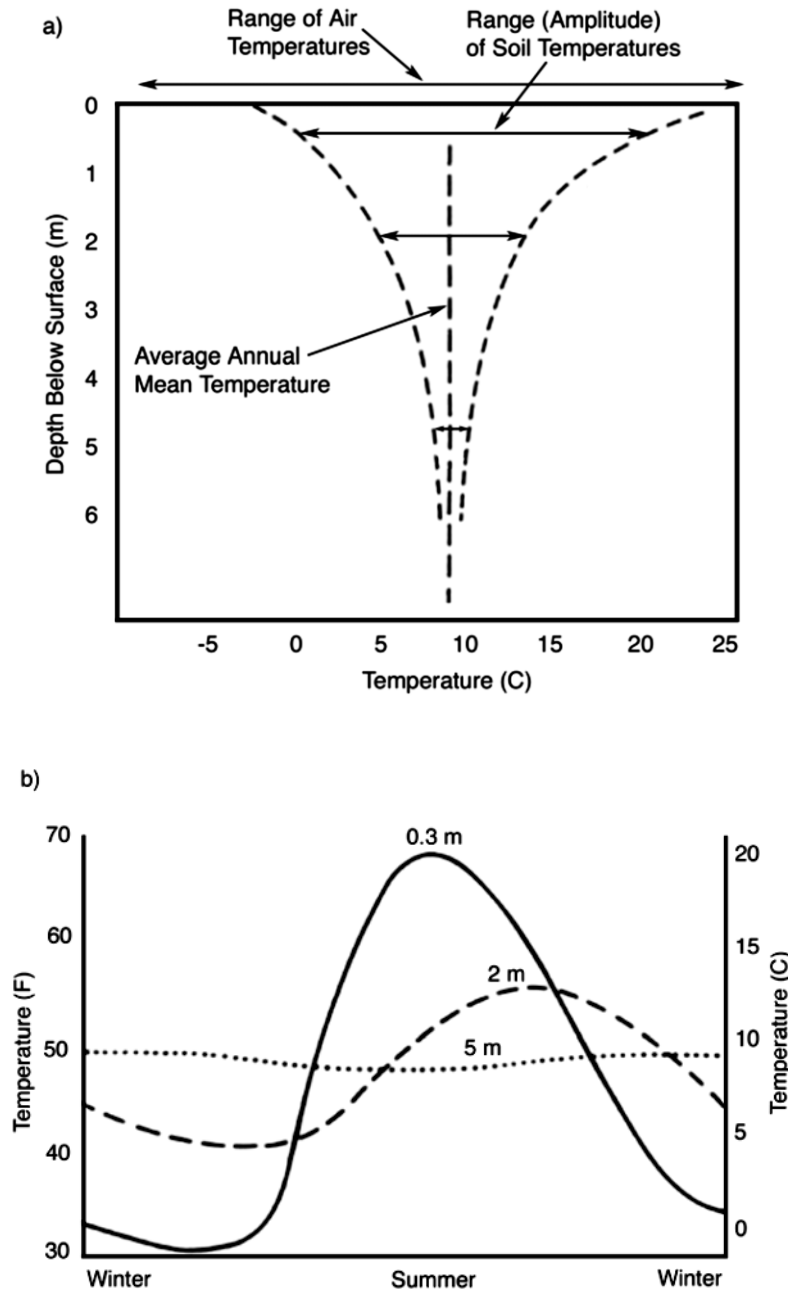


Fig. 2-3: Annual range of ground temperature in Ottawa, Canada [58]

If a ground heat exchanger, a borehole, or a well could transfer the heated water coming from a conditioner to the ground layer, cooling water temperatures would no longer rely on ambient weather conditions (e.g., wet-bulb and dry-bulb temperature, and relative humidity), but would instead vary according to soil temperature. If properly implemented and maintained, ground temperatures would remain reasonably constant throughout the year, offering a potentially reliable cooling source [58]. A comparative study by Eicker et al. [59] was performed on cooling tower, dry cooling, and ground heat rejection systems attached to a 15 kW absorption cooling system. It was found that the electrical COP varies between 6- 11.5 for wet cooling, 4-8 for dry cooling, and 13 for heat rejection to the ground. They also observed 30% lower electrical consumption for heat rejection to the ground. Another study by Palacín et al. [60] simulated the possibility of replacing a dry cooling tower in a LiBr/H₂O absorption cycle with a 25 m³ underground water tank. They found the geothermal unit improved the COP by 15.38%. The potential of using this cooling technique to replace ECT was investigated in the current study and is discussed further in Chapter 3.

2.1.5 Selected Heat Rejection Strategies

The performance of LDAC's strongly depends on the selected heat rejection system and its control strategy [61]. The existing literature confirms improvements can be made to a system using an ECT, specifically, by increasing the amount of cold water supplied to the system, or decreasing the electrical power consumed by an ECT.

The literature indicates that the use of a dry cooler in a absorption system does not provide sufficient cooling to the conditioner and can lead to crystallization of the

desiccant solutions, and lower system COP's. Cold water storage tanks offer beneficial load shifting capability, which have been shown to improve the COP_E of LDAC systems. Ground source heat exchangers allow access to a larger heat sink, allowing for greater heat transfer rates compared to a standard ECT. Therefore, this study focuses on these two cooling techniques for further investigations.

2.2 Previous Work at the Queen's Solar Calorimetry Laboratory

2.2.1 Queen's System Description

The LDAC systems installed at Queen's is configured as a dedicated outdoor air system (DOAS) intended to pre-condition ventilation air for commercial applications. It uses a unique low-flow, direct contact, laminar film absorber and regenerator design [62] with internally cooled and heated, parallel-plate, heat and mass exchangers (i.e., Falling-Film Desiccant Systems). In this design, desiccant flows down a thin wick on the exterior of the plates and process air and scavenging air are blown across the absorber and regenerator, respectively. During this process, moisture in the air is attracted to the plates and the desiccant solution became weak (i.e., its concentration decreased).

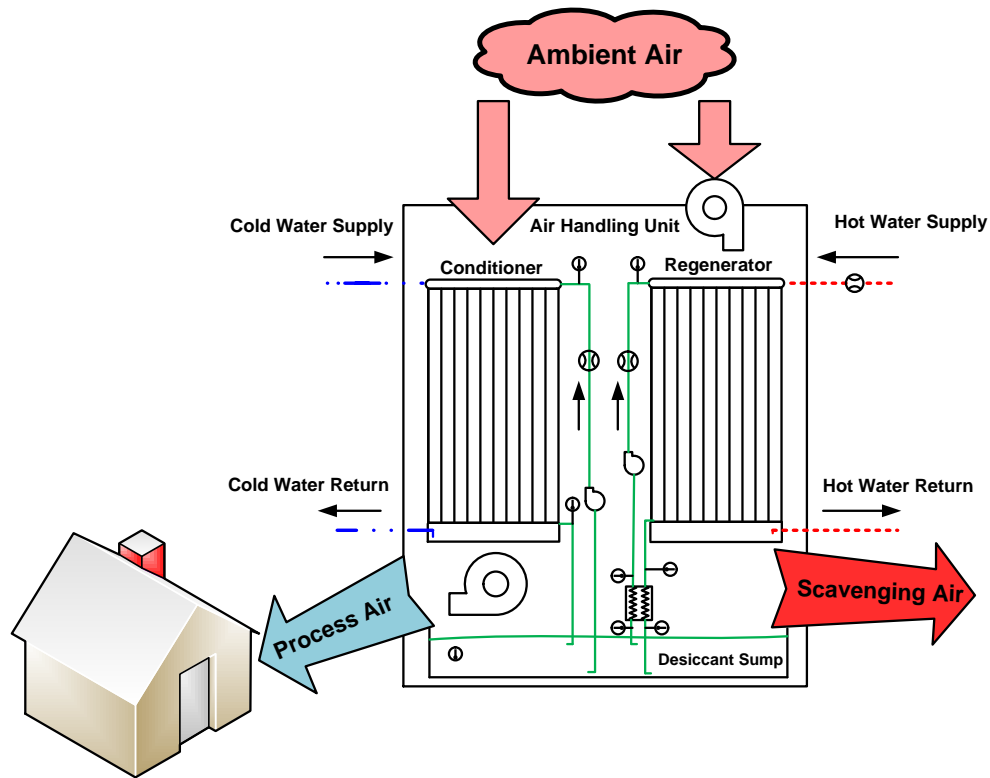


Fig. 2-4: Schematic of air handling unit

During operation, the weak desiccant is preheated by a heat exchanger, and pumped to the regenerator where it was heated and re-concentrated by a heat source (solar thermal system and auxiliary gas-fired boiler). After regeneration, cooling water is circulated through the conditioner to cool the desiccant. The driving force for the mass transfer of water into the desiccant is the difference between the partial pressure of water vapour in the air and the partial pressure of water vapour caused by the moisture absorbing desiccant. Cooling and concentrating the desiccant reduces the water vapour partial pressure induced by the desiccant, which increases the latent cooling rate. The cooling power and COP_T have been shown to be strongly dependent on the heat rejection [63] [64]. An evaporative cooling tower (ECT) is utilized for heat rejection from the system.



Fig. 2-5: Cooling water system at a commercial LDAC system at Queen’s University

Low-flow desiccant absorbers and regenerators were modeled and tested in 2006 by Mesquita using a single channel parallel-plate absorber [65]. The study revealed that both cooling water temperature and flow rate have a significant effect on the performance of the system [66].

The prototype DOAS system at Queen’s was originally procured, installed, and studied by Jones in 2008 [24]. The field performance of the unit was investigated using a gas fired boiler to simulate solar thermal heat input. System performance was determined for a range of heating water temperatures. Jones reported that the cooling power was between 4.3 kW and 22.8 kW, while the electrical COP ranged from 0.58-4.48, with high values of cooling power and COP_E at high heating water temperatures.

In 2012, Crofoot et al. [8] studied and installed a 95 m² evacuated tube solar thermal array as a heat source for a prior system. A full schematic of the system is shown in Fig. 2-6. The system could be operated with or without two buffer hot water storage tanks. In this system, the solar array supplied up to 40% of the energy required for a

liquid desiccant air handling unit. The results indicated that a solar LDAC system achieved a total cooling power (latent and sensible cooling powers) between 9.2- 17.2 kW with an overall COP_T of 0.40 and COP_E of 2.43. Crofoot et al. further developed a model in TRNSYS to predict the performance of the solar LDAC system and compared with experimental results with reasonable accuracy. This simulation model was used as a base model for this study.

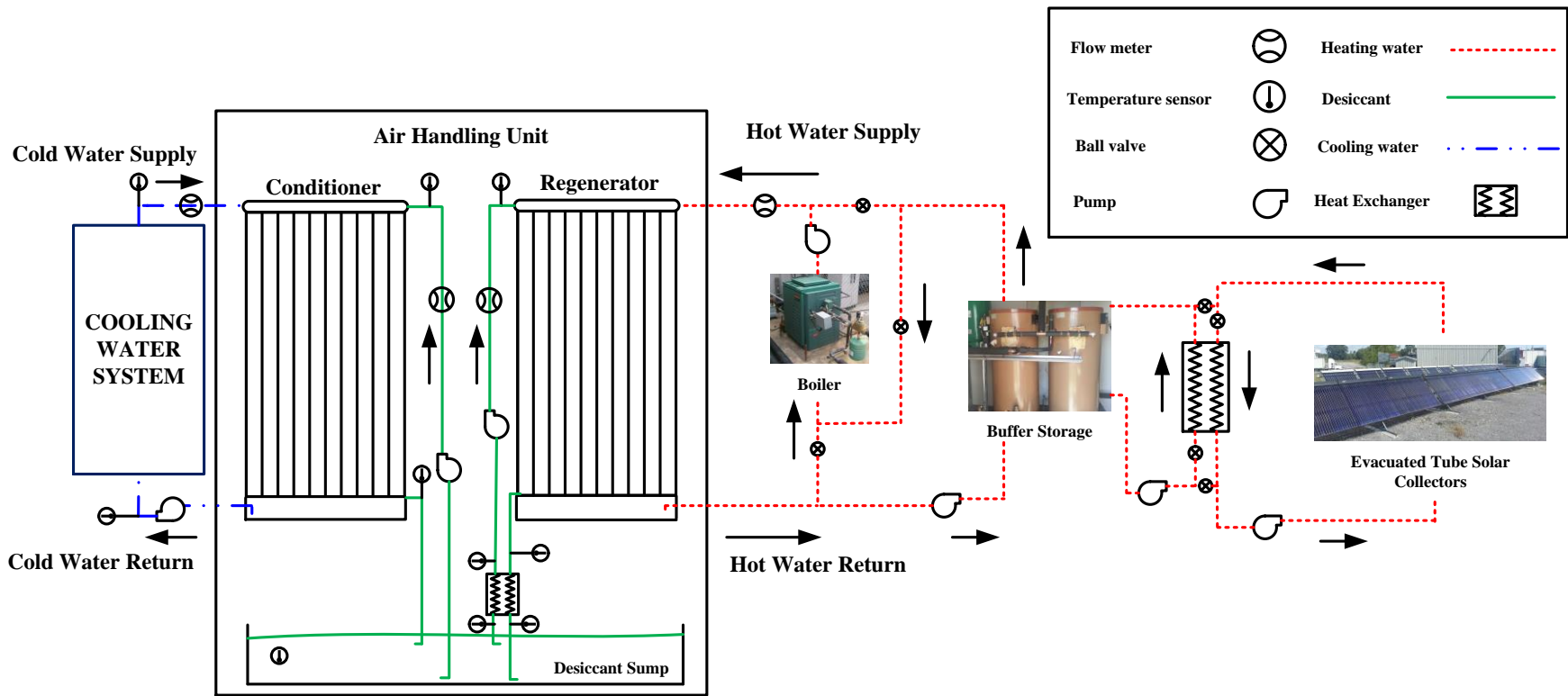


Fig. 2-6: Simplified schematic operation of solar driven liquid desiccant air conditioner

Chapter 3

Numerical and Experimental Modeling

Several heat rejection strategies were studied to determine their performance and effects on the LDAC system. The focus of this chapter is to describe the techniques and tools used to predict the system performance as well as the experimental methodology used to predict the performance of a stratified tank.

This chapter describes the base case which was investigated in previous studies. Following this, a description of several new heat rejection systems, and the simulations used to predict their performance characteristics, are detailed. The final section describes the experimental set-up used to support the modeling. Each of these different systems has been designated as follows:

1. Base Case: Evaporative cooling tower model;
2. Case A: Cooling water temperature model;
3. Case B: Cooling water storage system model (Load-shifting) ;
4. Case C: Ground source heat exchanger model;
5. Case D: The experimental investigation of a stratified cooling water storage tank (SCWS) and night cooling water storage (NCWS).

3.1 Basic Simulation Model of LDAC System

3.1.1 Introduction

Previous research performed at Queen's University, created empirical correlations of the absorber and regenerator effectiveness of the Queen's LDAC unit [8]. These were used as the basis for the simulations described in this work. These correlations can evaluate the performance of each component of the LDAC unit (i.e. the conditioner, regenerator, and desiccant sump) and determine the mass and energy balance for the given input conditions. These models were implemented in the transient system simulation software (TRNSYS). TRNSYS is made up of two parts: the first being a computational engine (that reads and processes an input file, iteratively solves the mass and energy balances associated with the system, determines convergence, and plots system variables at each time step); and, the second that allows systems to be configured using an extensive library of components (i.e., TYPES). Each TYPE is a sub-model used to predict the performance of a single component of a system. This makes the TRNSYS simulation program suitable for system design and refinement as different components can be switched into and out of the system and tested using different parameters. TRNSYS also allows the users to create custom TYPES coded in FORTRAN. In the current study, the custom TYPES previously created for the conditioner, regenerator, and desiccant sump were used in modeling of the LDAC system.

3.1.2 Basic TRNSYS Simulation

The TRNSYS simulation allowed individual component models (i.e., TYPES) to be connected to form a complete system model [67]. The base model was developed by Andrusiak, et al. [68] and was updated to include the solar thermal array by Crofoot [8].

Several standard TYPES provided by the TRNSYS component library were used in the simulation. Each TYPE calculates the performance and physical outputs based on specified inputs (time-dependent values) and parameters (time independent values). For example, weather conditions, inlet fluid conditions (temperature and flow rate), and control signals are typically used as inputs. Fluid properties (density, specific heat, etc.), thermal conductivity, and loss coefficients are examples of parameters.

A complete system model is built by joining library and custom components such that their interaction in terms of mass and energy flows is represented (i.e., outputs of one TYPE are linked to the inputs of the next TYPE). Simulations are run over specified time periods (e.g., days, months, or years), however, to accurately predict the system's interactions with time-dependent factors, the simulation period is broken into short discrete time steps. For each time step, component input and output values are solved iteratively until convergence is achieved. The complete initial TRNSYS simulation model is shown in Fig. 3-1 and a list of the TYPES used is provided in Table 3-1.

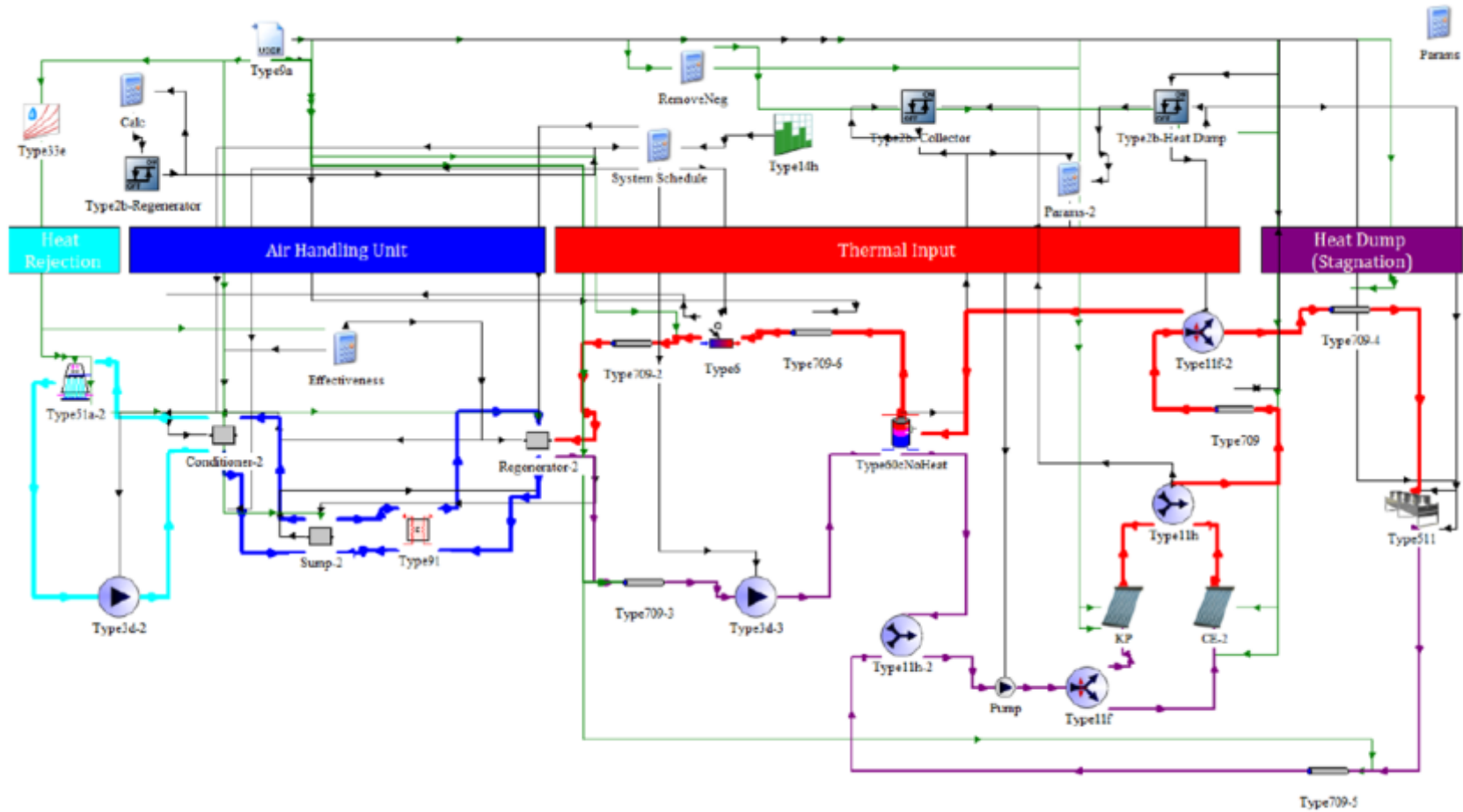


Fig. 3-1: Schematic of basic TRNSYS model (dark blue, light blue, and green lines represent desiccant, cooling water, and weather data connections respectively; purple, and red lines represent heating water loop [8].

Table 3-1: TRNSYS components used in the base case simulation including the standard TRNSYS library TYPES and custom TYPES.

Type Number	Models description
TYPE 2	differential controller
TYPE 3	pump
TYPE 6	natural gas boiler
TYPE 9a/ TYPE 109	local/typical meteorological year weather
TYPE 51	evaporative cooling tower
TYPE 91	heat exchanger
TYPE 60	hot water storage tank
TYPE 71	evacuated tube solar collectors
TYPE 511	dry cooler
TYPE 709	pipes
Custom TYPE 251	conditioner
Custom TYPE 250	regenerator
Custom TYPE 299	desiccant sump

3.1.2.1 Custom Components

In the conditioner, there were three working fluids: moist air (i.e., the process-air stream), the liquid desiccant solution, and the cooling water. Heat transfer occurs between all three fluids and mass transfer occurs between the air stream and the liquid desiccant solution. A detailed description of the heat and mass transfer processes can be found in Appendix A and was studied in more detail by Crofoot in 2012 [8]. Three experimentally determined effectiveness values were needed to solve the mass and energy balances for these streams. These effectiveness values were based on those developed by Khan and Martinez [69]. The dehumidification effectiveness, enthalpy

effectiveness, and desiccant-cooling water effectiveness values were needed to determine the outlet conditions of the LDAC unit's fluid streams. Custom component models for the conditioner were designed to make use of these effectiveness values by Andrusiak, Harrison, and Mesquita in [68]. As shown in Eq. (3.1.1), the dehumidification effectiveness of the conditioner, $\varepsilon_{dehumid}$, was defined as the ratio of the actual moisture removal to the maximum moisture removed. The enthalpy effectiveness, ε_h , shown in Eq. (3.1.2), was the ratio of actual enthalpy change of air across the conditioner to the maximum possible enthalpy change. Finally, in Eq. (3.1.3), the desiccant-cooling water effectiveness, $\varepsilon_{ld,cw}$, was the ratio of actual heat transfer between the desiccant and the cooling water stream to the maximum possible heat transfer. Similar equations were used to model the regenerator of the LDAC unit. The heat and mass transfer in the conditioner/regenerator can be found in Appendix A.

$$\varepsilon_{dehumid} = \frac{\omega_{in,cond} - \omega_{out,cond}}{\omega_{in,cond} - \omega_{min,cond}} = \frac{P_{a,in} - P_{a,out}}{P_{a,in} - P_{des,min}} \quad (3.1.1)$$

$$\varepsilon_h = \frac{h_{air,in,cond} - h_{air,out,cond}}{h_{air,in,cond} - h_{air,min,cond}} \quad (3.1.2)$$

$$\varepsilon_{ld,cw} = \frac{T_{ld,in,cond} - T_{ld,out,cond}}{T_{ld,in,cond} - T_{cw,in,cond}} \quad (3.1.3)$$

The terms $\omega_{in,cond}$ and $\omega_{out,cond}$ in Eq. (3.1.1), represented the inlet and predicted outlet humidity ratios of the conditioner. The variable $P_{des,min}$ was the minimum outlet partial vapour pressure that could occur (i.e. when the vapour pressure of the air was in equilibrium with the inlet desiccant partial vapour pressure at the inlet cooling water

temperature). $\varepsilon_{dehumid}$ can be also written in the form of humidity ratios, as seen in Eq. (3.1.1.). In Eq. (3.1.2), the enthalpy of the inlet process-air stream and the predicted outlet air enthalpy were $h_{air,in,cond}$ and $h_{air,out,cond}$, respectively. For an internally cooled system the minimum outlet enthalpy, $h_{air,min,cond}$, occurred when the air was at the inlet cooling water temperature and a had a humidity ratio of $\omega_{min,cond}$. In Eq. (3.1.3), $T_{ld,in,cond}$ and $T_{ld,out,cond}$ are the inlet and predicted outlet desiccant temperature, and $T_{cw,in,cond}$ is the cooling water inlet temperature.

The water vapour pressure is a function of both temperature and desiccant concentration; Conde [70] reported a formulation for the accurate prediction of this property. The water vapour pressure decreases as the temperature of desiccant decreases or as desiccant concentration increases as shown in Fig. 3-2.

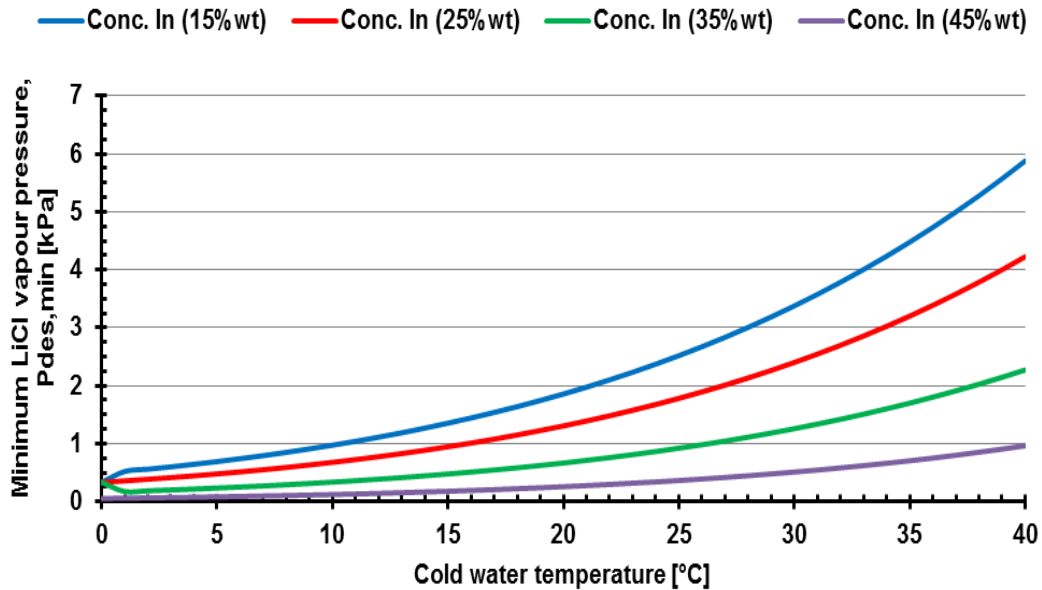


Fig. 3-2: Minimum water vapour pressure of Lithium Chloride [70]

The performance of the LD dehumidification system depended on heat and mass transfer between moist process air, desiccant solution and cold water inside the

conditioner. To predict performance and the outlet conditions of air-handling unit, three experimentally determined dehumidification ($\epsilon_{dehumid}$), enthalpy (ϵ_h), and desiccant-cooling water ($\epsilon_{ld,cw}$) effectiveness values were used (Table 3-2). These values can predict latent cooling, regenerator hot water load, and overall collector efficiency within 5%, 4%, and 1% respectively [8].

Table 3-2: Effectiveness values used in TRNSYS simulation [8]

Conditioner		Regenerator	
$\epsilon_{dehumid}$	0.5933	$\epsilon_{regenerator}$	0.2037
ϵ_h	0.4381	$\epsilon_{reg. h}$	0.2699
$\epsilon_{ld,cw}$	0.7784	$\epsilon_{ld,hw}$	0.6613

3.2 Case A: Cooling Water Temperature Model

3.2.1 Introduction

The heat rejection system in the LDAC system is not only responsible for approximately 40% of the electrical power consumption in the system, but it also has a strong effect on the cooling capacity of the LDAC system. Previous studies on the LDAC system were done by Jones in 2008, Andrusiak in 2010, and L. Crofoot in 2012, to investigate the effect of operating variables (such as ambient air conditions, hot water source, hot water temperature, etc.) on the performance of solar LDAC system. In this study, the performance of the LDAC system was simulated for a range of cooling water temperatures using a modified base case model. The results were compared to both the base case model and to the experimental data taken from the 2012 tests in Kingston [8].

From these results, the effect of the cooling water temperature on the LDAC system's COP_T was evaluated.

3.2.2 TRNSYS Simulation Model

Data recorded for the Queen's LDAC system during the summer of 2012 was used for this analysis. TRNSYS TYPE 9a was used to import actual weather data from test days into the simulation. A text file was generated from recorded data for the working hours of 8AM to 6PM. The data included the incident solar radiation, ambient temperature, and solar incidence angle for each minute. For the annual simulations modeling the summer cooling season (May to September), TYPE 109 was used to read Typical Meteorological Year (TMY) weather files for Toronto, Canada.

The simulated control system mirrored the physical system by activating the regenerator (at an 80°C set point temperature) when the relative humidity of the ambient air was above 30%. A controller (Type 2b) was used to model this operating condition. All components in the Case A model are similar to the previously built simulation model (Base Model) except for the heat rejection loop and weather input conditions. The heat rejection system was changed to provide a set cooling water temperature to the conditioner. An 'Equation Type' was used to determine the cooling water temperature

The selection of heat rejection system partially depends on the cooling water temperature range that cooling devices can produce. If the heat sink was ambient air, and a heat pump is not used, the lowest cooling water temperatures attainable are based on either the wet bulb temperature, as in the case of evaporative cooling (latent plus sensible cooling), or the dry bulb temperature (sensible cooling), as in the case of dry cooling. If the heat sink was the earth, the cooling water temperature supplied to the LDAC unit

would be close to the average annual ground temperature (assuming it is independence from the ambient air condition [23]). Therefore, various cooling water ΔT , at different fixed relative humidity percentages, were set as inputs to the conditioner model in the TRNSYS simulation to investigate how cooling water temperature and relative humidity could affect the cooling performance of a LDAC system. For the purpose of this analysis ΔT is defined by the following equations:

$$\Delta T = (\text{cooling water temperature} - \text{ambient air temperature}) \quad (3.2.1)$$

The modified simulation results were used to identify the most promising cooling techniques and to estimate the effect of cooling water temperature on the unit is COP_T for different weather conditions. The validated system model was then used to predict the average seasonal performance of the system in Toronto. The results are shown in Chapter 4.

3.3 Case B: Cooling Water Storage System (Load-shifting Model)

3.3.1 Introduction

The evaporative cooling tower (ECT) often operated in humid conditions which resulted in reduced heat rejection rates and ineffective operation. When the ambient air had a relatively high humidity, its capacity to absorb water in the ECT was reduced, as the ECT can only humidify air up to 80-90 % [71]. This directly reduced the rate of cooling by the ECT. The experimental results indicated that, as the ambient relative humidity increased, the COP_T was reduced. Utilizing cooling water storage (CWS) to

shift ECT usage to lower ambient humidity times was considered as a potential method improving performance. During normal operation, the ECT ran continuously during the operating hours of 8 AM to 6 PM. A sample of the experimental results showing the ambient relative humidity and temperature throughout the day is shown in Fig. 3-3. The high relative humidity of the ambient air in the morning resulted in a reduced cooling rate in the ECT.

The CWS system was designed to provide cooling water during of the morning period of high relative humidity. This allowed the heat rejection load to be shifted to times of lower ambient relative humidity and temperature (i.e. night time). In this design, the ECT did not operate during the early morning hours as water from the CWS system was used instead. This period was referred to as ‘standing time’ in Fig. 3-3.

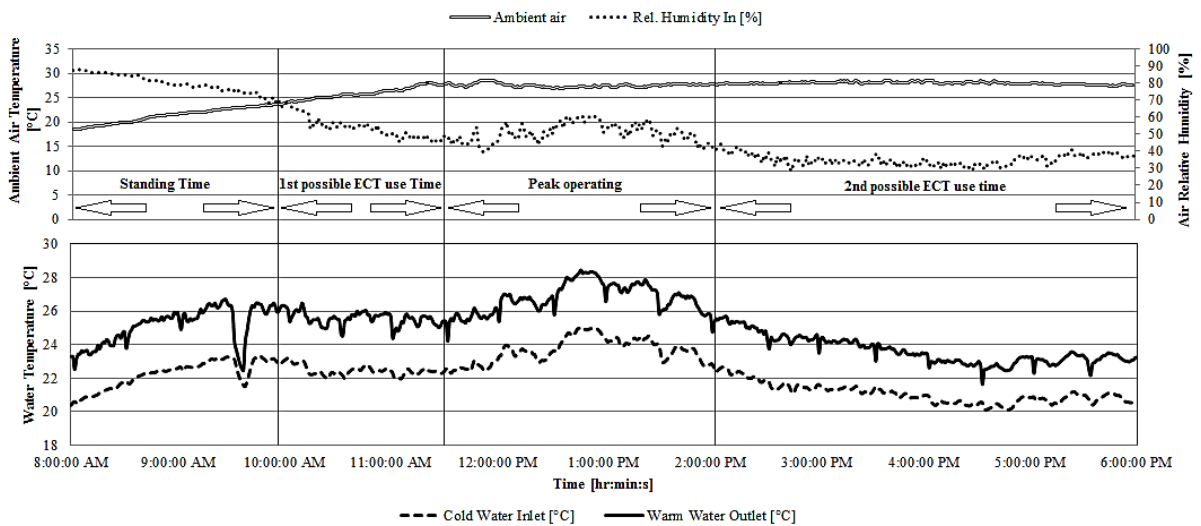


Fig. 3-3: Cooling pattern of ECT and operating conditions over a single test day

A CWS system was modeled in TRNSYS to determine if the LDAC system’s performance (in particular, the COPs of the system) could be improved. A base case

model was updated to include that had a well-mixed storage tank and the valves and controls required to redirect the cooling water.

3.3.2 TRNSYS Simulation Model

The proposed system consisted of an LD (liquid desiccant) air handling unit, a WS (water storage) tank, and an ECT (Fig. 3-4). These components, along with the required pumps, pipes, and valves, formed the conditioner heat rejection sub-system of the Case A LDAC system. The regeneration sub-system was unchanged for the Case A model.

The new Case A model was designed so that the temperature of the cooling water leaving the conditioner determined whether it was sent to either the CWS or the ECT. The CWS was used primarily during early morning operation because the ambient air relative humidity was relatively high, thus making the ECT the less effective method. This effect can be seen during the standing time period as shown in Fig. 3-3. The ECT was used once the air's relative humidity was low enough to provide cooling water at a lower temperature than the stored water. The CWS was used again if the ECT outlet temperature was greater than the CWS temperature. This occurred when the ambient relative humidity increased or when the temperature of desiccant inside the conditioner was increased (e.g. if the regenerator had been running for long periods of time).

The control system was set to switch off the ECT's fan when the CWS temperature was lower than the ECT's temperature. When the difference between CWS and ECT was greater than 3 °C ($T_{CWS} < T_{ECT}$) the stored cold water was used as the cooling water source. The control system also employed a leveling balance approach to maintain appropriate water levels in the CWS and ECT.

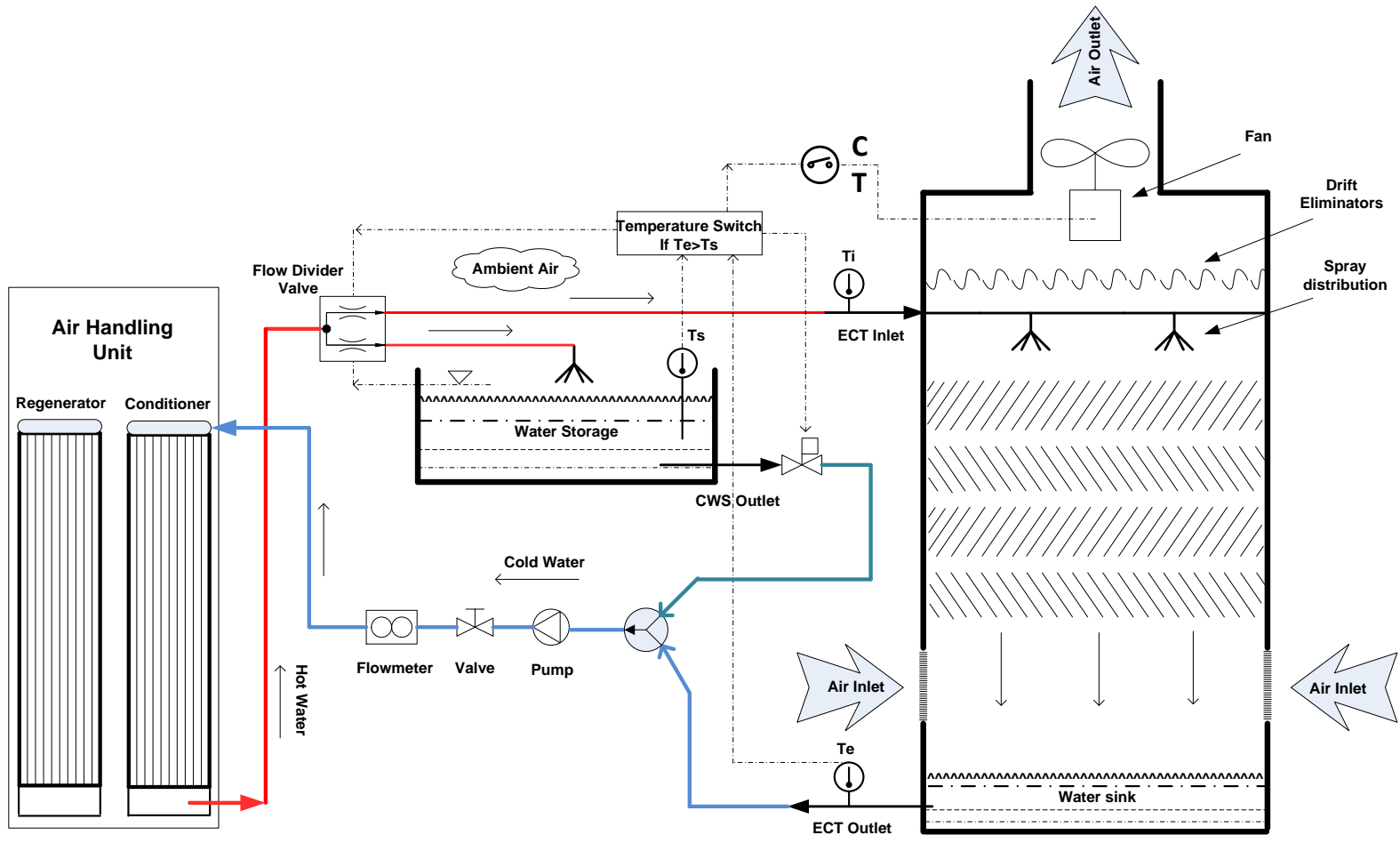


Fig. 3-4: Schematic of cooling water storage system integrated with the liquid desiccant air-conditioning system

A differential temperature controller (TYPE 2b) was used to determine if the warm conditioner outlet water should be stored or sent to the ECT. A dead band was set to prevent instability in the control signals sent to the flow diverting valve (TYPE 11). The valve was used to control the flow of water into either the CWS or the ECT. A cooling tower model (TYPE 51a) was used to model the ECT. The TYPE 51a was an effectiveness model developed by Braun [72] that used performance maps provided by the unit's manufacturer. This was the same TYPE used in the base case model.

The CWS tanks were modeled using a variable volume tank (TYPE 39). This was a fully-mixed storage tank with a constant cross-sectional area of 4 m². The tank had one inlet, warm water from the conditioner, and a single outlet, cold water being sent to the conditioner. The differential equations used to describe the rate of mass and energy change for a given time step were presented in Eq. (4.1.4) and (4.1.5).

$$\frac{dm}{dt} = \dot{m}_{in} - \dot{m}_{out} \quad (4.1.4)$$

$$c_p \left(\frac{dm}{dt} \right) (T_{in} - T_{out}) = \dot{m}_{in} c_p T_{in} - \dot{m}_{out} c_p T_{out} - UA(T_{out} - T_{amb}) \quad (4.1.5)$$

In these equations, \dot{m}_{in} and \dot{m}_{out} , were the inlet and outlet mass flow rates of water. Similarly, T_{in} and T_{out} were the inlet and outlet temperatures of the tank. The mass of water in the tank was represented by the term m and c_p was the heat capacity of the water, which was assumed to be constant. The UA term was the heat loss coefficient for the tank. The heat generation and LDAC unit models were not altered from the original system as designed, tested and verified by Crofoot [8]. The new CWS system was

simulated using experimental weather data gathered in 2012. The results of these simulations are shown in Chapter 4.

3.4 Case C: Ground-source Heat Exchanger Model

3.4.1 Introduction

Ground-source heat exchangers (GSHX) use the earth's relatively constant temperature below the surface as a heat sink to reject the heated water coming from a conditioner. It can be an efficient alternative to ECT due to independence from weather condition such as wet-bulb, dry-bulb, and relative humidity. Also, as the ground temperature is usually much lower than the ambient air dry-bulb and wet-bulb temperatures in summer, higher heat rejection rates can be achieved.

U-tube heat exchangers (Boreholes) are commonly used for ground-source heat exchangers. Boreholes consist of buried pipe loops in the ground which are connected to a pump for fluid circulation. Boreholes are often filled with a fill material (virgin soil or grout). These vertical U-tube heat exchangers were simulated using TRNSYS and compared to the base case heat rejection model (Fig. 3-5).

3.4.2 TRNSYS Simulation Model

The model of the ground-source heat exchanger LDAC system uses all the same TYPES as the Base Case model were used (as shown in Table 3-1) with the exception of the ECT based heat rejection loop. A new heat rejection sub-system model was created using vertical boreholes. The borehole array was modeled by TYPE 557. Different numbers of boreholes were tested under identical operating conditions. The cooling water

from the conditioner outlet was sent to the boreholes in the arrangement shown in Fig. 3-5. The cooling water leaving the conditioner was circulated through the ground heat exchanger, rejecting the heat to the ground, before being returned to the conditioner.

In a U-tube ground heat exchanger, a vertical borehole is drilled into the ground. A U-tube heat exchanger is then pushed into the borehole. The top of the ground heat exchanger is typically 0.5 m below the surface of the ground. The borehole is then back filled with a grout or the excavated soil. Fig. 3-5 shows one U-tube for each borehole with its dimensions; although up to 10 U-tubes can be installed per borehole.

In Type 557, the ground temperature was calculated from three parts; a global temperature, a local solution, and a steady-flux solution. The global and local values were calculated with using an explicit finite difference method. The steady flux solution is obtained analytically, and the ground temperature is then calculated using superposition methods. The component description and FORTRAN coding used for TYPE 557 can be found in the TRNSYS manual [67] and G. Hellstrom [73]. The mathematical modeling of TYPE 557 component follows the methodology specified in ASHRAE 1995 [74]. The accuracy of this model was validated by C. Yavuzturk, [75], G. Hellstrom, [76], and P. Pärish [77].

The TYPE 9a was used to import the weather data for Kingston recorded during the 2012 experimental phase. Three summer days (July 11th- sunny and dry, July 17th- sunny and humid and August 13th-overcast and humid) were modelled to quantify the effects of various weather conditions on the system performance. The simulation results obtained were compared with the base model to highlight the effects of variable weather conditions on system performance.

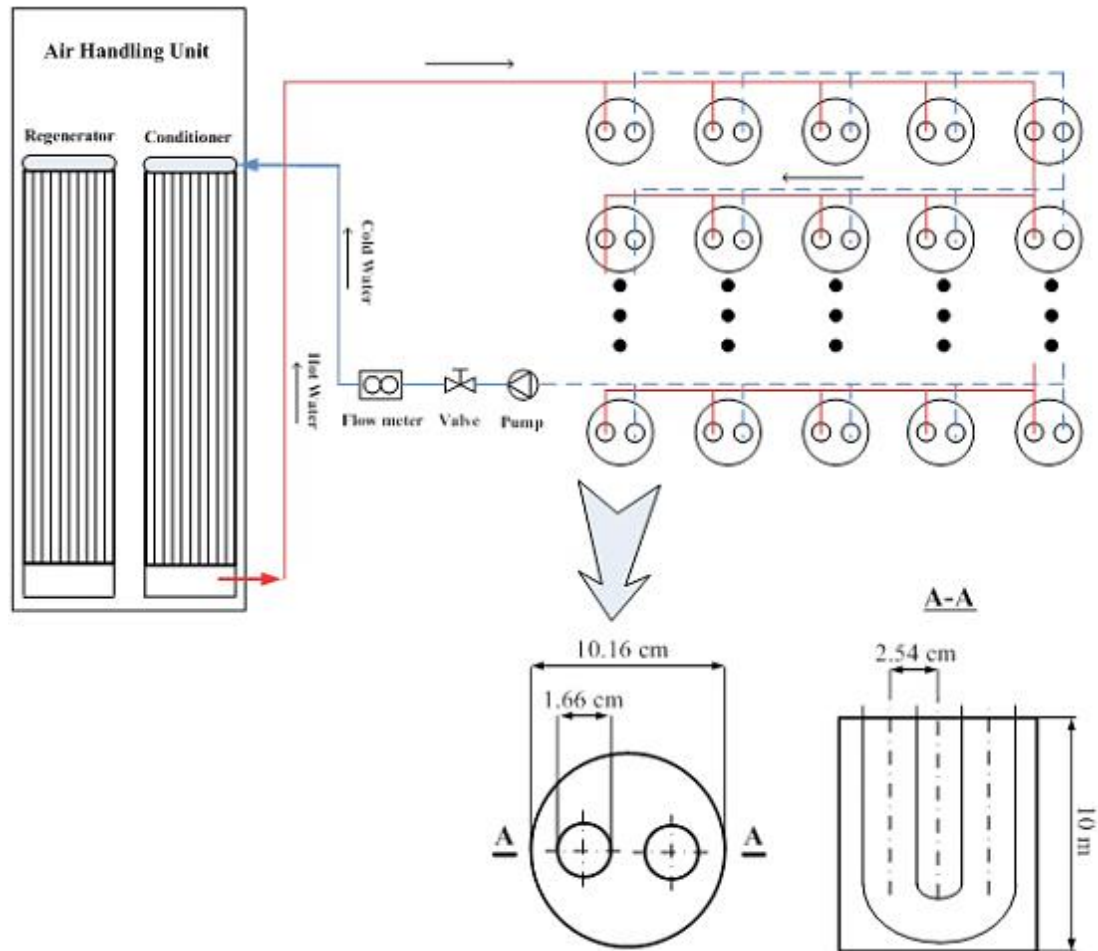


Fig. 3-5: Schematic of U-tube geo-exchanger integrated with the liquid desiccant air-conditioning system [78]

The model assumed that the boreholes were placed uniformly within a cylindrical storage volume in the ground. The heat transfer associated with each borehole consisted of convective heat transfer within the pipes and conductive heat transfer to the storage volume. The thermal conductivity of the grout, pipe and storage were assumed to be 2.8, 0.4, and 1.9 (W/m.K) for each borehole. The list of input parameters for TYPE 577 can be found in Table 3-3. These parameters were recommended by ASHRAE [78]. The results from these simulations are presented in Chapter 4.

Table 3-3: Input parameters used in Type 577.

Parameters	Values
Borehole depth	10 m
Header depth	0.5 m
Borehole radius	0.1016 m
Storage thermal conductivity	1.9 W/m.K
Storage heat capacity	2016 kJ/m ³ /K
Center-to-center half distance	0.0254 m
Fill thermal conductivity	2.8 W/m.K
Outer/inner radius of u-tube pipe	0.01664/0.01372 m
Pipe thermal conductivity	0.420 W/m.K
Gap thermal conductivity	1.4 W/m.K
Insulation thickness	0.0254 m
Thermal conductivity of layer	1.9 W/m.K
Number of boreholes	Varied (10,15, 20, 25)

3.5 Experimental Investigation of Stratified Cooling Water Storage Tank (SCWS) (Case D)

3.5.1 Introduction

The potential of using a CWS and an evaporative cooling tower (ECT) system with a LDAC system was experimentally investigated. A thermally stratified tank was studied to determine if the temperature gradient could be used to improve the systems performance. The cold water in the tank would remain cold if the return water, rather than mixing into the tank and raising the temperature of all the water, was contained within the higher levels of the tank. The tank would be cooled during the night.

The cooling water flow through the heat rejection system and the conditioner typically has a high mass flow rate ranging from 7200 kg/hr to 10800 kg/hr. Maintaining this high water flow rate can reduce the level of stratification in CWS tank. Stratified tanks rely on the buoyancy of warm water returning from the conditioner to reduce mixing in the storage tank water, but high velocity water can overcome these buoyant forces and cause the tank to mix. Higher degrees of stratification are possible at lower flow rates but this could affect the performance of the LDAC system. The solution to this was to employ a diffuser to reduce the fluid velocity at the inlet to the tank by increasing the outlet flow area. This allowed the same high flow rate but minimized the mixing the tank.

The initial temperature of the tank depended on the heat rejection rates during hours of non-operation. To achieve the lowest temperature possible with the available equipment night cooling water storage (NCWS) operating cycles were used as part of the stratified cooling water storage (SCWS) system. These systems were experimentally

evaluated over six days during September 2014. Fig. 3-6 shows the installed testing system at Queen's University.



Fig. 3-6: 6000 liter CWS tank at Queen's University

The performance of the LDAC system can be predicted by using the modified TRNSYS simulation model, accounting for different climate conditions. To undertake this study, first the SCWS tank was modeled utilizing TRNSYS software, and then the experimental testing was carried out to validate the model. After validation of the SCWS type, the liquid desiccant system types were integrated into the model. Appendix B describes this investigation in more details.

3.5.2 Experimental Set-up and Design

The storage tank consisted of a 6.6 m³ cylindrical tank (Table 3-4). This tank featured one outlet at the bottom of the tank and a larger vented inlet at the top of the tank. In order to achieve a high degree of thermal stratification in the storage, a perforated single-pipe diffuser (PSD) was used for the charging and improving the level of stratification in the CWS tank (Fig. 3-7). The PSD was used to minimize water mixing

at the tank inlet by distributing the flow through out of a series of equally sized and spaced holes along the length of the pipe. Table 3-4 indicates the dimensions of the PSD.

Table 3-4: CWS Tank and PSD Characteristics

Tank Specification		Perforated single-pipe diffuser Specification	
Height of tank (L)	1.67 m	Total Number of holes	20
Diameter (D)	2.24	Number of perforated rows	2
Maximum volume of the tank	6.6 m ³	Degrees of inclination between perforated rows	120°
Material	High-density polyethylene (HD-PE)	Diameter of a hole	0.015 m
Thermal conductivity	0.42 - 0.51 W/(m.K)	Distance between each hole	0.1 m

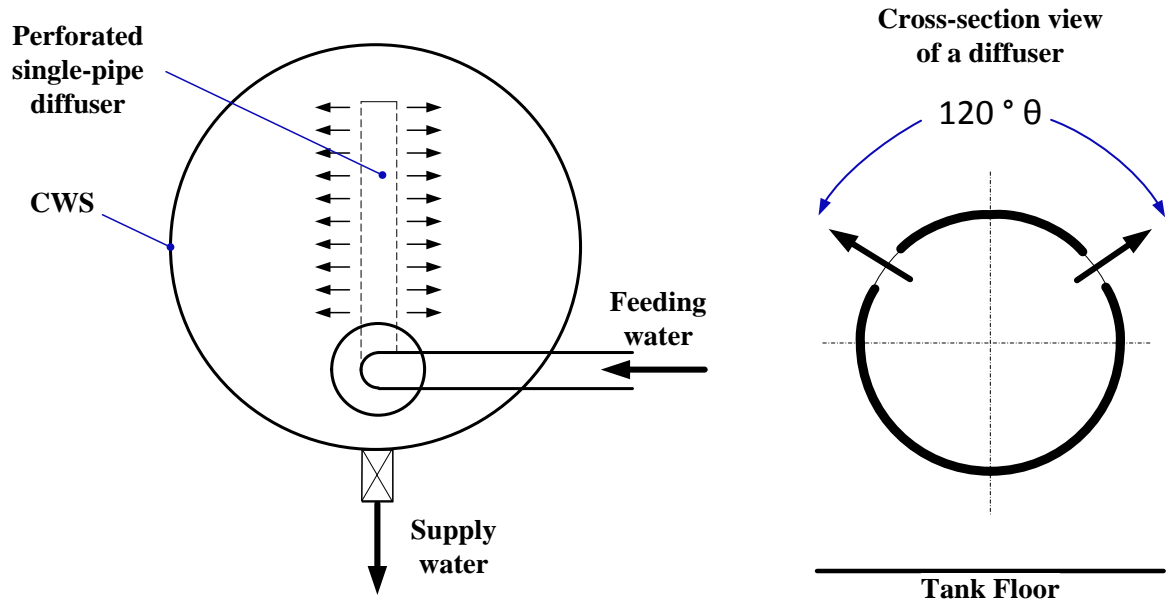


Fig. 3-7: Plan View and Details of the perforated single-pipe diffuser (PSD)

The SCWS tank was instrumented with a series of thermocouples positioned at regular intervals for the entire height of the tank. This enabled a data logger to record the tanks temperatures at different heights to monitor the level of stratification. The location of the eight temperature sensors inside the tank are shown in Fig. 3-8. The temperature sensors were installed with a vertical spacing of 30 cm (1 ft). The eight channel thermocouple and data logger system used to read the temperature had an accuracy of $\pm 0.5^{\circ}\text{C}$ accuracy. For the purpose of the present research, the water draw was at a nominal flow rate of approximately 41 L/min. The inlet water temperature of the tank depended on the amount of heat absorbed inside the conditioner during the dehumidification process.

When using the night cooling water storage (NCWS), warm water from the storage tank was circulated through the cooling tower (ECT) to reduce its temperature (Fig. 3-9). As previously discussed, the cooling water temperature achieved by the ECT depended on the ambient conditions (temperature and humidity) and the water flow rate. The ECT at Queen's University operated at a constant volumetric air flow rate of 8326 (m^3/hr) and a water mass flow rate in the range of 6600 to 7800 (kg/hr) [8]. The results of these experiments are described in Chapter 4.

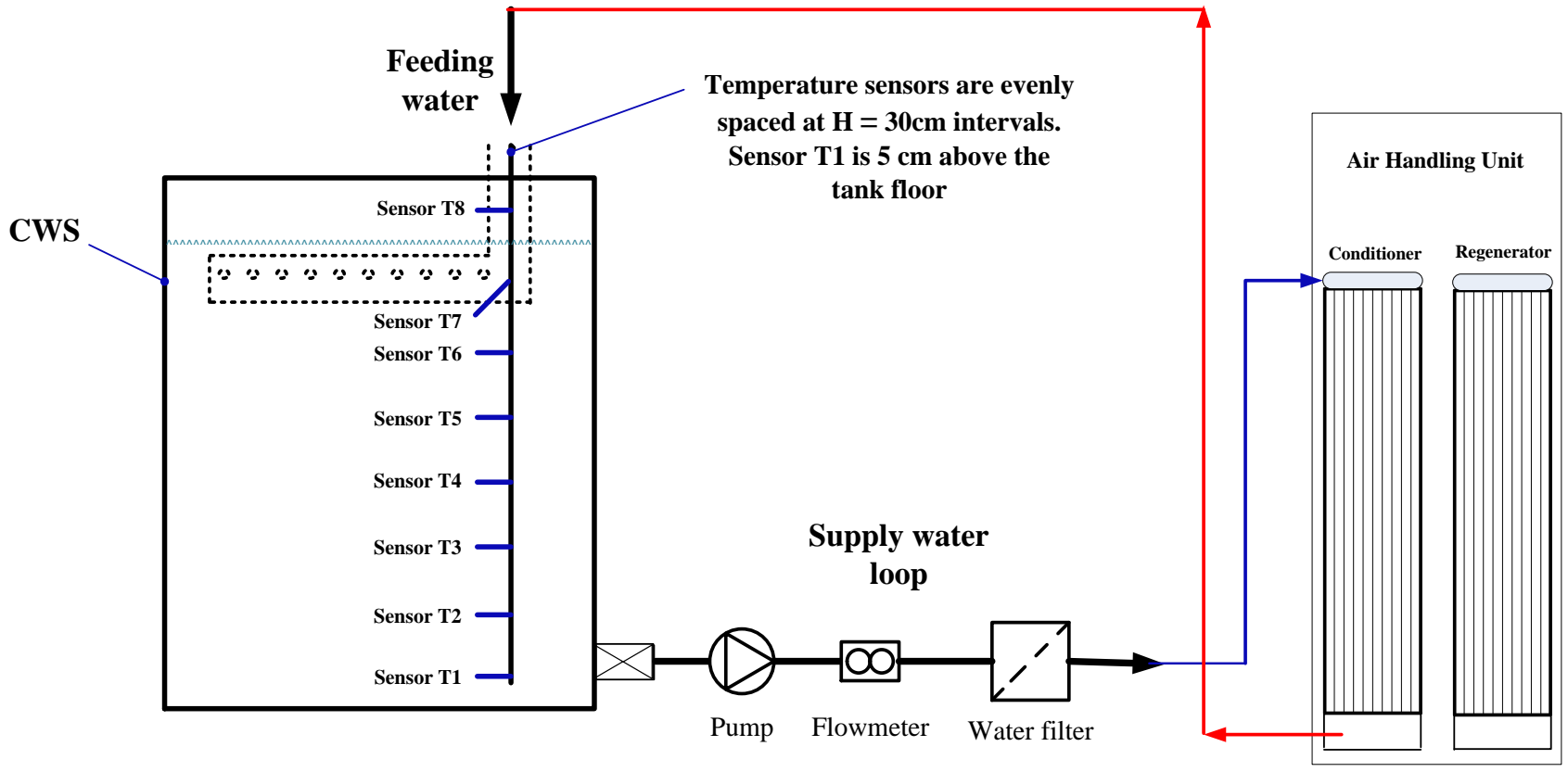


Fig. 3-8: Queen's University CWS tank instrumentation diagram

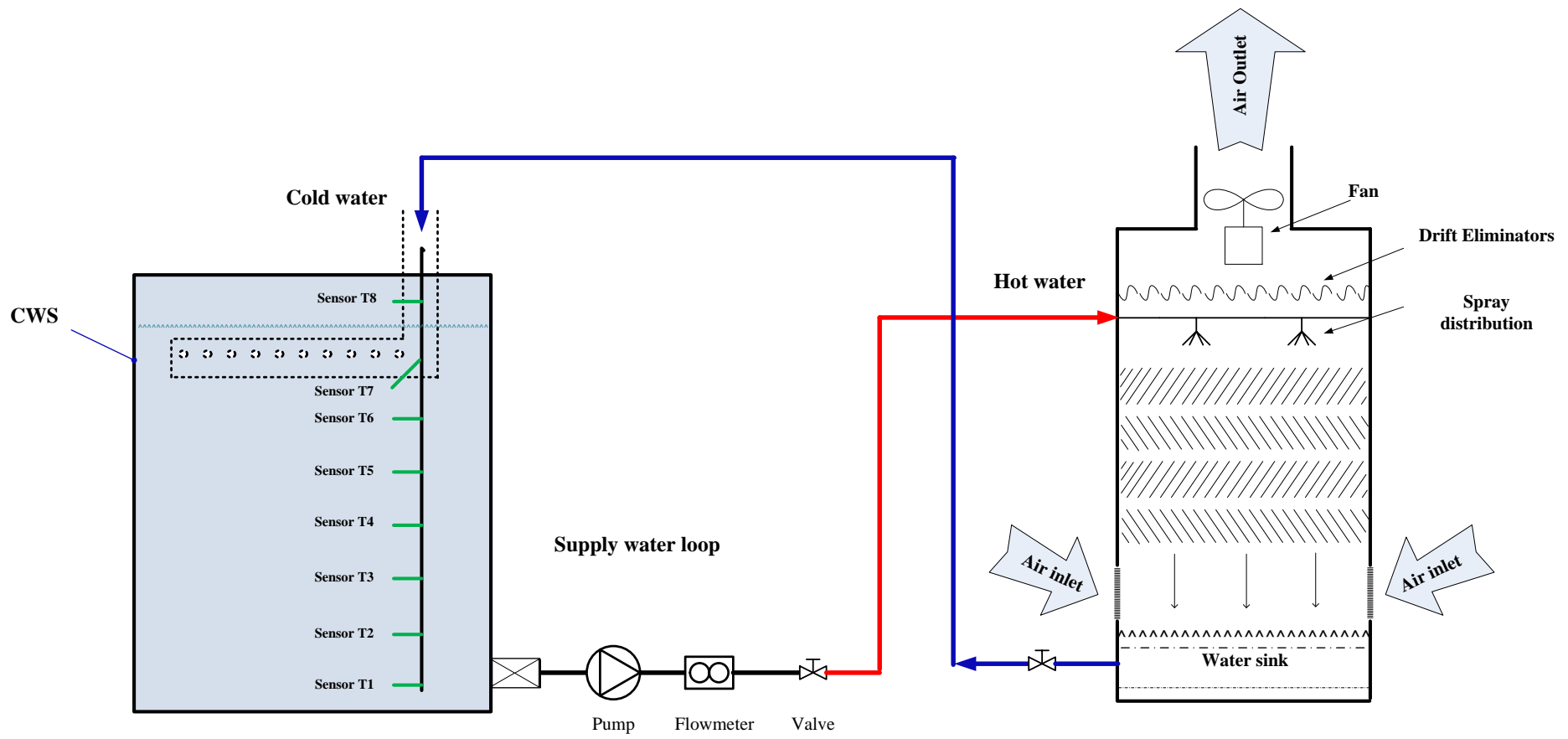


Fig. 3-9: Night cooling water storage (NCWS) system diagram

Chapter 4

Results and Analysis

This chapter presents the results obtained from both the numerical and experimental case studies (described in Chapter 3) and highlights parameters which can be used for the comparison and selection of new heat rejection systems. Results from this research are compared to the simulation and experimental results obtained for the Base Case to highlight their effects on the overall performance of the LDAC system. A discussion of these results is presented in Chapter 5 for each Case individually and in comparison.

4.1 Case A: Cooling Water Temperature Results

4.1.1 Daily System Performance

Simulations were conducted to determine the effect of the cooling water temperature on COP_T . The results were compared to the TRNSYS simulations and experimental results obtained by Crofoot [8]. The average of the weather conditions used for each simulated day is shown in Table 4-1. The actual data used for the simulations was recorded during the 2012 experiments in one minute time steps. The control methodology for the simulation was the same as was used in the Base Case, e.g., operation from 8 AM to 6 PM, hot water set point equal to 80°C, and the regenerator switched off when the relative humidity of the process-air was below 30%.

Table 4-1: Average value from day long operating condition

	July 11th	July 17th	July 23th	August 13th	August 15th
Air temperature (°C)	26.2	32.4	27.7	24.4	23.7
Relative humidity (%)	50.7	52	70.5	66.9	69.4
Abs. Humidity (g/kg)	10.3	16	16.5	12.7	12.6
Radiation (W/m²)	714	631	642	538	552

The effect the cooling water temperature and relative humidity had on the regenerator coefficient of performance (COP_R ; which is the ratio of $Q_{Desorption}$ to $Q_{Heat\ in}$) is shown in Fig. 4-1. The figure was plotted for the simulation using the weather conditions on July 11th and with constant relative humidities ranging from 55 to 85%. A wide range of ΔT values were simulated (ΔT representing the difference between the temperature of the cooling water entering the conditioner and the ambient air). The maximum and minimum COP_R were obtained for coldest and hottest water temperatures respectively, ranging from 0.54 for a ΔT of 5°C and 55% RH and 0.67 for a ΔT of -10°C and 85% RH.

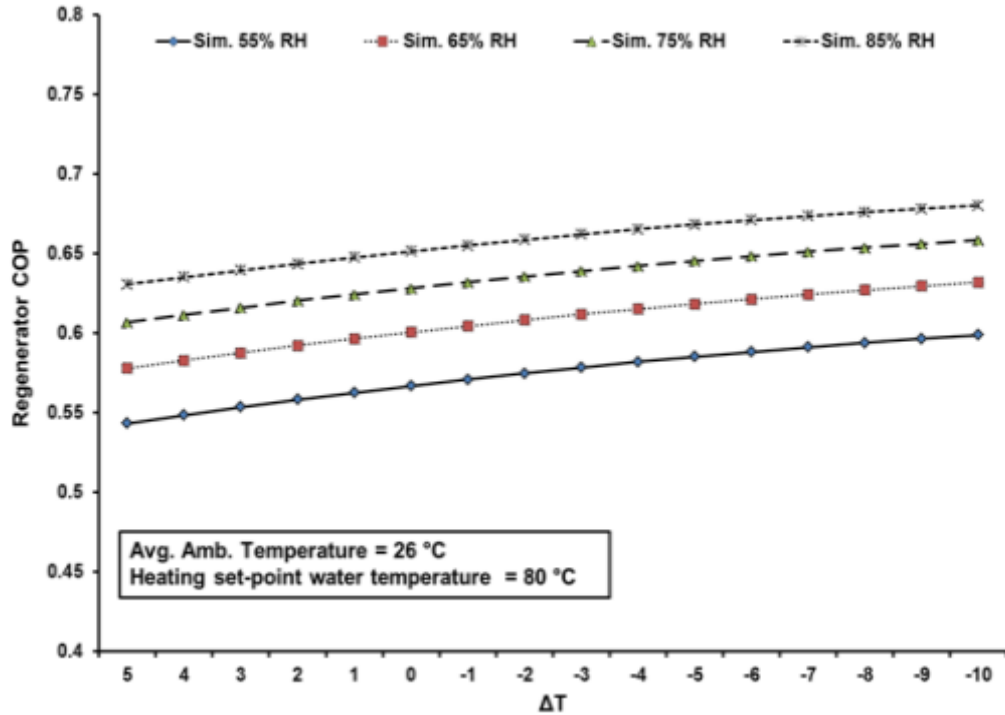


Fig. 4-1: Simulated average COP_R at different fixed relative humidity values determined using July 11th weather data.

Fig. 4-2 to Fig. 4-6 show the average COP_Ts of the LDAC system over the same range of ΔT and relative humidity values. Each figure shows one of five simulated days to highlight the effect of various weather conditions on system performance. The red circles indicate the average simulated COP_T of the LDAC system as determined using the Base Case simulation, and the green rectangles indicate the average experimental COP_T of the LDAC system. The simulation results indicate that the maximum COP_T was achieved at the lowest cooling water temperature (ΔT= -10) and ranged from 0.58 to 0.6 as the relative humidity varied. The effect of relative humidity on COP_T decreased as cooling water temperature was reduced.

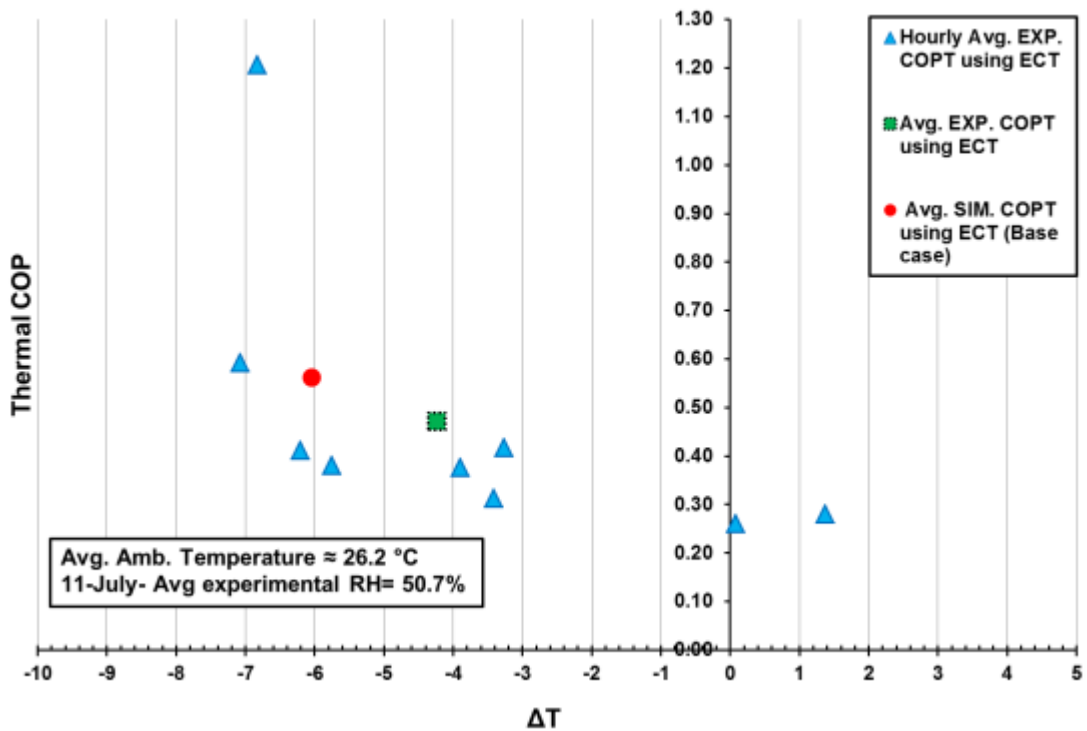
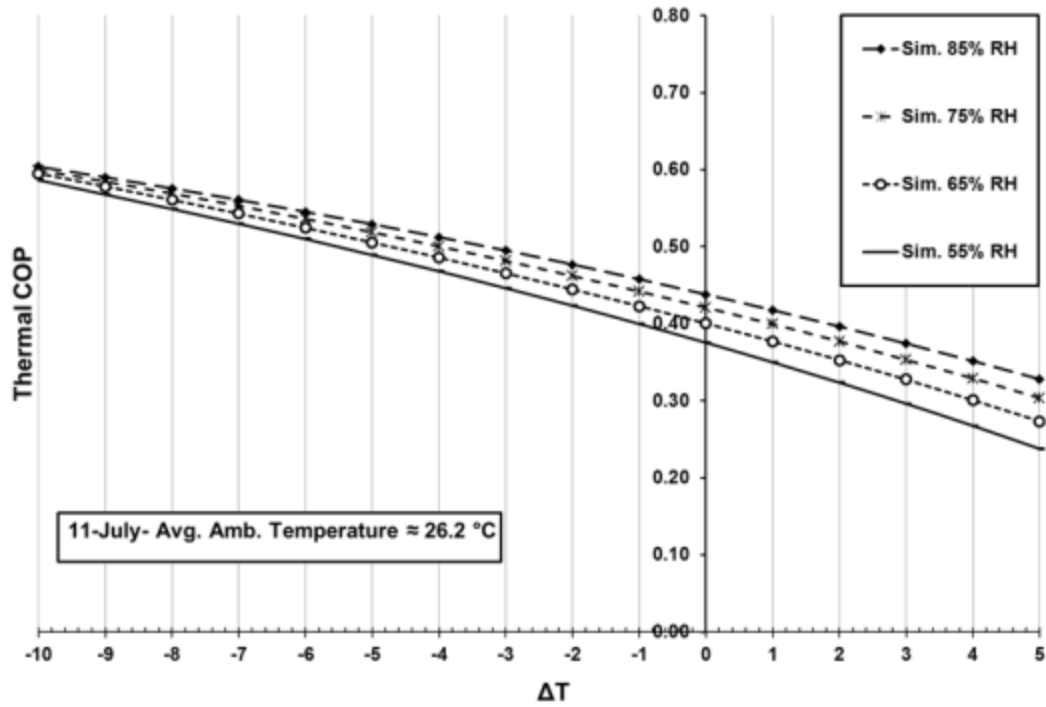


Fig. 4-2: Results for July 11th - Top: simulated values of average COP_T as a function of cooling water temperature and relative humidity; Bottom: Actual hourly and daily average values of COP_T measured over the day.

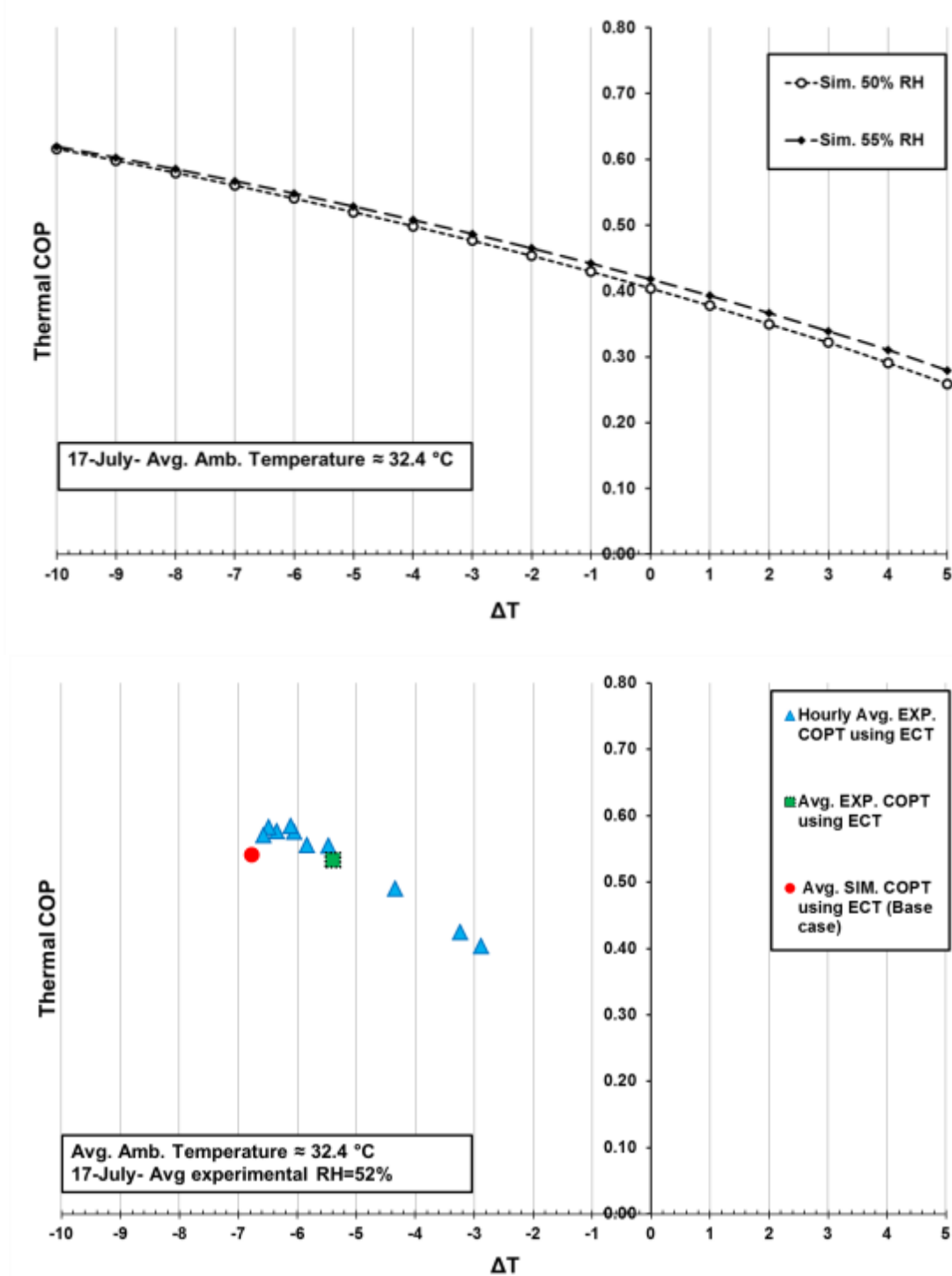


Fig. 4-3: Results for July 17th - Top: simulated values of average COP_T as a function of cooling water temperature and relative humidity; Bottom: Actual hourly and daily average values of COP_T measured over the day.

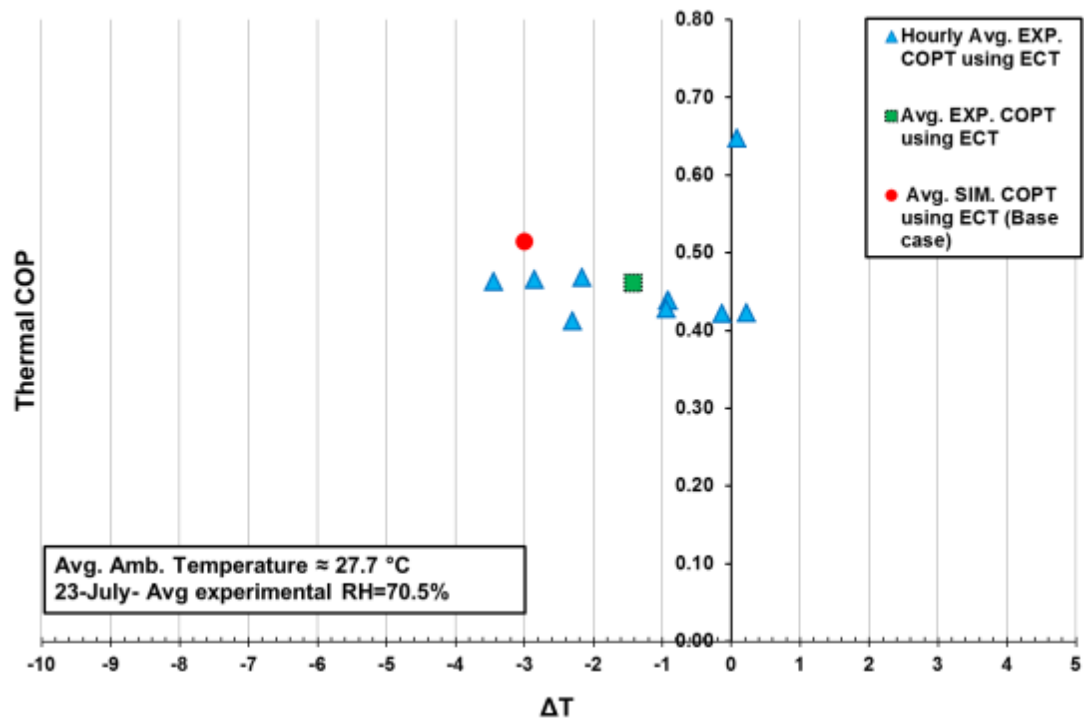
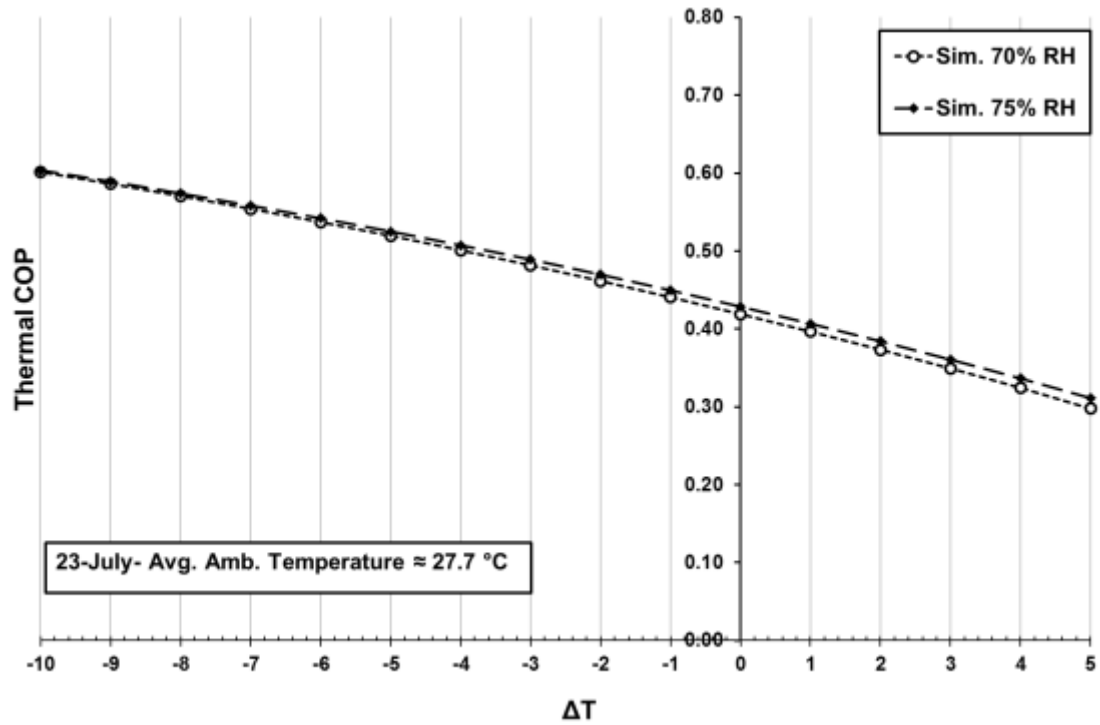


Fig. 4-4: Results for July 23rd - Top: simulated values of average COP_T as a function of cooling water temperature and relative humidity; Bottom: Actual hourly and daily average values of COP_T measured over the day.

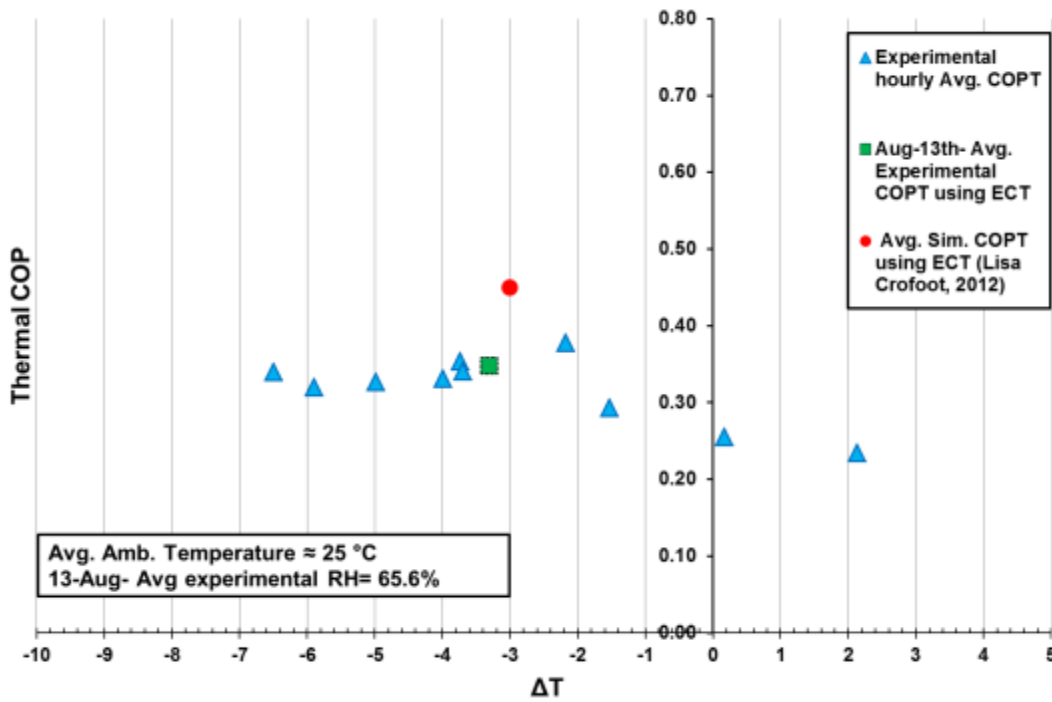
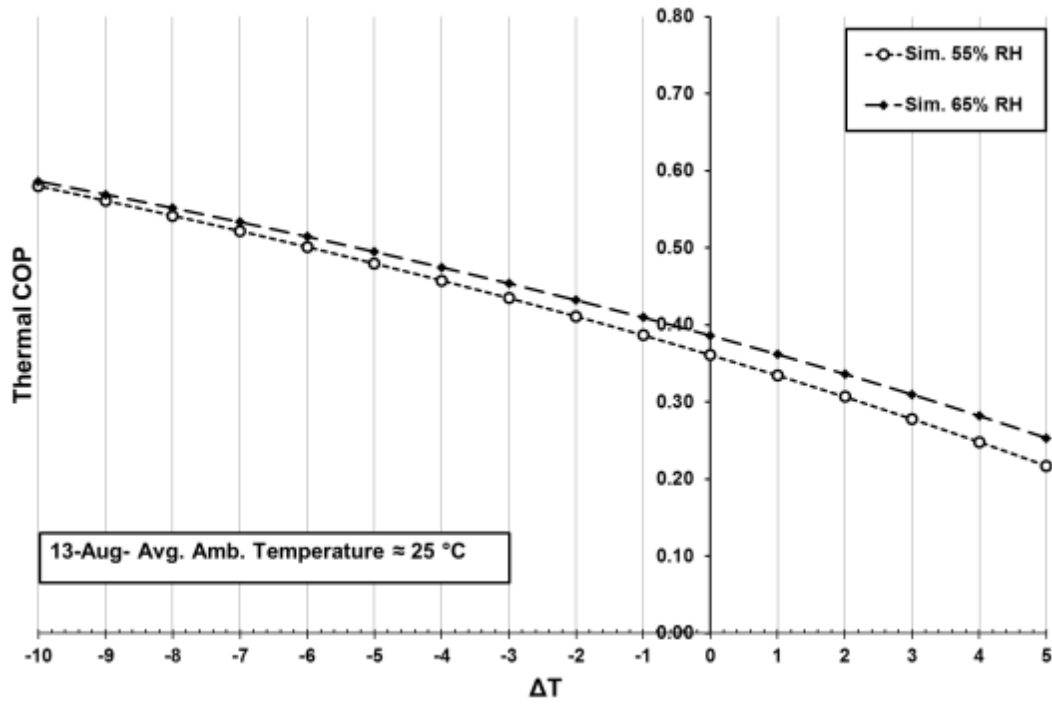


Fig. 4-5: Results for Aug 13th - Top: simulated values of average COP_T as a function of cooling water temperature and relative humidity; Bottom: Actual hourly and daily average values of COP_T measured over the day.

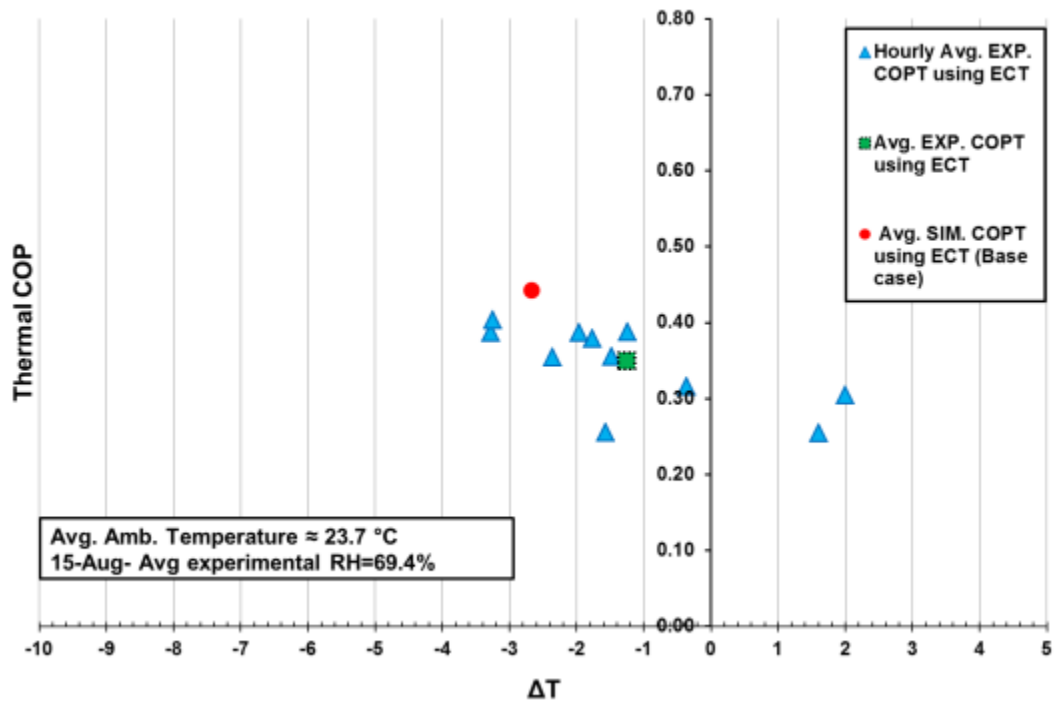
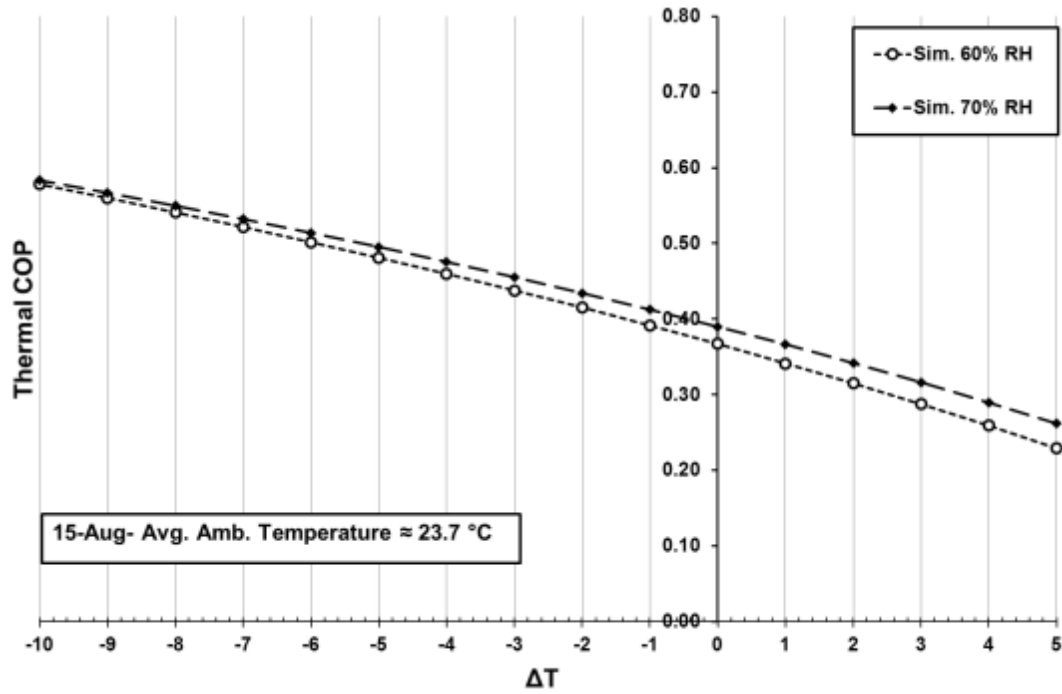


Fig. 4-6: Results for Aug 15th - Top: simulated values of average COP_T as a function of cooling water temperature and relative humidity; Bottom: Actual hourly and daily average values of COP_T measured over the day..

Fig. 4-2 to Fig. 4-6 also indicated the hourly average COP_T (blue triangles) taken from the 2012 experimental data. The evaporative cooler provided ΔT between 2°C and -7°C . While it was capable of performance at the maximum value (i.e. -7°C) this performance did not occur often. A heat rejection system with consistently high results would be preferable.

4.1.2 Thermal comfort and cooling water

When considering the effect of cooling water temperature on LDAC performance, the temperature and humidity should be considered to ensure the comfort of any users of the system. Discomfort can arise from both conditions that are too hot and humid as well as conditions that are too cold and dry.

The effect of cooling water temperature for the weather conditions that occurred on the 15th of August is shown in Fig. 4-7. Two fixed process air streams (Condition-1: 70% RH; Condition-2: 60% RH) were used as input air conditions. The recommended range of comfortable conditions is shown in pink for summer and blue for winter [3].

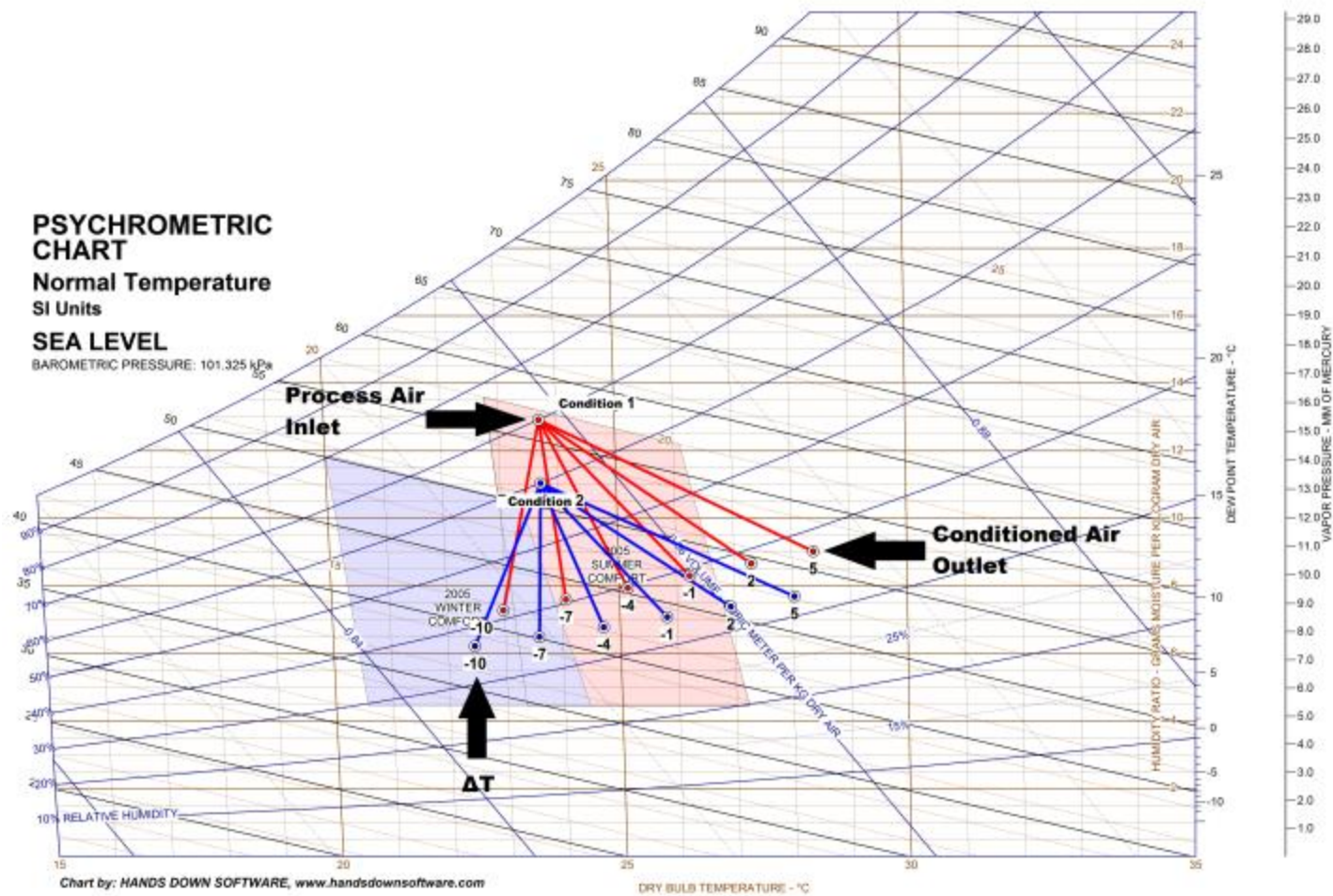


Fig. 4-7: Example of simulated process air inlet and outlet conditions (i.e., Condition 1: 70% RH; Condition 2: 60% RH) at different cooling water temperatures for August 15th 2012.

Conditions 1 and 2 represent different inlet air conditions. Each condition has been simulated at different ΔT 's (i.e., temperature differences between the cooling water and ambient air as previously discussed) to show the effect of the cooling water temperature. Each point represents the average process-air outlet condition over a single day using the specified constant inlet conditions. These results indicated that for inlet process-air at Condition-1, the cooling water temperature must be near the dry bulb temperature ($\Delta T=0$) to provide summer thermal comfort. If the LDAC system is operating at Condition 1 (Fig. 4-7), there is no need for the cooling water temperature to operate more than seven degrees below the ambient air temperature. Cooling water below this point would provide air too cold to be comfortable.

4.1.3 Annual System Performance

The annual performance of the LDAC system was simulated for the summer months (May to August). Typical meteorological year weather data (TMY) for Toronto were used to investigate the effect of cooling water operating temperature on COP_T during these summer months. The monthly average, minimum, and maximum ambient air temperatures from the Toronto TMY weather file are shown in Table 4-2.

Table 4-2: Ambient air temperature variations from May to August [67]

Months	Max. Temperature	Min. Temperature	Ave. Temperature
August	30.8	8.4	19.6
July	33	8.6	20.8
June	31.3	3.7	17.5
May	29.4	-4.6	12.4

As was shown earlier in Fig. 1-11, the operating range of cooling devices depends on their heat sink temperature. If the heat sink is ambient air, the lowest cooling water temperatures are based on either the wet-bulb temperature (evaporative cooling) or the dry-bulb temperature (sensible cooling). If the heat sink is the earth, the cooling water temperatures supplied to LDAC unit would be close to the average annual ground temperature [23].

The average overall COP_T values of the LDAC system using average relative humidity rates of 65% and 75% from May to September are presented in Fig. 4-8 and Fig. 4-9. The possible cooling range of heat rejection devices and their effect on the COP_T of the system indicates the feasibility of the different water cooling techniques.

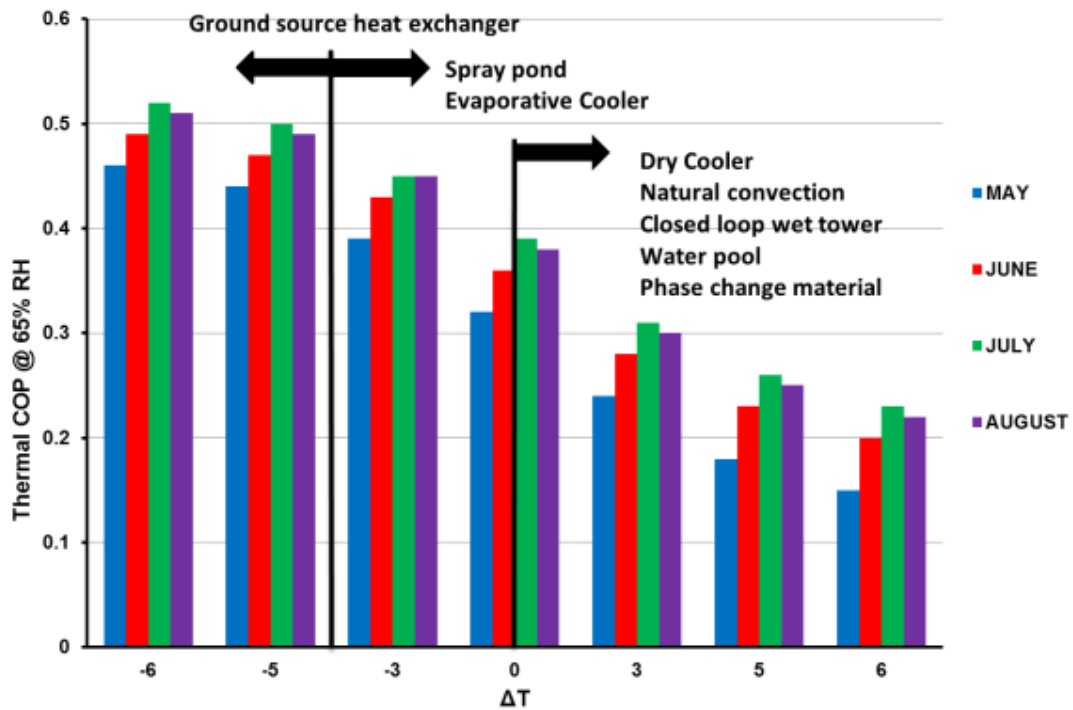


Fig. 4-8: Simulated average COP_T for each month and ΔT values at a fixed relative humidity of 65% in Toronto. The heat rejection technologies capable of producing each temperature are also shown.

Fig. 4-8 and Fig. 4-9 show that cooling devices with maximum cooling water temperature near ambient air dry-bulb temperature ($\Delta T = 0$) in summer months have the lowest COP_T with 0.32- 0.39 for 65% RH and 0.34- 0.41 COP_T for 75% RH. Evaporative cooling devices and a geo-exchanger can provide the coldest water temperature and highest COP_T .

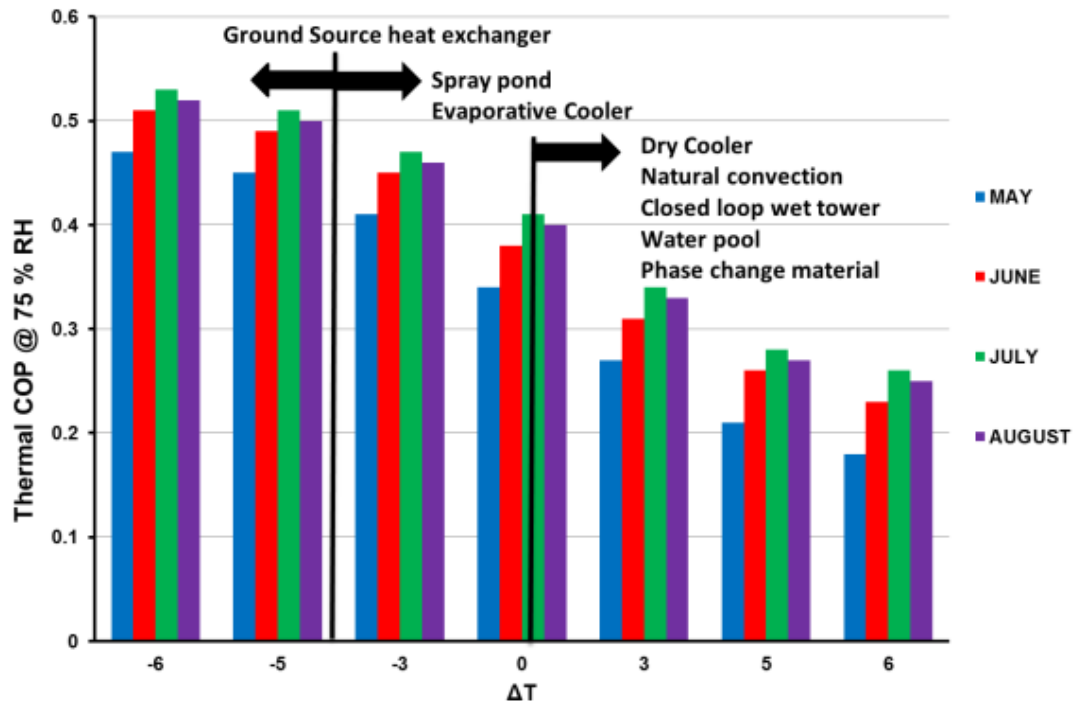


Fig. 4-9: Simulated average COP_T for each month and ΔT values at a fixed relative humidity of 75% in Toronto. The heat rejection technologies capable of producing each temperature are also shown.

4.2 Case B: Cold Water Storage System (Load shifting Model)

The addition of cooling water storage (CWS) allows cooling water to be supplied during times of high relative humidity. Fig. 4-10 shows experimental weather data recorded on July 11th, 2012 with clear sky conditions and an average absolute humidity of 10.3 (g_w/kg_a.) [8]. The data show that the ambient relative humidity was greater than 70% for the first 110 minutes of morning operation. This was followed by a period of low relative humidity in afternoon where the ECT could have been more effective at providing cooling than the CWS system. The proposed CWS system would allow the heat rejection load to be shifted out of the daytime periods and instead the heat could be rejected during the night. In this design, the ECT would not operate during the initial operating hours of the LDAC system, instead, the water from a CWS system would be used to cool the conditioner. Three different storage sizes were tested to find the optimum configuration.

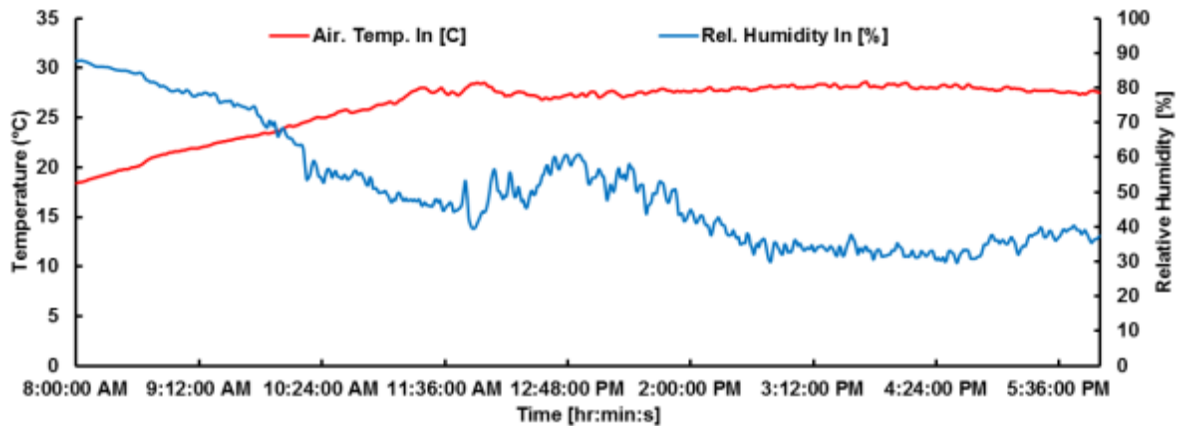


Fig. 4-10: Measured weather data for July 11th, 2013 [8].

Table 4-3 to Table 4-5 summarize the operation of the LDAC system using load shifting model for each testing day. The conditioner was operated from 8 AM to 6 PM.

Three system operations are shown for July 11th (sunny and dry), July 17th (sunny and humid) and August 13th (overcast and humid) to highlight the effect of various weather conditions on the system performance.

Table 4-3: Summary of the CWS simulation applied to experimental data recorded for the LDAC system on July 11, 2012.

11 th July					
	Initial volume of the tank (m ³)			SIM ¹	EXP ²
	10	15	20	-	-
Average ambient temperature (°C)	26.2				
Average ambient relative humidity (%)	50.7				
Average Radiation (W/m²)	714				
Average latent cooling rate (kW)	12.18	12.16	12.2	12.1	11.3
Average total cooling rate (kW)	12.7	12.74	12.8	12.6	11.0
Total electrical Consumption (kWh)	47.7	46.2	45.5	48.5	47.8
COP_T	0.55	0.55	0.55	0.52	0.47
COP_E	2.66	2.78	2.85	2.60	2.30
Total cooling rate improvement (%)	0.8	1.1	2	-	-
Energy consumption savings (%)	1.5	4.8	6.8	-	-
Cost savings³ (¢/day)	8.1	24.4	32.5	-	-

¹ simulation results according to Crofoot [8]

² experimental results from Crofoot for same period [8]

³ the average weighted hourly price of 10.9 (¢/kWh) before taxes and other fees.

Table 4-4: Summary of the CWS simulation applied to experimental data recorded for the LDAC system on July 17th 2012.

17 th July					
	Initial volume of the tank (m ³)			SIM ¹	EXP ²
	10	15	20	-	-
Average ambient temperature (°C)	32.4				
Average ambient relative humidity (%)	52.0				
Average Radiation (W/m²)	631				
Average latent cooling rate (kW)	17.8	19.40	18	17.6	16.9
Average total cooling rate (kW)	17.3	17.8	18	17.0	17.2
Total electrical Consumption (kWh)	47.3	46.6	45.8	50.1	50
COP_T	0.55	0.56	0.57	0.54	0.53
COP_E	3.65	3.85	3.93	3.4	3.4
Total cooling rate improvement (%)	1.8	4.8	6.1	-	-
Energy consumption savings (%)	5.6	7.3	9	-	-
Cost savings³ (¢/day)	29.1	37.2	45.3	-	-

Table 4-5: Summary of the CWS simulation applied to experimental data recorded for the LDAC system on Aug 13th 2012.

13th Aug					
	Initial volume of the tank (m³)			SIM¹	EXP²
	10	15	20	-	-
Average ambient temperature (°C)	24.4				
Average ambient relative humidity (%)	66.9				
Average Radiation (W/m²)	538				
Average latent cooling rate (kW)	16	16	16	16.0	14.6
Average total cooling rate (kW)	13.5	13.6	13.7	13.5	11.2
Total electrical Consumption (kWh)	49.5	48.8	47.3	50.1	50
COP_T	0.45	0.45	0.45	0.45	0.32
COP_E	2.74	2.79	2.90	2.70	2.20
Total cooling rate improvement (%)	0.6	0.9	1.4	-	-
Energy consumption savings (%)	1.1	2.6	5.8	-	-
Cost savings³ (¢/day)	5.7	13.8	30.1	-	-

4.3 Case C: Ground Source Heat Exchanger Results for LDAC System

As was mentioned earlier in Section 3.4, TRNSYS TYPE 557 was used to simulate four different borehole configurations using 10, 15, 20 or 25 boreholes. The operations of the air-handling unit are summarized in Table 4-6 to Table 4-8 for the same weather conditions as used in Case B (section 4.2). The results of these simulations, allows a direct comparison between the different systems and their performance. The Case B simulation has also been compared with previous Base Case experimental results (labeled EXP in tables) and simulation results (labeled SIM in tables). The results indicate that increasing the number of boreholes allows more heat to be rejected to the ground. As the heat rejection rate is increased, both the cooling rate and the COP_T of the LDAC system increased.

Table 4-6: Summary of geo-exchange (boreholes) simulation and experimental value from previous LDAC testing for 11th of July

11 th July						
	Number of boreholes (Rows X Columns)				SIM ¹	EXP ²
	10 (2X5)	15 (3X5)	20 (4X5)	25 (5X5)	-	-
Average ambient temperature (°C)	26.2					
Average ambient relative humidity (%)	50.7					
Average Radiation (W/m²)	714					
Average cold water supply (°C)	26.5	24	22.1	20.6	20.1	22
Average latent cooling rate (kW)	9.42	10.48	11.34	11.98	12.1	11.3
Average total cooling rate (kW)	6.72	9.04	1.82	12.22	12.6	11.0
Total electrical Consumption (kWh)	41	41	41	41	48.5	47.8
COP_T	0.38	0.46	0.51	0.55	0.52	0.47
COP_E	1.64	2.2	2.64	2.98	2.6	2.3
Energy consumption savings (%)	15	15	15	15	-	-
Cost savings³(¢/day)	81.7	81.7	81.7	81.7	-	-

¹ is in the simulation results recorded in 2012 by Crofoot, [8]

² is recorded experimental results from test site [8]

³ is the average weighted hourly price of 10.9 (¢/kWh) before taxing and other fees.

Table 4-7: Summary of geo-exchange (boreholes) simulation and experimental value from previous LDAC testing for 17th of July

17 th July						
	Number of boreholes (Rows X Columns)				SIM ¹	EXP ²
	10 (2X5)	15 (3X5)	20 (4X5)	25 (5X5)	-	-
Average ambient temperature (°C)	32.4					
Average ambient relative humidity (%)	52.0					
Average Radiation (W/m²)	631					
Average cold water supply (°C)	33.2	29.7	26.9	24.8	25.7	27.1
Average latent cooling rate (kW)	14.11	15.82	17.06	17.96	17.6	16.9
Average total cooling rate (kW)	9.79	13.20	15.73	17.70	17.0	17.2
Total electrical Consumption (kWh)	42.5	42.5	42.5	42.5	50.1	50
COP_T	0.37	0.46	0.52	0.56	0.54	0.53
COP_E	2.3	3.10	3.7	4.16	3.4	3.4
Energy consumption savings (%)	15	15	15	15	-	-
Cost savings³(¢/day)	82.8	82.8	82.8	82.8	-	-

Table 4-8: Summary of geo-exchange (boreholes) simulation and experimental value from previous LDAC testing for 13th of August

13 th Aug						
	Number of boreholes (Rows X Columns)				SIM ¹	EXP ²
	10 (2X5)	15 (3X5)	20 (4X5)	25 (5X5)	-	-
Average ambient temperature (°C)	24.4					
Average ambient relative humidity (%)	66.9					
Average Radiation (W/m²)	538					
Average cold water supply (°C)	28.4	25.5	23.3	20.3	22	21.75
Average latent cooling rate (kW)	13.10	14.31	15.22	15.90	16.0	14.6
Average total cooling rate (kW)	7.15	9.81	11.81	13.36	13.5	11.2
Total electrical Consumption (kWh)	42.6	42.6	42.6	42.6	50.1	50
COP_T	0.27	0.35	0.41	0.45	0.45	0.32
COP_E	1.68	2.30	2.77	3.13	2.70	2.20
Energy consumption savings (%)	15	15	15	15	-	-
Cost savings³(¢/day)	81.7	81.7	81.7	81.7	-	-

An example of the simulated performance of the LDAC system is illustrated in Fig. 4-11 for 25 boreholes, on July 11th. On this particularly dry day, the regenerator did not function between 2:45 PM and 5:30 PM because the process-air humidity was below the set-point (30%). As such, less heat was rejected to the ground during this time period. This led to reduced conditioner inlet desiccant solution temperatures and thus, lower cooling water outlet temperatures.

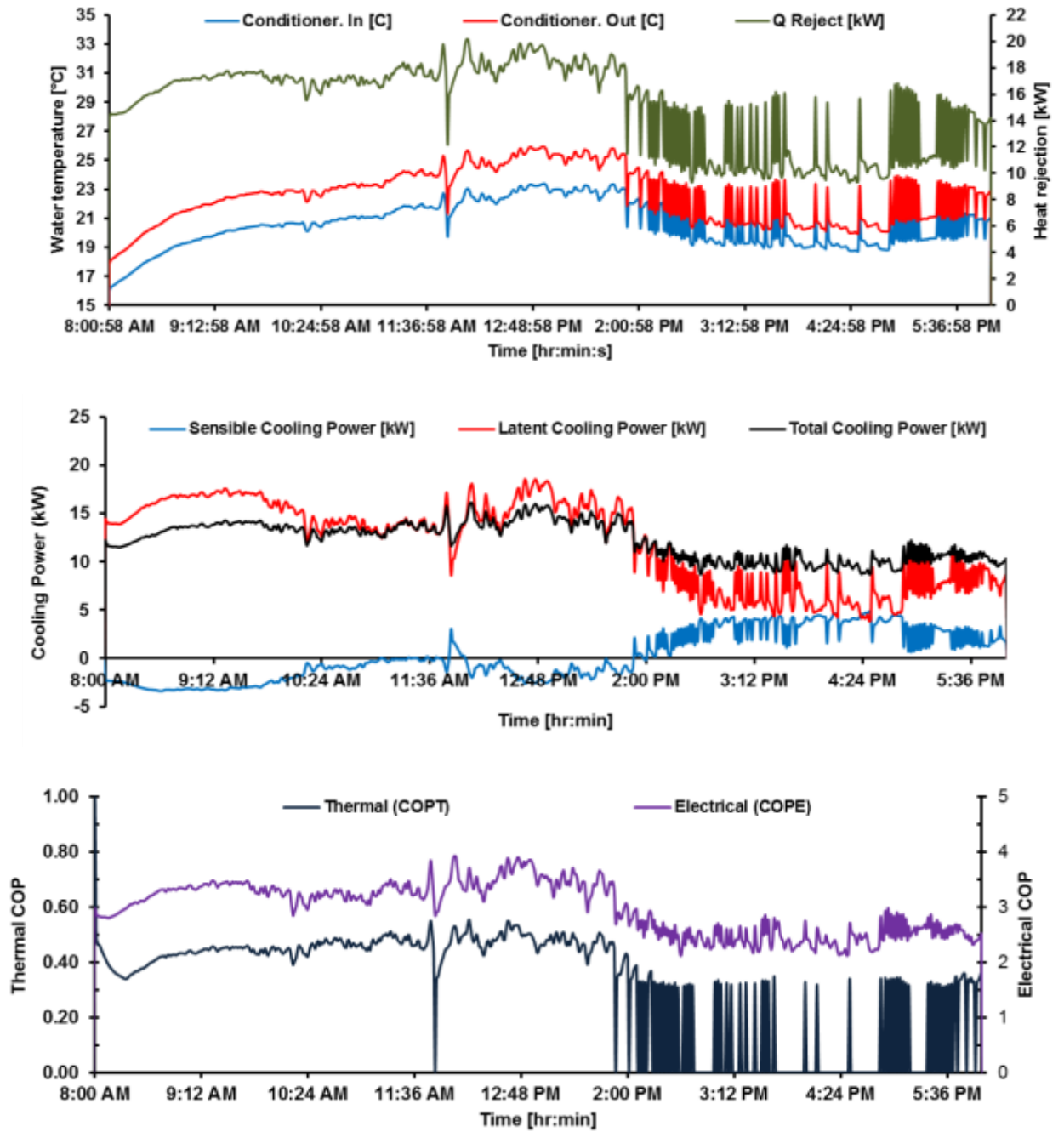


Fig. 4-11: Simulated performance for 25 boreholes on July 11th.

4.4 Experimental Investigation of a Stratified Cooling Water Storage Tank (SCWS) (Case D)

The effects on system performance of a stratified 6 m³ cold water storage tank were numerically and experimentally investigated. As was mentioned in section 3.5, in this configuration, cold water was provided to the conditioner during daylight hours (i.e., 8 AM - 5 PM) and heat rejection from the tank was accomplished using the ECT during the night hours (i.e., 5 PM - 8 AM).

To determine the level of thermal stratification inside the tank, temperature profiles in the SCWS were measured for the 9th, 16th and 17th of September, 2014. The results are shown in Fig. 4-12 to Fig. 4-14. Each temperature profile was plotted at each hour of the day during the LDAC's operation.

September 9th started with cold and humid ambient conditions of approximately 13 °C and 90 % relative humidity. After 10 AM, however, the relative humidity reduced to 50% as the ambient temperature increased to 20°C where it remained relatively unchanged for the rest of the day. Similar conditions were observed on the 16th of September with a 6°C cooler ambient temperature. In the afternoon, the relative humidity decreased to 47% with increasing air temperature up to 14°C. Similarly, cold and humid conditions were observed on the morning of September 17th. The ambient air temperature increased over the first four hours from 8°C to 19°C and resulted in a reduction in the relative humidity from 92% to 60%. This condition remained relatively unchanged after 11 AM.

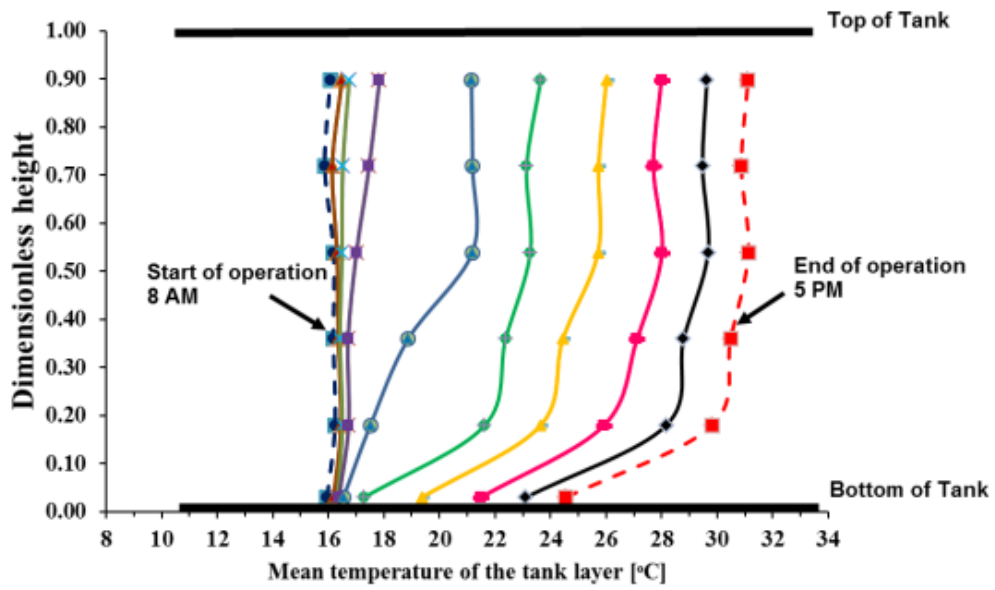


Fig. 4-12: Tank stratification for ten hours of operation for on September 9th

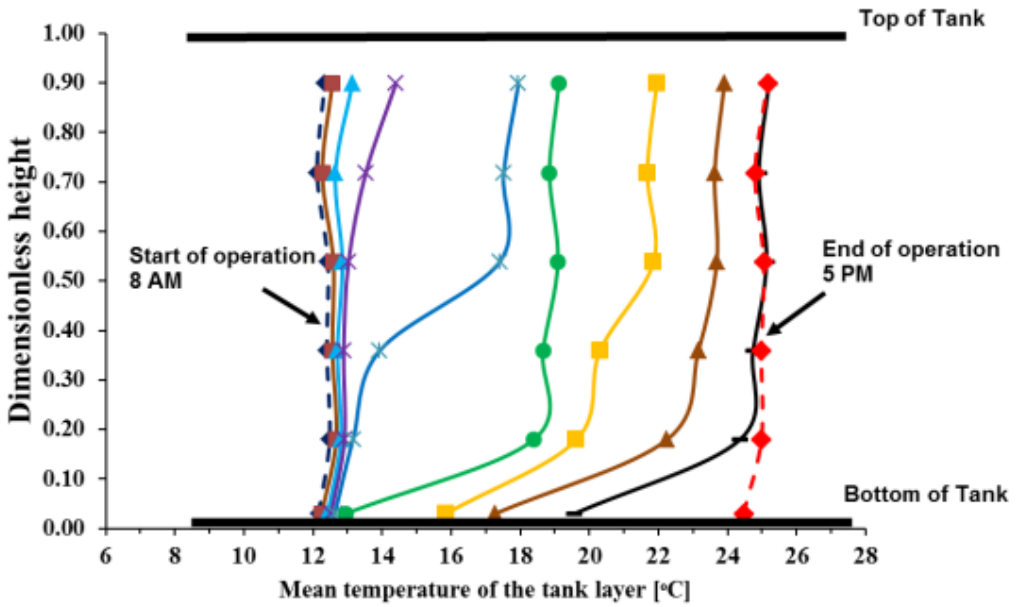


Fig. 4-13: Tank stratification for ten hours of operation on September 16th

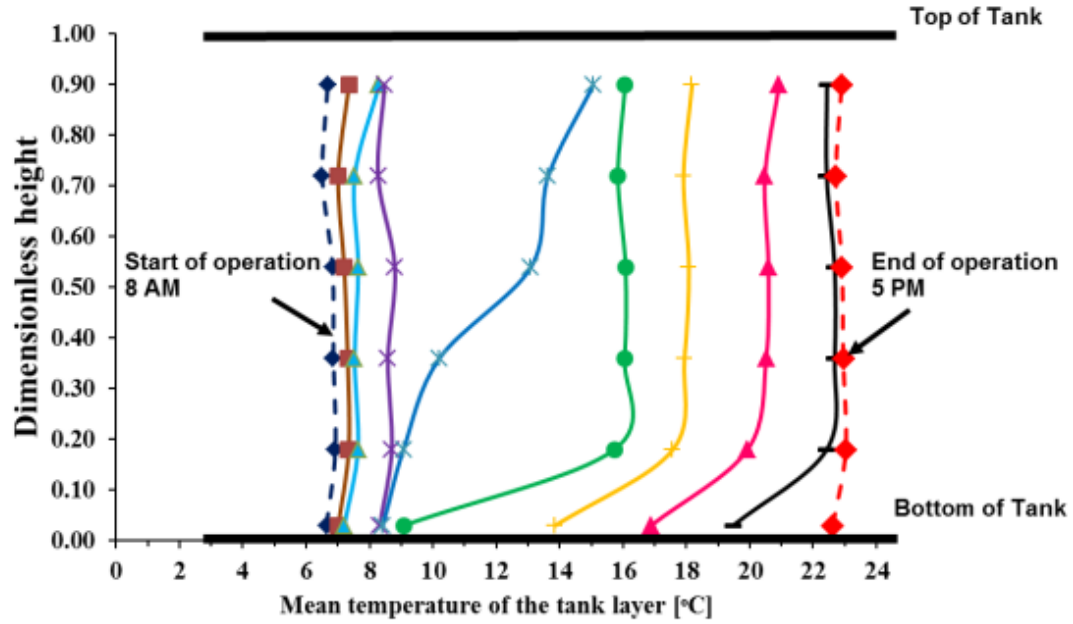


Fig. 4-14: Tank stratification for ten hours of operation on September 17th

Fig. 4-15 and Fig. 4-16 show the experimental data for night cooling taken from the evaporative cooler on two separate nights. The results indicate NCWS can cool the water tank between 6 °C and 16 °C and provide a low initial cold water temperature for the conditioner. To evaluate the water cooling performance of NCWS operation, the efficiency of evaporative cooling as defined by Berman, [79] was calculated. It is based on dimensionless parameter η_{ECT} , and can be written as,

$$\eta_{ECT} = \frac{T_{w,in} - T_{w,out}}{T_{w,in} - T_{lim}} \quad (4.2.1)$$

where $T_{w, in}$ is the temperature of hot water entering into the cooling water, $T_{w, out}$ is the average temperature of the cooled water in the pool of the cooling tower, and T_{lim} is the wet-bulb temperature. T_{lim} is the limiting temperature for an evaporative cooler at a given air temperature T_a and a relative humidity of ϕ and is obtained as follows:

$$\rho_s (T_a) \cdot \phi = \rho_s (T_{lim}) \quad (4.2.2)$$

where ρ_s is the density of saturated vapour, dependent on temperature, and T_a is the dry bulb temperature. η_{ECT} values calculated based on the simulated results in Fig. 4-15 and Fig. 4-16 indicate a relatively low average efficiency for period between 5 PM and 8 AM. The low efficiency is particularly evident during the nighttime hours where, as the ambient temperature drops, the relative humidity increases to the point that the capacity of the cooling tower is significantly reduced. This situation is a function of the local climatic conditions and an appropriate operational strategy may have to be modified to account for this situation. It is possible that an alternative cooling source or heat sink may be required for night operation; however, there is the potential of using off-peak power during the night.

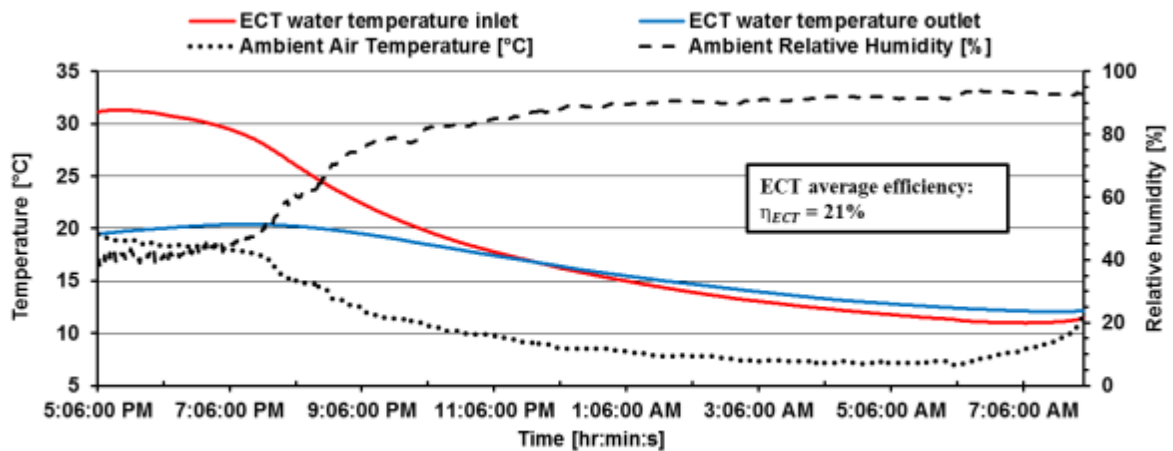


Fig. 4-15: Evaporative cooling tower operating condition and average efficiency for 8th and 9th of September

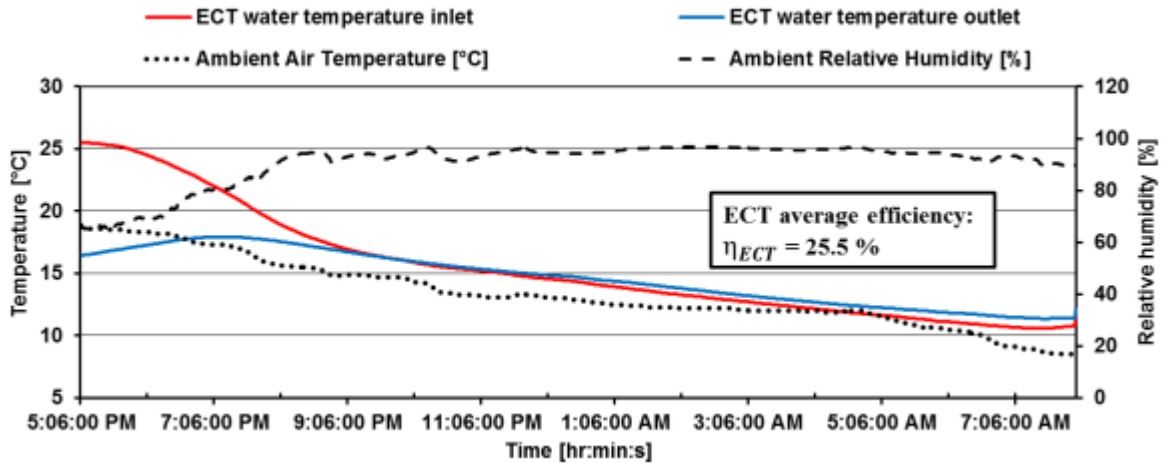


Fig. 4-16: Evaporative cooling tower operating condition and average efficiency for 15th and 16th of September

4.4.1 SCWS Simulation

The experimental results were used to verify the simulation model of the stratified storage tank. This model was then integrated into the Case B simulation. Under this scenario, the simulated SCWS tank operated in the same two distinct modes of operation as was used for the standard CWS: i.e., providing cold water to the conditioner, or rejecting thermal energy from the tank. As mentioned in section 3.5, cold water was provided to the conditioner during daytime hours (i.e., 8 AM to 5 PM) and heat rejection from the tank was done using the ECT during nighttime hours (i.e., 5 PM to 8 AM). A more detailed discussion of the simulation is given in Appendix B.

The stratification of the tank was found to significantly influence the performance of the system. As well, the cooling water flow rate influenced the level of stratification in the storage tank. Simulations were run at different flow rates to find the optimal value.

The results of these new simulations are shown in Fig. 4-17. Further results and analysis are discussed in Appendix B.

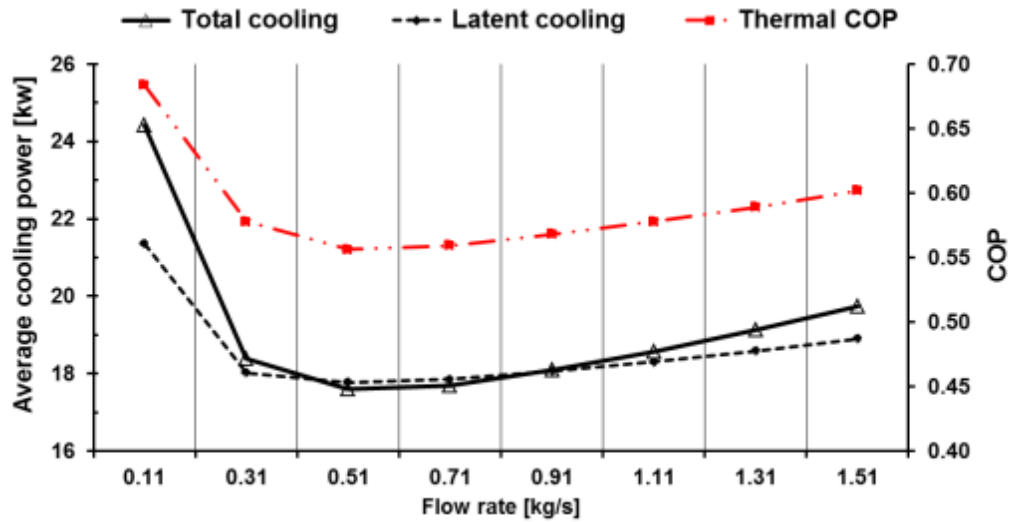


Fig. 4-17: Simulated average air cooling power and thermal COP for various cooling water flow rates on July 17th.

Chapter 5

Discussion of Results

Several different heat rejection methods were described in Chapter 3 and the results obtained for these heat rejection methods via simulation and experimentation are presented in Chapter 4. This chapter provides a discussion on these results and highlights differences between the current and previously available research.

5.1 Case A: Cooling Water Temperature Model

Finding an appropriate range of cooling water temperatures is a useful tool that can be used for selecting an appropriate heat rejection system. For the LDAC unit studied, the desiccant dehumidifier maintains a low desiccant vapour pressure by circulating the cooling water through channels in the absorber plates. This increases the effectiveness of the dehumidification process (i.e., increases the humidity absorption rate). The cooling water temperature also affects the sensible cooling of the process-air stream, which improves the heat and mass transfer [80] [81].

The simulation results shown in Fig. 4-2 to Fig. 4-6 indicated that the COP_T of the LDAC system increases with decreasing cooling water temperatures. The heat exchange between the desiccant and the cooling water inside the conditioner reduces the partial pressure of the concentrated desiccant and increases the moisture removal rate. This increase in the latent cooling rate along with an increase in the sensible cooling rate improve the COP_T of the unit.

It is also evident from Fig. 4-2 to Fig. 4-6 that increasing the process-air relative humidity, at fixed process-air temperature, results in increases to the latent cooling power and COP_T of the LDAC system. However, the effect of relative humidity on the COP_T becomes insignificant as the temperature of the cooling water reaches 7°C below the average ambient temperature for all simulated days. This is due to the fact that the rate of reduction in the desiccant partial pressure reduces with lowering cooling water temperature (see 3.1.1).

The cooling water temperature also affects the regenerator's performance. Reducing cooling water temperature reduces the temperature of the dilute solution leaving the absorber which increases the regenerator's demand for heat. However, the lower concentrations in the regenerator enhance the desorption rate that normally leads to higher regenerator COP_R , and potentially, a higher overall COP_T (Fig. 4-1).

The percent improvement of COP_T for every three degree reduction in cooling water temperature is shown for July 11th, July 17th, July 23th, August 13th, August 15th in Fig. 5-1. Although the colder water temperature results in a higher COP_T , the cooling-rate improvements are greater at higher water temperature values. In other words, the improvement seen between, 5°C above ambient to 2°C above ambient, is greater than the improvement seen from reducing the temperature, from 2°C above ambient to 1°C , below ambient. It can be seen from Fig. 5-1 that the improvement in COP_T is 22.5% higher, for a change from 5°C to 2°C , than for a change of -7 to -10°C . This trend is seen for all humidity values.

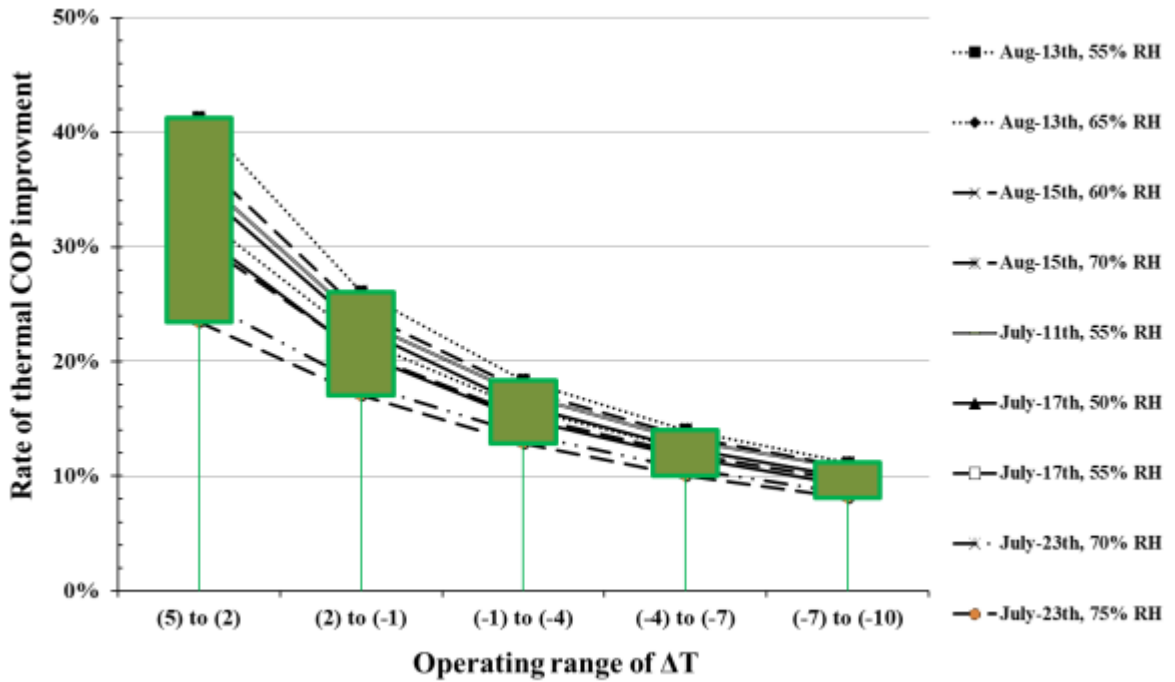


Fig. 5-1: Case A, thermal COP improvement for every three degree change in cooling water temperature for different operating days in Kingston.

Cooling water temperature affects the cooling performance, and thus the thermal comfort of the outlet process-air stream. Fig. 4-7 displays an example of outlet air conditions on a psychrometric chart at different cooling water temperatures. For an inlet process-air relative humidity of 70%, thermal discomfort would be present if the cooling water temperature is more than 1°C above the dry-bulb temperature. On the other hand, a cooling water temperature 7°C below the ambient temperature (i.e., $\Delta T = -7^\circ\text{C}$) will no longer deliver process air within the summer thermal comfort zone.

The goal of the cold water temperature simulations was to find appropriate cooling water technologies. Fig. 4-8 and Fig. 4-9 indicate several different heat rejection devices along with their typical cooling ranges, categorized depending on the heat sink temperature. While, the annual simulation results indicated that the performance of the LDAC system was higher, for July and August, than for, May and June (due to the higher

ambient temperatures seen later in the summer), the trends in the performance of the various heat rejection devices remained similar. The analysis in Chapter 4 showed that technologies that produced with the lowest cooling water temperature resulted in the highest COP_T .

Consequently, ground-source heat exchangers (e.g., bore-hole storage) and evaporative coolers showed the best cooling performance, especially when compared to dry coolers that are limited by the ambient dry-bulb temperature.

5.2 Case B: Cold Water Storage System (Load shifting Model)

When the ECT was operated in humid conditions, the heat rejection rates were reduced leading to an ineffective operation. To improve performance, cooling water storage (CWS) was investigated as a way to reduce ECT usage during periods of higher ambient humidity. As expected, the simulation results for different CWS volume capacities (i.e., 10, 15, and 20 m³) revealed that higher volumes will provide increased cold water storage capacity (Fig. 5-2). This leads to lower average cooling water temperatures and improved LDAC performance.

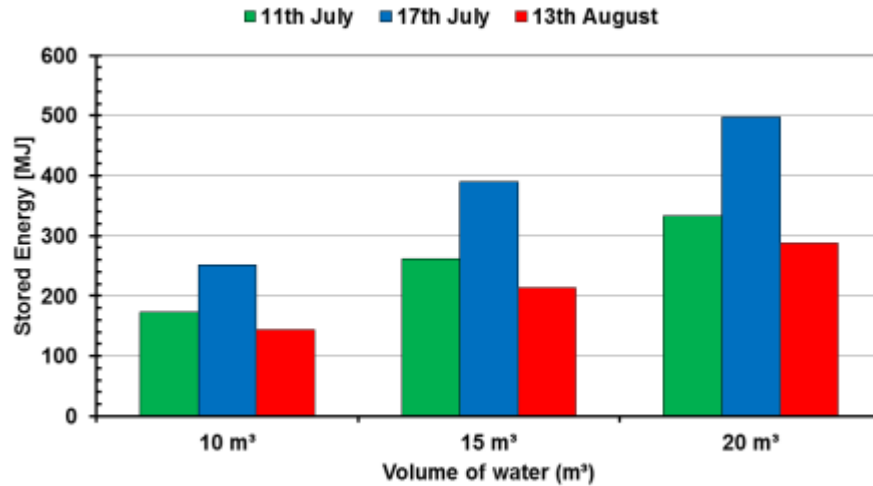


Fig. 5-2: Stored cooling energy at various storage volume.

Comparing the cooling water storage simulation (CWS) to the ECT simulation (base case) indicated that total cooling rate and COP_T increased up to 6%. The simulation results showed that the 10-20 m³ CWS increased the COP_E by 2.5-10 % on 11th July, by 8-16 % on 17th July, and by 1-7 % on 13th August. The improvement in COP_E was due to the ECT's fan electrical consumption being reduced (since it was not operated for as long during the day), and the increase in total cooling rate. The fan's power consumption was assumed to be constant at 746 W (1 horsepower) while the cooling tower was running and zero when the CWS system was running.

The CWS reduced the total power consumption, as shown in Table 4-3. This reduction occurred partially during peak energy demand times when the utility companies charge a higher rate. For estimating the cost savings, the mid-peak price of electricity was assumed to be 10.9 ¢/kWh, not considering other fees (tax, delivery, etc.) [82].

5.3 Case C: Ground-source Heat Exchanger Results for LDAC System

Type 577 was used to model a ground-source heat rejection system. TRNSYS simulations were conducted using four different configurations which each used a different number of boreholes (10, 15, 20, or 25 boreholes, with five boreholes per series). All boreholes were set at a depth of 10m below the ground surface. To highlight the effect of various weather conditions the on systems performance, three different weather conditions were simulated. The results indicate that increasing the number of boreholes ensured that more heat was dumped into the ground and thus both the cooling rate and the COP_T of the LDAC system were increased.

The use of ground-source heat exchangers as a method for rejecting heat to the earth was compared to the base case that consisted of only using the evaporative cooling tower. The performance was compared for the reference days previously described (e.g., July 11, 17, and August 13). Simulation results indicated that only the 25 borehole configuration (arranged in a 5 x 5 array) improved the overall system performance. For example, the COP_T of the LDAC system was improved by up to 6% over the base system with ECT only. From the average simulation results presented in Fig. 5-3, it was observed that, over the course of each of the tested days (i.e., Aug 13th followed by July 7th and 11th), at least 25 boreholes were required to provide the same COP_T as the base case using ECT.

The improvement in the COP_E was due to the removal of the ECT fan's electrical power consumption. The simulation results in Fig. 5-4 showed that the 20 and 25 boreholes could increase the COP_E by: 1 and 15%, respectively, on July 11th; 8 and 23%, respectively, on July 17th; and, 2 and 16%, respectively on Aug 13th.

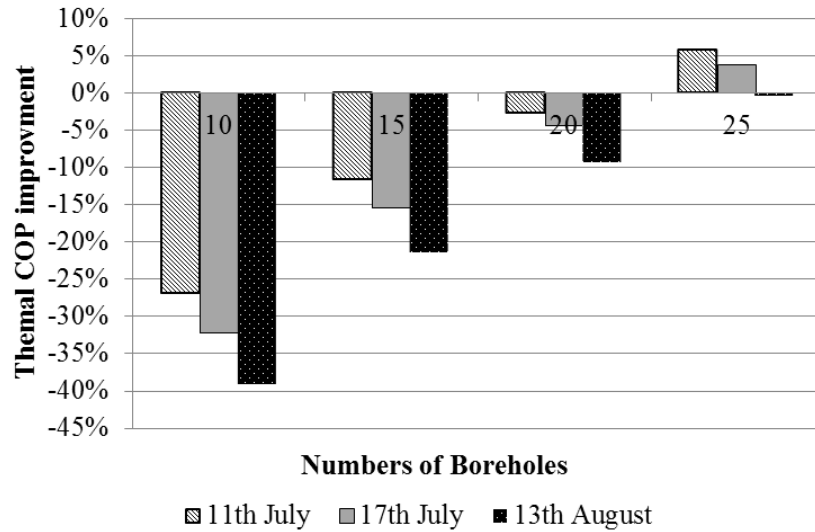


Fig. 5-3: Improvement in system COP_T as a function of the number of boreholes as compared to the base case (ECT only system) for three reference days

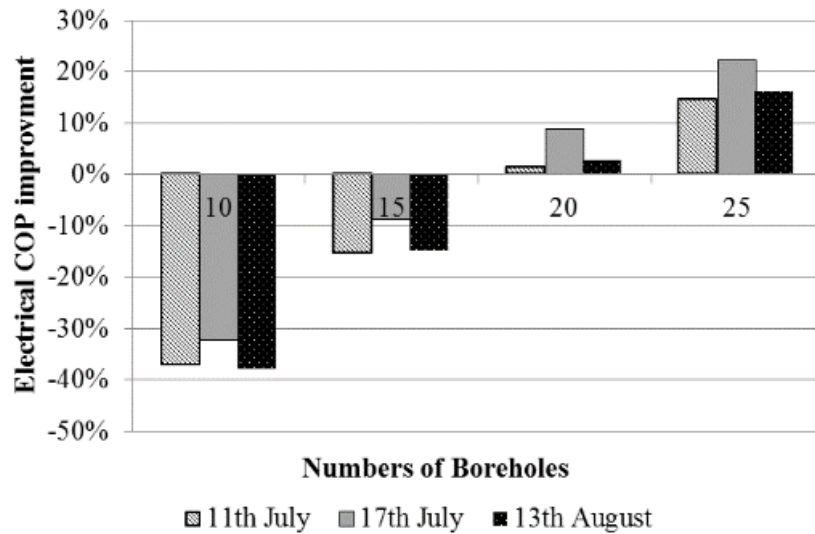


Fig. 5-4: Improvement in system COP_E as a function of the number of boreholes as compared to the base case (ECT only system) for three reference days

The cost of a geothermal installation is relatively high in comparison with other heat rejection techniques although, the cost varies depending on the location, type of ground (clay, wet shale, limestone, etc.), drilling methods, available equipment and materials, etc. The high capital cost tends to be due to the cost of drilling and lining the

boreholes. This is usually one of the more important contributing factors to the overall cost of a geothermal system, and the price increases with depth. In 2006, the costs of drilling, pipe, and grout were estimated to be \$33.00/m, \$1.31/m, and \$0.199/m, respectively [83]. Even with inflation at moderate levels over the last decade, the cost of a borehole storage can be significant (Fig. 5-5).

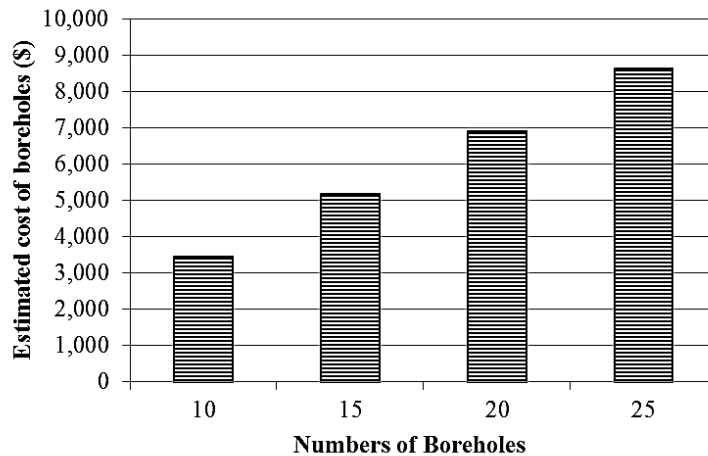


Fig. 5-5: Cost of borehole storage based on 2006 estimates [83]

5.4 Experimental Investigation of Stratified Cooling Water Storage Tank (SCWS) (Case D)

As described in Chapter 4, the use of a stratified cooling water storage was studied both experimentally and by simulation. From the experimental results displayed in Fig. 4-12 to Fig. 4-14, the level of thermal stratification attained during the operation of the LDAC system can be seen. Values are plotted for each hour of operations and at various dimensionless heights (H/L). The results indicate that the top of the storage tank attained a temperature 7°C warmer than the bottom of the tank. The time for the thermocline to pass from the initial (top of the tank) to the final (bottom of the tank) depended on the amount of heat rejected from the LDAC system. This typically took

approximately 3 to 4 hours. Under this operational scheme, the storage tank was cooled during the night by circulating the water through the cooling tower. Depending on the conditions of the night prior to the test days, this resulted in an initial morning tank temperature between 6°C to 16°C.

The experimental results demonstrated the potential of using night cooling to precondition the storage tank (i.e., lower its temperature) in preparation of offsetting the daytime load. However, as discussed previously, Fig. 4-15 to Fig. 4-16 indicated that continuously operating the ECT during the night (i.e., after 12 PM) resulted in decreased evaporative cooling and efficiency, due to cold and humid weather conditions observed during this period. This observation is important for the optimization of night cooling water storage (NCWS) which may result in decreased ECT performance but may shift peak electrical demand to night off-peak periods. Further research in the apparent tradeoffs is recommended accounting for variations in regional climatic conditions.

In the base case, the ECT operational performance depended on the ambient air humidity and temperatures, while the SCWS operational performance (case D) depends on the initial temperature of the tank and the degree of stratification obtained.

The SCWS simulation results for the three reference days are shown in Table B-1 of Appendix B and indicate that the COP_E of SCWS was improved up to 26% when compared with based case system using ECT only. The simulation results also indicated that reducing the cooling water flow rate resulted in a higher degree of stratification, increased the duration of the cold water delivery, and increased the temperature leaving the conditioner. It was also observed in Fig. B-5 that increasing the inlet cooling water temperature into the conditioner during the later hours of the day had a negative impact

on the cooling performance of the LDAC unit. Therefore, the cooling water flow rate should be adjusted so that the storage can supply cooling water for the duration of the LDAC operating hours.

5.5 Comparison of Different Cases

To accomplish this study, a detailed simulation previously developed to model a base case LDAC configuration was used. The base case utilized an evaporative cooling tower to reject heat in an on-demand configuration [8]. This simulation was validated by comparison with twenty days of experimentally monitored data take over the summer of 2012. For the current study, three representative day's data were selected from the monitored data and used as the basis for the performance evaluation presented in thesis. Four main cases were considered and the simulation of the base case system modified to allow these alternative heat rejection approaches to be evaluated.

In Case A, the effect of cooling water temperature on cooling performance (COP_T) was simulated. The results indicated that the effect of cooling water temperature on COP_T diminishes as the cooling water temperature reduces.

System operation and performance were compared in Case B and Case C for two alternative heat rejection approaches that were devised to provide different cooling water temperatures at different times. In particular, the use of a cooling water storage tank, and geo-exchangers (i.e., using boreholes at the ground temperature to improve cooling) were simulated for the three reference days (i.e., 11 July, 17 July and 13 August).

For Case B, the comparison between the mixed cooling water storage tank with a volume of 10 m^3 , and the base case, indicate that the average COP_E could be improved by 4.5% with a 2% improvement in COP_T . A goal of Case B was to shift daytime heat rejection loads to “off-peak” time periods. The success of this scheme depends on a number of factors that relate to the storage capacity and temperature, and to local climatic conditions (particularly if an ECT is to be used during high-humidity night times). For this reason, further study in this area would be of value.

In Case C, the LDAC system was modeled with a borehole field to allow heat rejection to the earth at an assumed constant temperature. The results indicate that the average COP_E improved by 18% with 25 boreholes while, for comparison, for Case B, with 20 m^3 tank, the average COP_E was improved by 11%. In addition, the results showed that, for both cases B (with a 20 m^3 tank) and Case C (with 25 boreholes at greater than 10 m deep); the COP_T was improved by 6% at the same cold water flow rate.

The percent improvement in COP_E over the base case for Case B (at different tank volumes) and Case C (for different number of boreholes) is shown for the three reference days in Fig. 5-6 to Fig. 5-8. In case B, electrical power consumption was due to the operation of the LDAC unit’s fans and pumps and the periodic operation of the cooling tower (although the latter could be shifted to off-peak times). In case C, cooling tower operation was not considered and so variations in COP_E were primarily due to increased LDAC cooling capacity that increase with the number and capacity of the borehole field. It should also be noted that from an economic point of view, the capital cost of Case C would most likely be higher than Case B but the operational costs of Case C would lower than Case B.

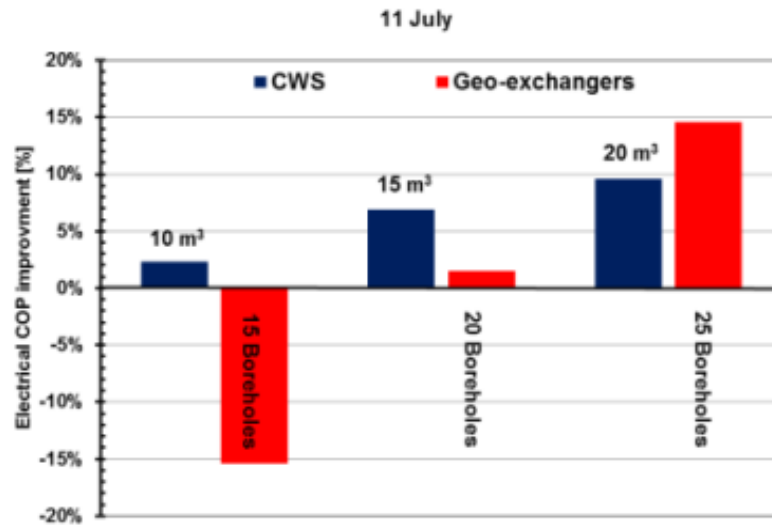


Fig. 5-6: Electrical COP improvement comparison for case B and C for July 11th

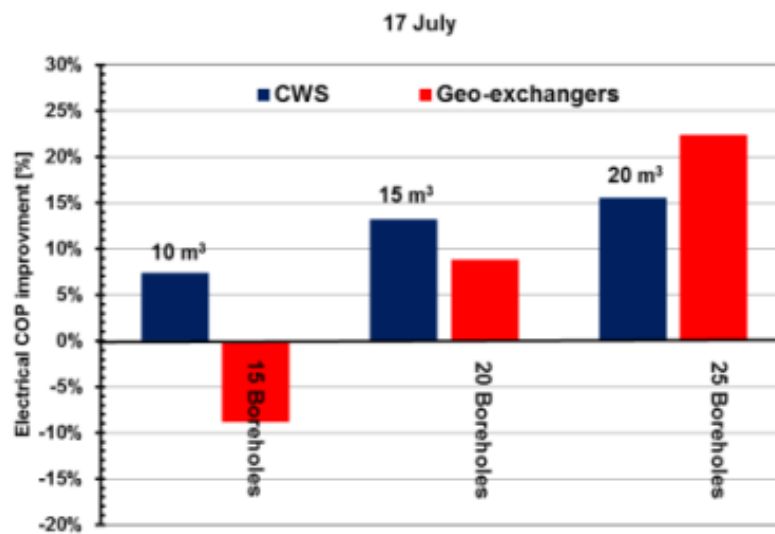


Fig. 5-7: Electrical COP improvement comparison for case B and C for July 17th

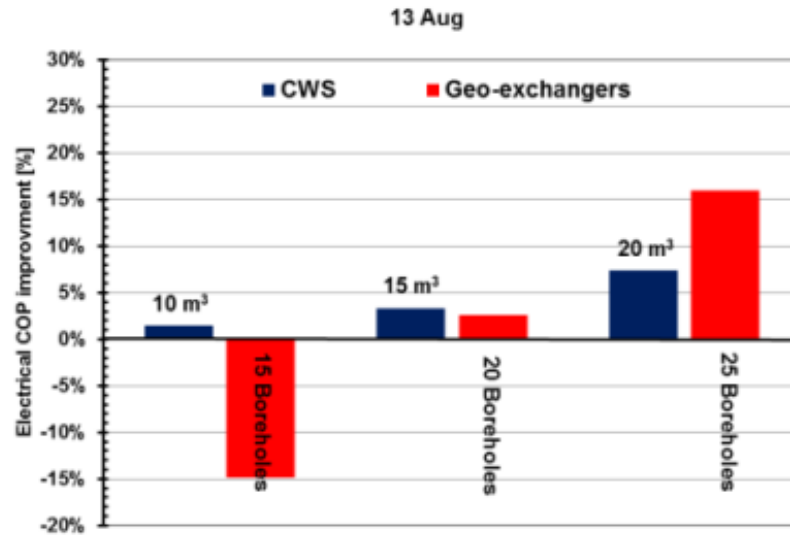


Fig. 5-8: Electrical COP improvement comparison for case B and C for August 13th

From the results given in Table 4-3 to Table 4-5 it can be seen that the high tank storage capacity (mixed water tank) and low initial temperature of Case B resulted in better electrical and thermal performance. This system's performance was further analyzed by varying the tank volume and initial temperature.

In Case D, a 6 m³ stratified CWS tank (SCWS) and night cooling was studied experimentally and by computer simulation. In this case, the large stratified water storage tank was used to store cooling water that was generated during the night cooling operation of the ECT. The stored cooling water was then used during the daytime to absorb heat rejected by the LDAC unit.

In case D, stratification existed for 3 to 4 hours. This meant that cool water was delivered for a longer period of time for Case D than for Case B, as mixing of the Case B tank contributed to a steadily increasing supply temperature. Therefore, it was concluded that a smaller storage could be used for the Case D while maintaining a high performance.

Simulations conducted for a 6 m³ SCWS tank (Case D) are presented in Appendix B and indicate that the average COP_E was improved by 9% over the base case for and initial tank temperature equal to the early morning ambient air temperature. If lower initial tank temperatures can be achieved by the night cooling system, higher COP_E and COP_T can be achieved.

Overall, by analyzing the performance in each of the presented cases, it can be concluded that Case C with 25 boreholes showed better COP_E than Case B whereas the COP_T improvement of Cases C and B is almost same. When comparing Cases B (with a mixed tank) and D (with a stratified tank) it was observed that stratified tank has a higher potential to improve the COP of the system, depending upon the water flow rate.

Chapter 6

Conclusions and Recommendations

6.1 Conclusions

Various heat rejection methods for a liquid desiccant air-conditioning system were evaluated using both simulations and experiments. Three different cases (Cases A, B, and C) were modeled in TRNSYS and compared to the base case to evaluate their performance. Each of these different systems has been designated as follows:

- Base Case: LDAC with Evaporative cooling tower;
- Case A: Cooling water temperature model;
- Case B: Cooling water storage system model (Load-shifting) ;
- Case C: Ground source heat exchanger model;
- Case D: The experimental investigation of a stratified cooling water storage tank (SCWS) with night cooling (i.e., NCWS).

In Case A, the effect of cooling water temperature on the COP_T of a LDAC system was investigated based on daily and annual performances. From these results, the following outcomes can be highlighted:

- Reducing the temperature of the inlet cooling water improved the COP_T of the LDAC system, but caused diminishing returns as the temperature range was lowered.

- It was also shown that with an increase of inlet air humidity at constant cooling water temperatures, a higher COP_T was achieved. However, the effect of relative humidity on COP_T became negligible as the inlet cooling water temperature reached 7°C below the ambient air temperature.
- The range of inlet cooling water temperatures that could provide adequate thermal comfort for the occupants in the cooling space was found to be 1 to 7°C degrees below the ambient conditions.

Cases B and C were simulated using a cooling water storage tank and geo-exchangers. The results of the simulations were compared with the base case simulation results under the same weather conditions. From these results, the following outcomes can be realized:

- The COP_T for cases B and C was improved by up to 6% for the same cooling water flow rate.
- The average COP_E for case B was up to 11% higher than the base case, based on operation over three separate days.
- For case B, increasing the storage tank volume resulted in increased values of COP_E and COP_T for the system as the CWS was able to store more cooling energy. This allowed the system to operate for longer periods of times without running the cooling tower.
- The average COP_E for Case C (bore-hole heat exchange) was improved by up to 18% over the base case when compared over three separate days.

- From an economic point of view, the capital cost of Case C is higher than Case B. However, the operational cost of Case C is lower than Case B due to elimination of the fans.

In order to evaluate the volumetric capacity of the cooling water storage tank and validate the simulation model used, the stratification of a SCWS with a capacity of 6 m^3 was numerically and experimentally investigated. The numerical results were found to be in good agreement with the experimental results.

- The comparison with the base case resulted in an average COP_E improvement of 9%. It was also noted that stratification exists for 3- 4 hours with a flow rate of 41 L/min.
- Maintaining a stratified tank led to higher LDAC performance. Lower flow rates lengthened the amount of time cold water could be supplied to the LDAC unit. In this way the COP_T could be increased up to almost 0.7.

In conclusion, the results obtained in the cases mentioned above, showed that case C has a higher COP_E improvement than case B, whereas the COP_T improvements of cases C and B are similar. When comparing cases B and D it was observed that the stratified tank has the better potential of improving the COP value.

6.2 Recommendations for Future Research

There are still several other avenues of research open to potentially improve the LDAC system's performance. An alternative approach to reducing demands on the "grid-supplied" electricity is to power fans with photovoltaic modules. Recent cost reductions in PV solar cells have yielded positive results with sufficient solar insolation values.

Pre-cooling the air before it enters the conditioner can be an effective strategy to increase the cooling performance, since this will result in a higher relative humidity which enables an increase in latent cooling. This can be achieved with a sensible heat exchanger or heat pump.

Future work in this area could involve the application of alternative control systems to control regenerator operation. The regenerator is currently controlled by an ambient air relative humidity sensor, which is triggered by a pre-determined set-point. This control system can be replaced with a water level sensor, which would indicate the volume of desiccant in the sump. This could result in a reduction in natural gas consumption of the boiler as it will only be operated when desiccant regeneration is required.

References

- [1] Statistics Canada, "Report on Energy Supply and Demand in Canada,1990–2010," Natural Resources Canada, Ottawa, 2012.
- [2] ASHRAE 62.1, "Ventilation for acceptable indoor air quality," *ANSI/ASHRAE*, 2013.
- [3] ASHRAE, "Ventilation and acceptable indoor air quality in low-rise residential buildings," *ANSI/ASHRAE*, 2013.
- [4] M. Mujahid Rafique, P. Gandhidasan, Shafiqur Rehman, and Luai M. Al-Hadhrami, "A review on desiccant based evaporative cooling systems," vol. 45, pp. 145-159, May 2015.
- [5] Henning and Hans-Martin, "Solar-Assisted Air-conditioning in Buildings: A Handbook for Planners," 2, Ed., New York, Springer-Verlag Wien.
- [6] Harriman L G, Plager D, and Kosar D, "Dehumidification and cooling loads from ventilation air," vol. 39, no. 11, 1997.
- [7] Lewis G. Harriman III, Dean Plager, and Douglas Kosar, "Dehumidification and cooling loads from ventilation air," *ASHRAE Journal*, 1997.
- [8] L. Crofoot, "Experimental evaluation and modeling of a solar liquid desiccant air conditioner," Master's Thesis, Queens University, Kingston, Ontario, 2012.
- [9] Michael J. Moran and Howard N. Shapiro,, *Fundamentals of Engineering Thermodynamics*, 4 ed., John Wiley & Sons, pp. 529-531.
- [10] SOLAIR, "Technology," SOLAIR, 2009. [Online]. Available: <http://www.solair-project.eu/114.0.html>.
- [11] Ali Al Alili, Isoroku Kubo, Yunho Hwang, and Reinhard Radermacher, "Review of Solar Cooling Technologies,," vol. 14, May/2008.
- [12] Keith E. Herold, Reinhard Radermacher, and Sanford A. Klein, *Absorption chillers and Heat pumps*, New York: CRC press, 1996.

- [13] S. C. Kaushik and J. V. Kaudinya, "Open cycle absorption cooling: a review," *Energy Conversion and Management*, vol. 29, no. 2, 1989.
- [14] Pietro Mazzei, Francesco Minichiello, and Daniele Palma, "HVAC dehumidification systems for thermal comfort: a critical review," *Applied Thermal Engineering*, vol. 25, no. 5–6, pp. 677-707, April 2005.
- [15] P. N. Ananthanarayanan, *Basic Refrigeration and Air-Conditioning*, New Delhi: Tata McGraw-Hill Education, 2013.
- [16] ASHRAE Standard, *Method of Test for rating Desiccant-Based Dehumidification Equipment*, Atlanta, GA: ASHRAE , 2009.
- [17] Henning and Hans-Martin, "Solar-Assisted Air-conditioning in Buildings: A Handbook for Planners," 2, Ed., New York, Springer-Verlag Wien.
- [18] R.Z. Wang, T.S. Ge, C.J. Chen, Q. Ma, and Z.Q. Xiong, "Solar sorption cooling systems for residential applications: Options and guidelines," *International Journal of Refrigeration*, vol. 32, no. 4, pp. 638-660, 2009.
- [19] Solar Heating and Cooling, "Technology Roadmap," OECD/IEA, 2012.
- [20] IEA SHC Task 38, "Solar Cooling Position Paper," Solar Air-Conditioning and Refrigeration, October 2011.
- [21] Herbert W. Stanford. III, *HVAC Water Chillers and Cooling Towers: Fundamentals, Application, and Operation*, 2 ed., CRC Press, 2012, pp. 23-24.
- [22] McNevin, C., and Harrison, S., "Performance improvements on a solar thermally driven liquid desiccant air-conditioner," Toronto, Canada, 2014.
- [23] Michael Becker, Martin Helm, and Christian Schweigler, "Subtask A Report A2, Collection of selected systems schemes "Generic Systems"," IEA SHC Task 38 Solar Air-Conditioning and Refrigeration, November 2009.
- [24] B. M. Jones, *Field Evaluation and Analysis of a Liquid Desiccant Air Handling System*, Kingston, Ontario: Master's Thesis, Queen's University, 2008.
- [25] W. P. Jones, *Air Conditioning Engineering*, New York: taylor & francis group, 2011.

- [26] ASHRAE, "AIR-COOLING AND DEHUMIDIFYING COILS," in *HVAC Systems and Equipment (SI)*, Handbook, ASHRAE, 2012.
- [27] A. Y. Khan, "Cooling and dehumidification performance analysis of internally-cooled liquid desiccant absorbers," *Applied Thermal Engineering*, vol. 15, no. 5, pp. 265-281, 1998.
- [28] Pradeep Bansal, Sanjeev Jain, and Choon Moon, "Performance comparison of an adiabatic and an internally cooled structured packed-bed dehumidifier," *Applied Thermal Engineering*, vol. 31, no. 1, pp. 14-19, 2011.
- [29] Oh MD, Kim SC, Kim YL, and Kim Y., "Cycle analysis of air-cooled, double-effect absorption heat pump with parallel flow type.," in *International Absorption Heat Pump*, New Orleans, 1994.
- [30] Kwon, Jung-In Yoon, and Oh-Kyung, "Cycle analysis of air-cooled absorption chiller using a new working solution," *Energy*, vol. 24, no. 9, pp. 795-809, 1999.
- [31] Izquierdo, M., Lizarte, R., Marcos, J.D., Gutierrez, G., "Air-conditioning using an air-cooled single effect lithium bromide absorption chiller: Results of a trial conducted in Madrid in August 2005," *Appl. Thermal. Eng.*, vol. 28, no. 8-9, pp. 1074-1081, 2008.
- [32] A. González-Gil, M. Izquierdo, J.D. Marcos, and E. Palacios, " Experimental evaluation of a direct air-cooled lithium bromide–water absorption prototype for solar air conditioning,," *Applied Thermal Engineering*, vol. 31, no. 16, pp. 3358-3368, 2011.
- [33] ASHRAE, COOLING TOWERS, ASHRAE Handbook-HVAC Systems and Equipment (SI), 2012.
- [34] C. Ruef, "Nosocomial Legionnaires' disease — strategies for prevention," *Journal of Microbiological Methods*, vol. 33, no. 1, pp. 81-91, 1998.
- [35] Environment Canada, "Wet cooling tower guidance for particulate matter," 2012. [Online]. Available: <http://www.ec.gc.ca/inrp-npri/>
- [36] Lu, Ronghui Qi and Lin, "Energy consumption and optimization of internally cooled/heated liquid desiccant air-conditioning system: A case study in Hong

- Kong," *Energy*, vol. 73, pp. 801-808, 2014.
- [37] K. Gommed and G. Grossman, "Experimental investigation of a liquid desiccant system for solar cooling and dehumidification," *Solar Energy*, vol. 81, no. 1, pp. 131-138, 2007.
- [38] W. Kessling, E. Laevemann, C. Kapfhammer, "Energy storage for desiccant cooling systems component development," *Solar Energy*, vol. 64, no. 4-6, pp. 209-221, 1998.
- [39] N. Hartmann, C. Glueck, and F. P. Schmidt, "Solar cooling for small office buildings: Comparison of solar thermal and photovoltaic options for two different European climates," *Renewable Energy*, vol. 36, no. 5, pp. 1329-1338, 2011.
- [40] B. Jones, "First results of a solar-thermal liquid desiccant air conditioning concept," in *1st International Congress on Heating, Cooling and Building*, Lisbon, Portugal, 2008.
- [41] Sioros and Donna, *Integrated solutions for energy and facility management*, The Association of Energy Engineering, 2002.
- [42] W.M.G. Fields, D.E. Knebel, *Cost effective thermal energy storage, Heat-Piping-Air Conditioning*, 1991, p. pp. 59-72.
- [43] M.J. Sebzali, P.A. Rubini, "The impact of using chilled water storage systems on the performance of air cooled chillers in Kuwait," *Energy and Buildings*, vol. 39, pp. 975-984, 2007.
- [44] Osama Ayadi, Alberto Mauro, Marcello Aprile, and Mario Motta, " Performance assessment for solar heating and cooling system for office building in Italy," *Energy Procedia*, vol. 30, pp. 490-494, 2012.
- [45] Francis Agyenim, Ian Knight, and Michael Rhodes, " Design and experimental testing of the performance of an outdoor LiBr/H₂O solar thermal absorption cooling system with a cold store," *Solar Energy*, vol. 84, no. 5, pp. 735-744, 2010.
- [46] Yonggao Yin, Xiaosong Zhang, Geng Wang, and Lei Luo, "Experimental study on a new internally cooled/heated dehumidifier/regenerator of liquid desiccant systems,"
- [47] Un Liu, Tao Zhang, Xiaohua Liu, and Jingjing Jiang, "Experimental analysis of an

- internally-cooled liquid desiccant dehumidifier," *Building and Environment*, vol. 63, pp. 1-10, 2013.
- [48] Gao, W., Shi, Y., Cheng, Y., and Sun, W., "Experimental study on partially internally cooled dehumidification in liquid desiccant air conditioning system," *Energy and Buildings*, vol. 61, pp. 202-209, 2013.
- [49] Un Liu, Tao Zhang, Xiaohua Liu, and Jingjing Jiang, "Experimental analysis of an internally-cooled/heated liquid desiccant dehumidifier/regenerator made of thermally conductive plastic," *Energy and Buildings*, vol. 99, pp. 75-86, 2015.
- [50] Henning, Hans-Martin, "Solar-Assisted Air-Conditioning in Buildings: A Handbook for Planners," Freiburg, SpringerWienNewYork, 2007.
- [51] A. Abhat, "Low temperature latent heat thermal energy storage: heat storage materials," 30 (1983).
- [52] Belen Zalba, Jose M, Marin, Luisa F. Cabeza, and Harald Mehling, "Review on thermal energy storage with phase change: materials, heat transfer analysis and applications," *Applied Thermal Engineering*, no. 23, p. 251–283, 2003.
- [53] Manish K. Rathod, Jyotirmay Banerjee, "Thermal stability of phase change materials used in latent heat energy storage systems: A review," *Renewable and Sustainable Energy Reviews*, vol. 18, pp. 246-258, February 2013.
- [54] Wang, Shan K., Handbook of air conditioning and refrigeration, 2 ed., New York: McGraw-Hill, 2001.
- [55] M. Helm, C. Keil, S. Hiebler, H. Mehling, and C. Schweigler, "Solar heating and cooling system with absorption chiller and low temperature latent heat storage: Energetic performance and operational experience," *Journal of Refrigeration*, vol. 32, no. 4, pp. 596-606, 2009.
- [56] Martin Helm, Kilian Hagel, Werner Pfeffer, Stefan Hiebler, and Christian Schweigler, "Solar Heating and Cooling System with Absorption Chiller and Latent Heat Storage - A Research Project Summary," *Energy Procedia*, vol. 48, pp. 837-849, 2014.
- [57] Ibrahim Dincer, Sadik Dost, and Xianguo Li, "Performance analyses of sensible heat

- storage systems for thermal applications," *International Journal of Energy Research*, vol. 21, pp. 1157-1171, 1997.
- [58] G.P. Williams, L.W. Gold, "Ground Temperatures Canadian Building Digest CBD-180.," July 1976. [Online]. Available: <http://archive.nrc-cnrc.gc.ca/eng/ibp/irc/cbd/building-digest-180.html>.
- [59] Ursula Eicker, Dirk Pietruschka, and Ruben Pesch, "Heat rejection and primary energy efficiency of solar driven absorption cooling systems," *International Journal of Refrigeration*, vol. 35, no. 3, pp. 729-738, 2012.
- [60] F. Palacín, C. Monné, and S. Alonso, "Improvement of an existing solar powered absorption cooling system by means of dynamic simulation and experimental diagnosis," *Energy*, vol. 36, no. 7, pp. 4109-4118, 2011.
- [61] P. Kohlenbach, "Solar cooling with absorption chillers: control strategies and transient chiller performance," Technische Universität Berlin, Berlin, 2006.
- [62] Lowenstein, A., Slayzak, S., and Kozubal, E., "A Zero Carryover Liquid-Desiccant Air Conditioner for Solar Applications," in *ASME International Solar Energy Conference, National Renewable Energy Laboratory*, Denver, Colorado, 2006.
- [63] Andrusiak, M., and Harrison, S. J., "The modeling of a solar thermally-driven liquid desiccant air conditioning system," in *ASES National Conference*, Buffalo, NY, 2009a.
- [64] D. Salimizad, C. McNevin, and S. J. Harrison, "Evaluation of cooling water storage for liquid desiccant air conditioning system," in *ASME International Mechanical Engineering*, Kingston, Ontario, Nov, 2014.
- [65] L. C. Mesquita, Analysis of a Flat-Plate Liquid-Desiccant Dehumidifier and Regenerator, Kingston, Ontario: PhD thesis, Queen's University, 2007.
- [66] Gao, W., Shi, Y., Cheng, Y., and Sun, W., "Experimental study on partially internally cooled dehumidification in liquid desiccant air conditioning system," vol. 61, pp. 202-209, 2013.
- [67] "TRNSYS: A Transient Simulation Program", 16 ed., , Madison, WI: Solar Energy Laboratory, University of Wisconsin-Madison, 2006.

- [68] Andrusiak, M., Harrison, S., and Mesquita, L, "Modeling of a solar thermally-driven liquid-desiccant air-conditioning system," in *ASES National Solar Conference*, Phoenix, AZ, 2010.
- [69] Khan, A. Y. and Martinez, J. L, "Modelling and parametric analysis of heat and mass transfer performance of a hybrid liquid desiccant absorber," *Energy Conservation and Management*, vol. 39, no. 10, pp. 1095-1112, 1998.
- [70] Conde, Manuel R., "Properties of aqueous solutions of lithium and calcium chlorides: formulations for use in air conditioning equipment design," *International Journal of Thermal Sciences*, vol. 43, p. 367–382, 2004.
- [71] H. Stanford, *HVAC Water Chillers and Cooling Towers: Fundamentals, Application, and Operation*, Second ed., CRC Press, 2012, pp. 23-24.
- [72] J. Braun, *Methodologies for the Design and Control of Central Cooling*- Ph.D. Thesis, Madison, Wisconsin.: University of Wisconsin-Madison, 1988.
- [73] G. Hellstrom, "Heat Storage in the Ground Duct Ground Heat Storage Model, Manual for Computer Code," Department of Mathematical Physics, University of Lund, Lund, Sweden, 1989.
- [74] ASHRAE, "Commercial/institutional ground-source heat pump engineering manual," *ASHRAE*, 1995.
- [75] Yavuzturk, C., J.D. Spitler, and S.J. Rees., "A Transient Two-dimensional Finite Volume Model for the Simulation of Vertical U-tube Ground Heat Exchangers," *ASHRAE Transactions*, vol. 105, no. 2, pp. 465-474, 1999.
- [76] G. Hellstrom, "Ground heat storage. Thermal analysis of Duct Storage Systems," Thesis, Department of Mathematical Physics, University of Lund, Sweden, 1991.
- [77] Peter Pärish, Oliver Mercker, Phillip Oberdorfer, Erik Bertram, Rainer Tepe, and Gunter Rockendorf, "Short-term experiments with borehole heat exchangers and model validation in TRNSYS," *Renewable Energy*, vol. 74, pp. 471-477, 2015.
- [78] Mikael Philippe, Michel Bernier, and Dominique Marchio, "Sizing Calculation Spreadsheet: Vertical Geothermal Borefields," *ASHRAE Journal*, vol. 52, no. 7, p. 9, 2010.

- [79] L. Berman, *Evaporative Cooling of Circulating Water*, London: Pergamon, 1961, p. 710.
- [80] Yin YG, Zhang XS, "Comparative study on internally heated and adiabatic regenerators in liquid desiccant air conditioning system," *Building Environment*, vol. 45, no. 8, pp. 1799-807, 2010.
- [81] Lu, Ronghui Qi and Lin, "Energy consumption and optimization of internally cooled/heated liquid desiccant air-conditioning system: A case study in Hong Kong," *Energy*, vol. 73, p. 801–808, 2014.
- [82] "Ontario Energy Board," 2014. [Online]. Available:
<http://www.ontarioenergyboard.ca/OEB/Consumers/Electricity/Electricity+Prices>.
- [83] M. Bernier, "Close loop Ground-Coupled Heat pumps systems," *ASHRAE Journal*, vol. 48, no. 9, p. 9, 2006.
- [84] B. Newton, "Modeling of Solar Storage Tanks," M.S. Thesis, University of Wisconsin-Madison, 1995.
- [85] Cruickshank, C.A. and Harrison, S.J, "Simulation and Testing of Stratified Multi-tank, Thermal Storages for Solar Heating Systems," in *EuroSun*, Glasgow, Scotland, 2006.

Appendix A- Modeling of a Conditioner/Regenerator

A.1. Conditioner Model (TYPE 2511)

In the conditioner, there are three working fluids: moist air, liquid desiccant, and cooling water. Heat transfer occurs between all three fluids, and mass transfer occurs between the air and the liquid desiccant. Figure. A-1 shows the heat and mass transfer in the conditioner.

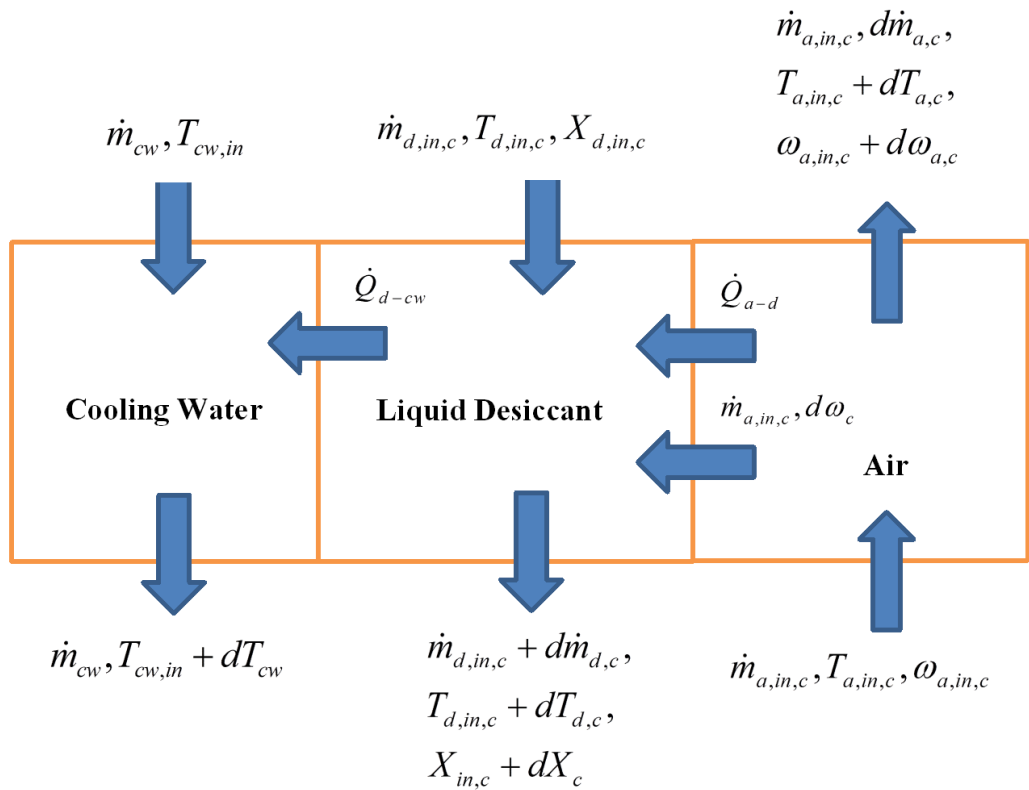


Fig. A-1: Schematic of heat and mass transfer in liquid desiccant conditioner.

There are therefore eight coupled heat and mass balance expressions that describe the operation of the conditioner. These eight equations have been simplified to the five, given below. The mass and energy balance of the moist air stream are given in Eq.s A-1 and A-2,

$$\dot{m}_{a,in,c} \omega_{in,c} = \dot{m}_{abs} + \dot{m}_{a,in,c} \omega_{out,c} \quad (\text{A-1})$$

$$\dot{m}_{a,in,c} (\omega_{in,c} h_{f,in,c} + h_{a,in,c}) = \dot{m}_{a,out,c} (\omega_{out,c} h_{f,out,c} + h_{a,out,c}) + \dot{m}_{abs} (h_{fg}) + \dot{Q}_{a-d} \quad (\text{A-2})$$

where $\dot{m}_{a,in,c}$ and $\dot{m}_{a,out,c}$ are the mass flow rates of incoming and outgoing air; \dot{m}_{abs} is the absorption rate; $\omega_{in,c}$ and $\omega_{out,c}$ are the absolute humidity of the air flowing into and out of the conditioner; $h_{f,in,c}$ and $h_{f,out,c}$ are the enthalpies of the water vapour into and out of the conditioner; $h_{a,in,c}$ and $h_{a,out,c}$ are the enthalpies of dry air into and out of the conditioner; h_{fg} is the latent heat of vaporization; and, \dot{Q}_{a-d} is the heat transfer rate between the air and the desiccant.

The mass and energy balance Eq.s for the desiccant stream are given in Eq.s A-3 and A-4. The energy balance is only valid if it is assumed that the moisture transferred into the desiccant \dot{m}_{abs} is very small, compared to the total desiccant flow rate $\dot{m}_{d,in,c}$.

$$\dot{m}_{d,in,c} X_{in,c} = \dot{m}_{d,out,c} X_{out,c} = (\dot{m}_{d,in,c} + \dot{m}_{abs}) X_{out,c} \quad (\text{A-3})$$

$$\dot{m}_{d,in,c} h_{d,in,c} + \dot{Q}_{a-d} = \dot{m}_{d,out,c} h_{d,out,c} + \dot{m}_{abs} (h_{dil}) + \dot{Q}_{d-cw} \quad (\text{A-4})$$

where $X_{in,c}$ and $X_{out,c}$ are the desiccant concentrations into and out of the conditioner; $h_{d,in,c}$ and $h_{d,out,c}$ are the desiccant enthalpies into and out of the conditioner; h_{dil} is the enthalpy of dilution; and \dot{Q}_{d-cw} is the heat transfer rate between the desiccant and cooling water.

In Eq. A-3 and A-4, $\dot{m}_{d,in,c} \cdot X_{in,c}$ is a liquid desiccant inlet property that operates at constant variables such as flow rate, concentration and temperature. However, change of heat and mass transfer of the desiccant ($\dot{m}_{d,out,c} \cdot X_{out,c}$) depends on unknown variables such as \dot{Q}_{a-d} , \dot{Q}_{d-cw} , \dot{m}_{abs} and $T_{d,out,c}$. As a result, we can conclude that increasing the heat transfer between the desiccant and air, and the desiccant and the water cooling temperature, results in reducing the liquid desiccant temperature $T_{d,out,c}$, and increasing the absorption rate of moist (dehumidification) \dot{m}_{abs} . Finally, the energy balance of the cooling water stream is given in Eq. A-5,

$$\dot{m}_{cw} h_{cw,in} + \dot{Q}_{cw-d} = \dot{m}_{cw} h_{cw,out} \quad (A-5)$$

where \dot{m}_{cw} is the cooling water mass flow rate; and $h_{cw,in}$ and $h_{cw,out}$ are the enthalpies of the cooling water into and out of the conditioner. The heat transfer between the cooling water and the desiccant can be increased by either reducing the cooling water mass flow rate or reducing the temperature of water that goes into the conditioner.

As previously mentioned, the current study uses a modification of a model created by L. Crofoot (2012). Figure. A-2 shows the schematic of inputs, outputs, and parameters for the TYPE251 (conditioner) TRNSYS model that was created. Parameters are defined within the component by the user and are constant for the duration of the simulation. The outputs are connected to other components, or are used in calculations to determine the system performance.

The following assumptions were made in order to model the conditioner:

- the dehumidification, enthalpy, and desiccant-cooling water effectiveness are constant.

- the specific heats of the working fluids are constant with respect to temperature (and concentration);
- mass flow rates of the air and cooling water are constant;
- the inlet volumetric flow rate of the desiccant is constant;
- the conditioner is adiabatic (i.e., no heat losses to surroundings);
- Desiccant mass is conserved and there is no carryover into the air streams.

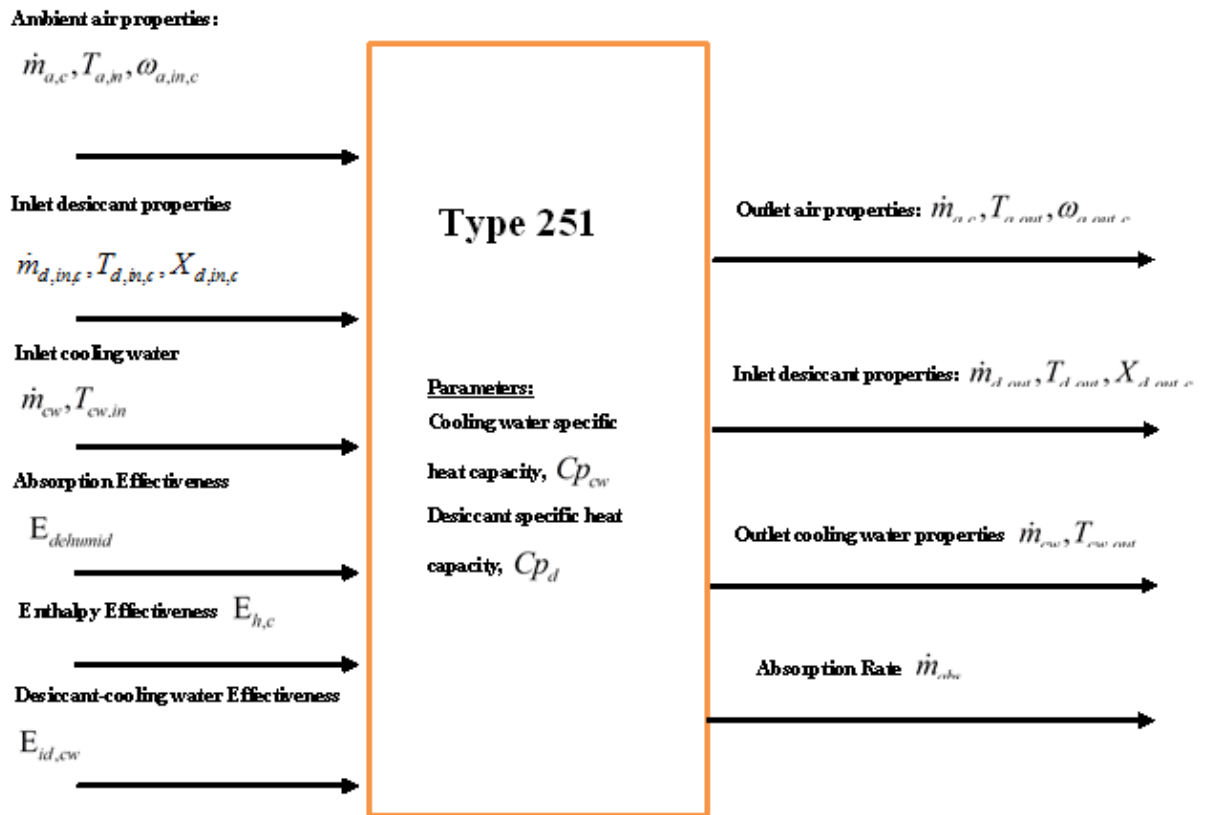


Fig. A-2: Schematic of inputs, outputs, and parameters for the TYPE251

A.2. Regenerator Model (TYPE 250)

The regenerator operates in the reverse manner as the conditioner by transferring (desorbing) the moisture from heated desiccant into a secondary scavenging-air stream.

Fig. A-3: shows a schematic of the heat and mass transfer.

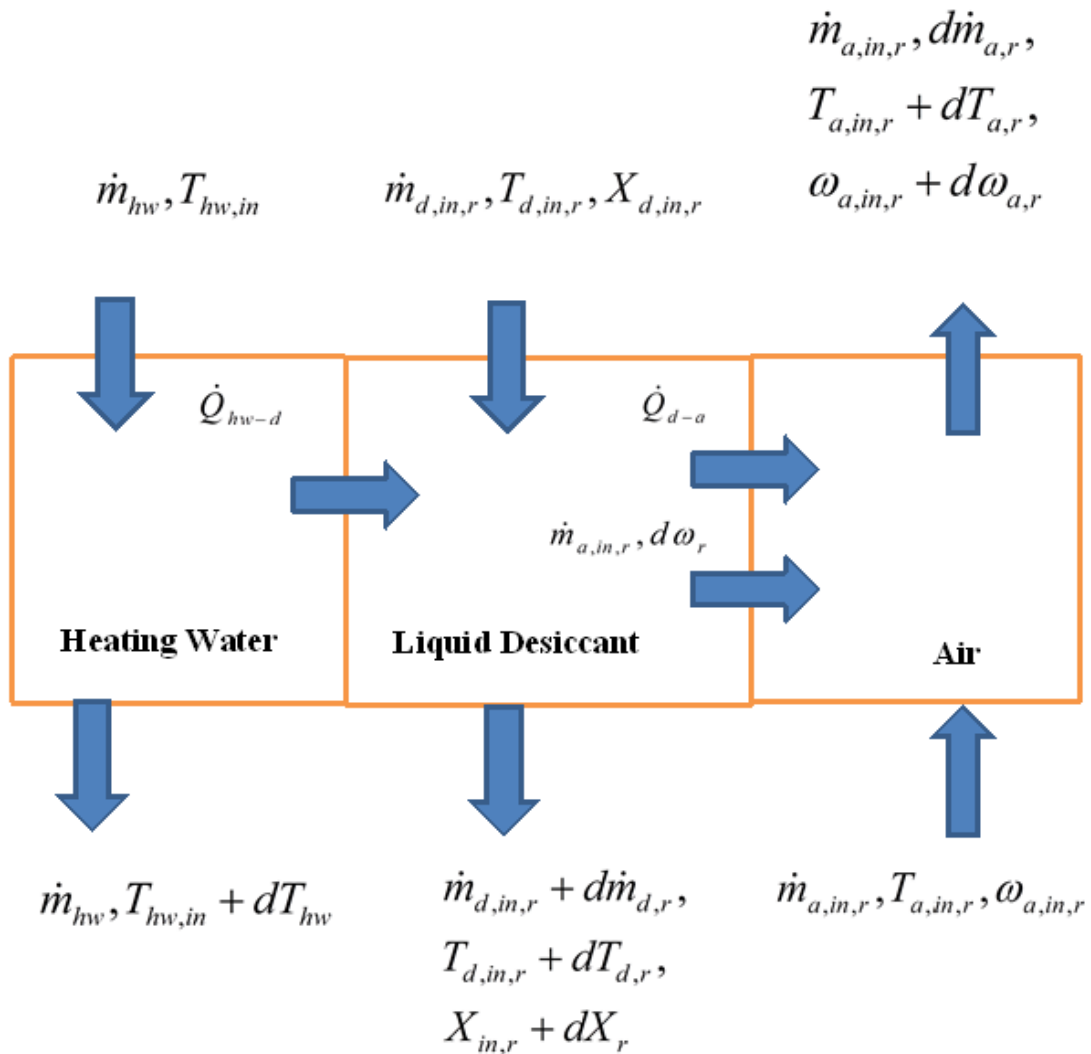


Fig. A-3: Schematic of heat and mass transfer in internally heated regenerator

Similar to the conditioner, the regeneration, enthalpy, and desiccant-heating water effectiveness parameters were defined and are given in Eq.s (A-10) - (A-12).

$$\varepsilon_{regen} = \frac{\omega_{out,r} - \omega_{in,r}}{\omega_{out,max} - \omega_{in,r}} = \frac{P_{a,out} - P_{a,in}}{P_{d,in,c} - P_{a,in}} \quad (\text{A-10})$$

$$\varepsilon_{r,h} = \frac{h_{a,out,r} - h_{a,in,r}}{h_{a,max,r} - h_{a,in,r}} \quad (\text{A-11})$$

$$\varepsilon_{ld,hw} = \frac{T_{d,out,r} - T_{d,in,r}}{T_{d,out,r} - T_{hw,in}} \quad (\text{A-12})$$

Appendix B- Stratified tank simulation

B.1. Introduction

A TRNSYS simulation was used to investigate the performance of the LDAC system using stratified cooling water storage (SCWS) tank. To undertake this study, the SCWS tank was simulated based on 2014 experimental testing (Case D) and then validated SCWS model incorporated into a LDAC system simulation as a cooling water supply.

B.2. TRNSYS simulation model

The accurate modeling of the components within the system is an important aspect in predicting the LDAC system performance. For this reason, the simulation modelling of stratified tank process was divided into two steps. The first step was to validate a SCWS tank model. In this step, the tank's water draw was set with a flow rate of 41 l/min similar into the experimental results (Case D). The tank's inlet water temperature depended on the recorded amount of heat absorbed inside the conditioner throughout the experiment. To measure the energy that delivered to the tank, inlet and outlet temperatures were recorded for every minute. TYPE 9a, was used to input experimentally observed weather conditions and heat source data. The simulation schematic is shown in Fig. B-1.

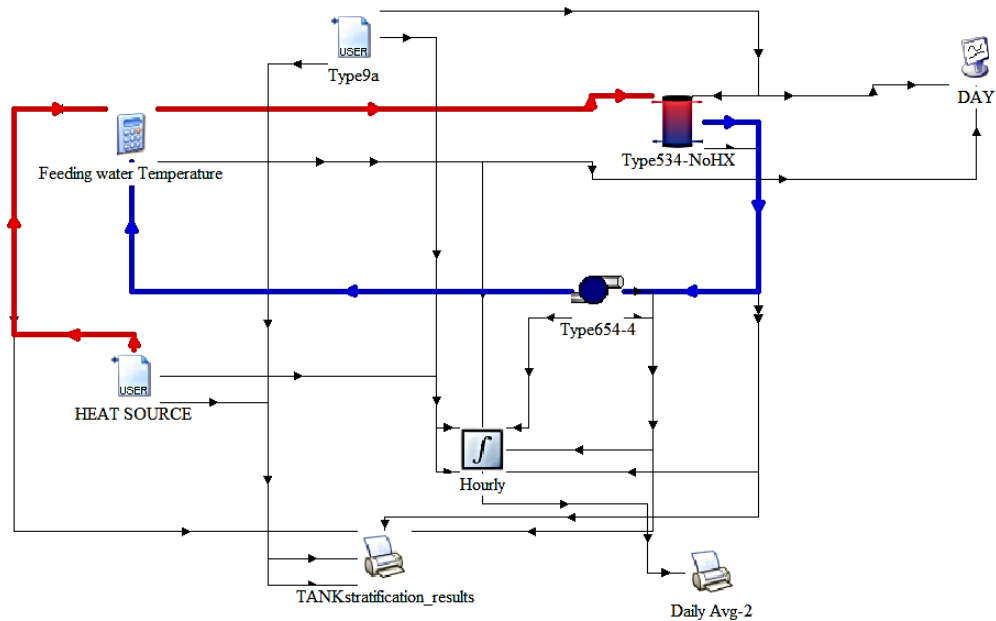


Fig. B-1: Schematic of components used for TRNSYS simulation validation

In the second step, the validated SCWS simulation model was used as a cooling water supply for the conditioner in the LDAC simulation model. To accomplish this, the heat rejection loop using the ECT (TYPE 51) in the base case was replaced with the SCWS tank (TYPE 534) and all other components remained the same.

B.2.1. Modeling of Stratified Storage tank (Type 534)

TYPE 534, a cylindrical storage tank with vertical configuration [84], was used to investigate the vertical temperature distribution and degree of stratification. The model assumes that the tanks consist of N fully-mixed equal volume segments. Each constant-volume node is assumed to be isothermal and interacts thermally with the nodes above and below through two mechanisms: thermal conduction between nodes, and through fluid movement (either forced movement from inlet flow streams or natural de-stratification mixing due to temperature inversions in the tank).

The number of nodes determines the resolution of the vertical temperature distribution modeled in the storage tank (i.e., increasing N will allow for temperature gradients to be more accurately modeled [85]). The main advantage of TYPE 534 over other stratified storage tank components such as TYPE 60 or TYPE 4, is the capability of setting a higher number of nodes (500 nodes) which allows for a larger tank to be simulated accurately. TYPE 534 uses an analytical solution rather than a numerical solution to solve the differential equation. This method eliminates simulations dependence on time-step, but it requires an iterative solution inside the subroutine to solve the differential equation [67].

Energy and mass balance equations describing the various modes of heat transfer for a segment (j) of a vertical storage tank are shown in Fig B-2. These modes of heat transfer are as follows:

- thermal losses to the environment through the top of the storage tank
- thermal losses to the environment through the sides of the storage tank
- thermal losses to the environment through the bottom of the storage tank
- conduction between adjacent tank nodes
- mixing between nodes to eliminate thermal instabilities
- mixing between nodes due to load flow through the storage tank

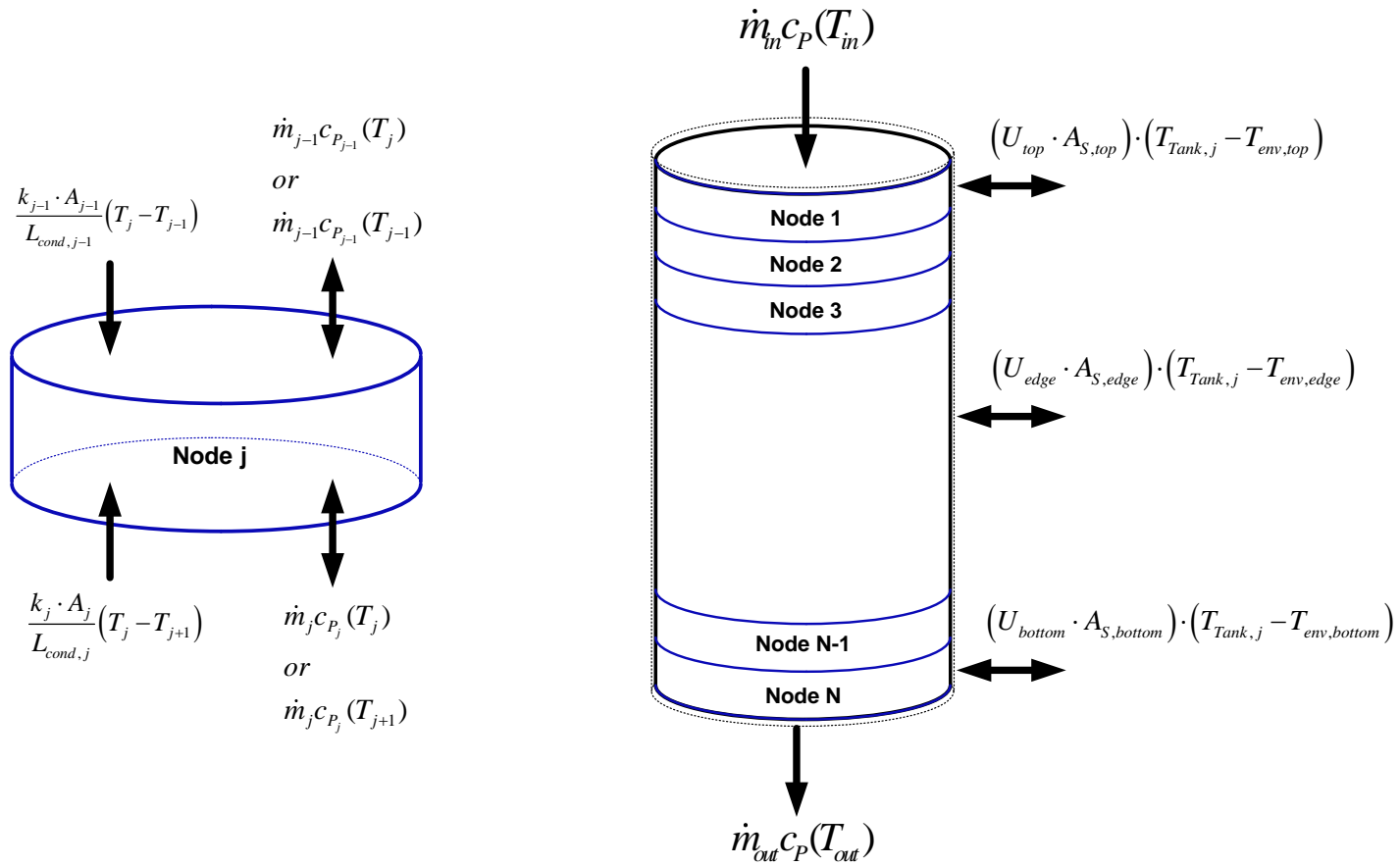


Fig. B-2: Schematic of liquid tank stratification nodes and heat and mass flow into and out of a node [67].

The energy and mass flows into and out of each node from adjacent nodes are estimated based on the node temperatures that existed at the beginning of each time-step. In this tank model, the influx of fluid into a node is completely mixed with the storage tank fluid at every time-step before this fluid flows to the next node. As in all TRNSYS components, the OUTPUTs from the model are assumed to be average values over the time-step. The differential equations used to generate the output of the tank nodes can be written as:

$$\frac{dT_{Tank,j}}{dt} = \frac{(Q_{in,Tank,j} - Q_{out,Tank,j})}{C_{Tank,j}} \quad (B-1)$$

$$\begin{aligned} \dot{m}c_p \frac{dT_{Tank,j}}{dt} = & \frac{k_{j-1} \cdot A_{j-1}}{L_{cond,j-1}} (T_j - T_{j-1}) + \frac{k_j \cdot A_j}{L_{cond,j}} (T_j - T_{j+1}) \\ & + (U_{top} \cdot A_{S,top}) \cdot (T_{Tank,j} - T_{env,top}) + (U_{edge} \cdot A_{S,edge}) \cdot (T_{Tank,j} - T_{env,edge}) \\ & + (U_{bottom} \cdot A_{S,bottom}) \cdot (T_{Tank,j} - T_{env,bottom}) \\ & + \dot{m}_j c_{P_j} (T_j - T_{j+1}) + \dot{m}_{j-1} c_{P_{j-1}} (T_j - T_{j-1}) \end{aligned} \quad (B-2)$$

where $A_{S,top}$ and $A_{S,bottom}$ are the top and bottom surface areas of the tank U_{top} , U_{bottom} and U_{edge} are the loss coefficients for the storage tank top, bottom, and edge, respectively. Two values of for the heat loss coefficients were used in this simulation, $U= 70 \text{ W/m}^2\cdot\text{K}$ (at the bottom of the tank) and $U= 1.3 \text{ W/m}^2\cdot\text{K}$ (best estimate of the edge loss and top loss coefficients); k_j is thermal conductivity of fluid in node j (evaluated at the average temperature between 'j' and the node above), and k_{j-1} is the thermal conductivity of the fluid at node j (evaluated at the average temperature between 'j' and the node below);

$L_{cond,j}$ and $L_{cond,j-1}$ are the vertical distances between the centroid of 'j' and the centroid of the nodes below and above respectively.

B.3. Results and Discussion

B.3.1. SCWS simulation and validation results

The SCWS experimental results (Case D) were used to verify the SCWS simulation model. This simulation was set up with the same operational conditions as seen experimentally. The experimental and simulation temperature profiles indicated that stratification happens in 100-130 min and at the initial tank temperature. The comparison of experimental and simulation stratification for 16th of September is shown in Fig. B-3.

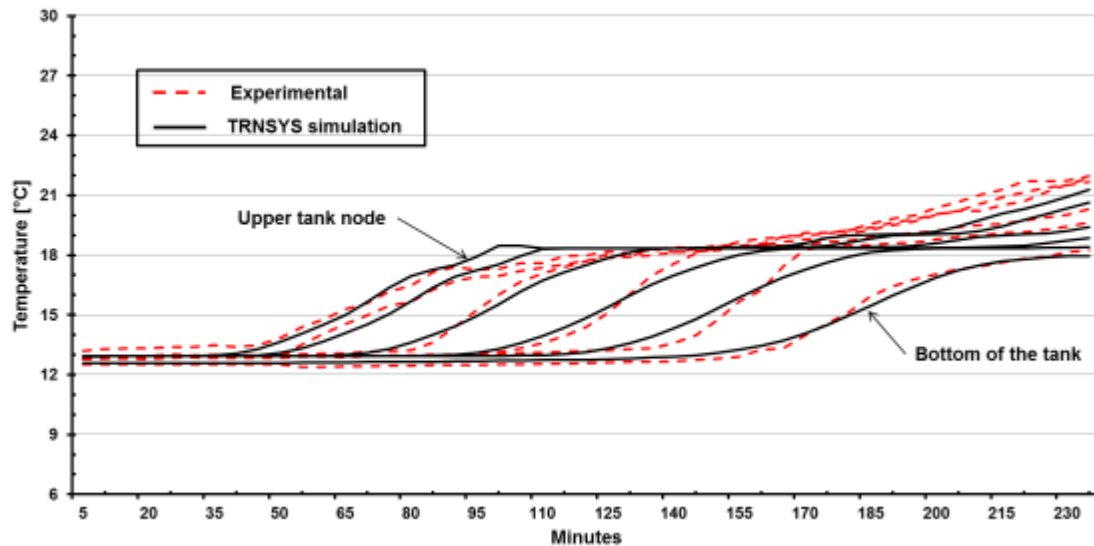


Fig. B-3: Comparison of experimental and simulation stratification for September 16th.

The simulated and experimental average water temperatures of each node over nine operating hours for three days of operation are shown in Fig. B-4. The result indicated that the simulated model could predict average water temperature within 15% for both cold water supply to the conditioner (Outlet) and hot water return to the tank (Inlet).

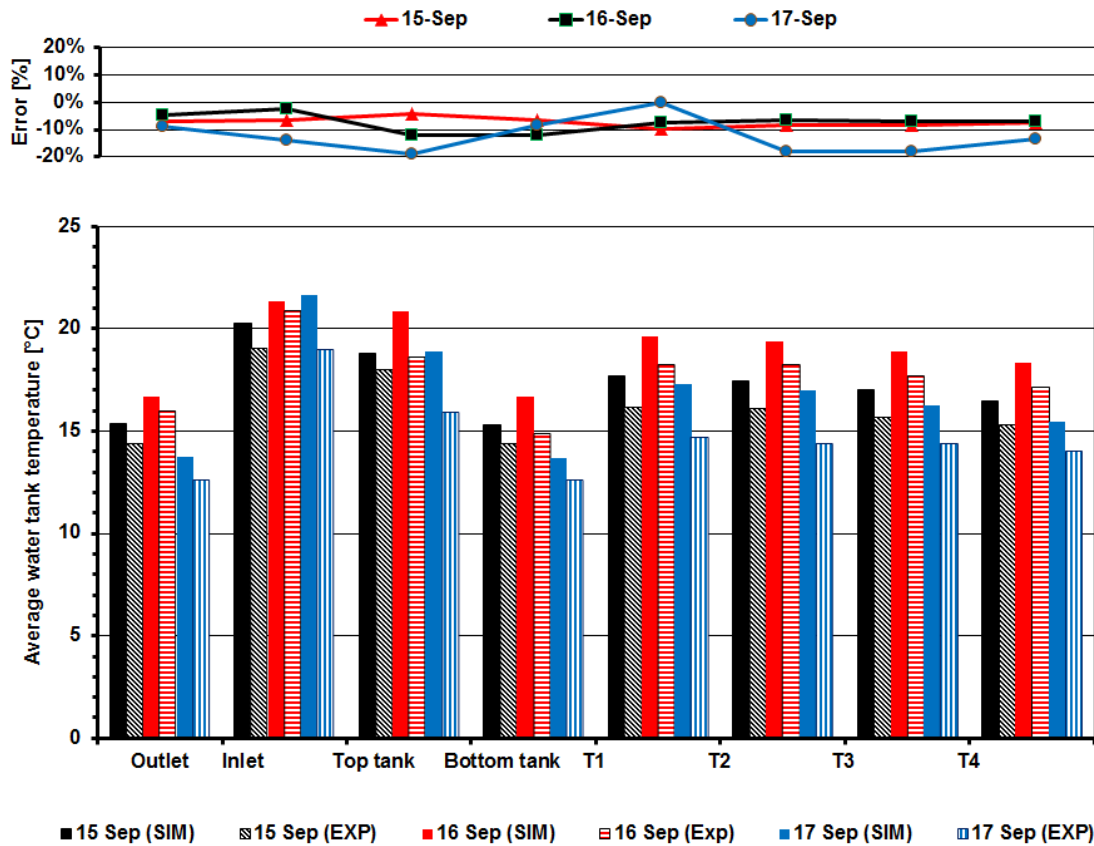


Fig. B-4: Comparison of experimental (EXP) and predicted (SIM) average water temperature for three operating days in September.

B.3.2. LD-SCWS results

The experimental and simulated results were compared in the previous section and proved the stratification model's accuracy. This model was integrated into a systems scale model of a LDAC system (LD-SCWS). The cold water was pumped at 41 L/min from the stratified cooling water storage tank into the conditioner.

Three typical weather conditions the system would experience were simulated. The chosen days were July 17th (sunny and humid), July 30th (sunny and dry), and August 13th (cloudy and humid). The LD-SCWS simulation results were compared with previous experimental and simulation results using an ECT. Table B-1 summarized the operation of both SCWS and ECT cooling systems.

Three different initial tank water temperatures were used for each testing day. In the experimental testing, the night cooling system (section 3.5) was designed to reject heat from the tank. Therefore, the early morning ambient dry-bulb temperature was used as a maximum initial temperature of the tank for each simulated day, and two lower initial tank temperatures were used for finding the effect initial tank temperature had on the LDAC performance.

July 17th was sunny and humid with an average ambient air temperature of 32°C and absolute humidity of 15.4 g_w/kg_a. The simulation results indicated that the SCWS at 41 kg/min flow rate could supply cold water for 146 minutes at the initial temperature. The COP_T and total cooling power results showed 5.5% and 9% improved for tank initial temperature at 12°C and no improvement at the maximum tank initial temperature (at 16°C).

July 30th was also sunny and warm, but the humidity was 2.4 g_w/kg_a lower than July 17th. The low ambient relative humidity (below the regenerator set-point of 30% RH) between 2:30 PM- 4 PM resulted in the regenerator shutting off and low absorption rates in the conditioner. Comparing LD-SCWS and base case results for this day indicated that the LD-SCWS system provided constant cold water temperature and with no total cooling power improvement. This is due to better operating ECT (base case) in the dry condition.

August 13th's humidity was 2.7 g_w/kg_a lower than July 17th's. The ambient temperature was noticeably lower due to the cloudy conditions (24°C compared to 32°C). The maximum initial temperature of the tank on 13th August was set as 18°C (equal to the dry-bulb temperature in the early morning). Similar to other days, the simulation results indicated no cooling power improvement was achieved at the tank's highest initial temperature. In all three days, electrical COPs were improved due to the decrease in electrical power consumption of the ECT's fan. Comparing the SCWS to the ECT systems indicated that COP_E increased by 8-16% on July 30th, 14-26% on July 17th, and up to 18% on August 13th.

Table B-1: Summary of LD-SCWS simulation and experimental values from LDAC testing in summer

	30 th July					17 th July					13 th August				
	SCWS-LD			ECT		SCWS-LD			ECT		SCWS-LD			ECT	
	Cold water flow (l/min)			NUM	EXP	Initial Tank Temperature (°C)			NUM	EXP	Initial Tank Temperature (°C)			NUM	EXP
	12.0	14.0	16.0	-	-	12.0	14.0	16.0	-	-	14.0	16.0	18.0	-	-
Average ambient temperature (°C)	26.4					32.4					24.4				
Average ambient relative humidity (%)	62.3					52.0					66.9				
Average Radiation (W/m ²)	716					631					538				
Cold water flow rate (kg/min)	42.6					42.6					42.6				
Average latent cooling rate (kW)	19.1	18.7	18.3	19.2	12.4	18.2	17.8	17.4	17.6	16.9	15.4	15.7	14.8	16.0	14.6
Average total cooling rate (kW)	18.7	17.9	17.1	18.6	10.9	18.5	17.7	16.8	17.0	17.2	13.9	13.04	12.1	13.5	11.2
Total electrical Consumption (kWh)	42.6			50.1	50.0	42.6			50.1	50.0	42.6			50	51.1
COP _T	0.63	0.62	0.60	0.64	0.38	0.57	0.56	0.54	0.54	0.53	0.44	0.42	0.40	0.45	0.32
COP _E	4.3	4.2	4.0	3.7	2.2	4.3	4.1	3.9	3.4	3.4	3.2	3.0	2.8	2.70	2.20
Total cooling rate improvement (%)	0	-3	-8	-	-	8.8	4	-1	-	-	3	-3.4	-10	-	-
Electrical reduction (%)	15			-	-	15			-	-	15			-	-

The simulation results indicate that reducing the cooling water flow rate resulted in increasing the duration of the cold water supply at the tank's initial temperature, and higher stratification rate. The effect of flow rate on the cooling power and thermal COP for a 14°C initial water temperature on July 17th can be seen in Fig. B-5.

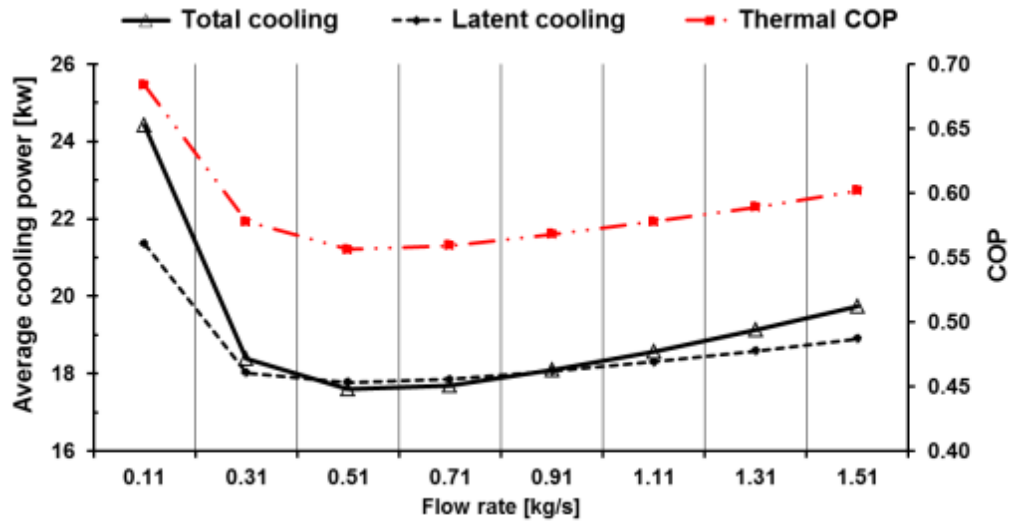


Fig. B-5: Simulated average air cooling power and thermal COP for various tanks cooling water flow rate on July 17th.

B.4. Conclusion

The use of SCWS tank as an alternative to ECT was evaluated both experimentally and through TRNSYS simulations. The SCWS tank simulation model was validated based on the experimental testing and then used in LDAC simulation model.

The LD-SCWS simulation results indicate the lower initial tank resulted in higher total cooling and COP_T when compared to the previous ECT system. This improvement over the ECT system was found to be up to 9% and 6% for total cooling and COP_T respectively. For all three days, the COP_E was improved (by up to 26%) due to the elimination of the ECT fan's electrical consumption. The study of cold water flow rate on the LD-SCWS system indicated that a lower water flow rate can provide high COPs and delay the mixing of the stratified tank. ECT performance depends on ambient air humidity and temperature while LD-SCWS depends on initial tank temperature and stratification rate.